SUPPORTING INFORMATION

Iridium(III) bis(thiophosphinite) pincer complexes: Synthesis, ligand activation and applications in catalysis

Alexander Linke[a], David Decker[a], Hans-Joachim Drexler[a], and Torsten Beweries*[a]

Leibniz-Institut für Katalyse e.V., Albert-Einstein-Str. 29a, 18059 Rostock, Germany. E-mail: torsten.beweries@catalysis.de

Table of contents

1 Experimental Section

General Information. If not stated otherwise, all manipulations were carried out under oxygen- and moisture-free conditions under an inert atmosphere of argon using standard Schlenk or glove box techniques. All glassware was heated three times *in vacuo* using a heat gun and cooled under argon atmosphere. Solvents were transferred using syringes, which were purged three times with argon prior to use. Solvents and reactants were either obtained from commercial sources or synthesised as detailed in Table S1. THF, toluene, dichloromethane, and *n*-hexane were dispensed from a solvent purification system (SPS) (PureSolv, Innovative Technology) into thick-walled glass Schlenk bombs equipped with Young-Type Teflon valve stopcocks, cannula transferred onto activated molecular sieves (3 Å, 0.3 nm, Carl Roth) and stored under argon in a conventional Schlenk flask.

Table S1. Origin and purification of solvents and reactants.

Substance	Origin	Purification
CH_2Cl_2	local trade	taken from SPS and stored over molecular sieves (3 Å)
THF	local trade	taken from SPS and stored over molecular sieves (3 Å)
benzene	local trade	dried over Na/benzophenone stored over molecular sieves (3 Å)
toluene	local trade	taken from SPS and stored over molecular sieves (3 Å)
mesitylene	abcr	degassed and distilled on molecular sieves (3 Å)
n-pentane	local trade	dried over Na/benzophenone stored over molecular sieves (3 Å)
n-hexane	local trade	taken from SPS and stored over molecular sieves (3 Å)
CD_2Cl_2	Eurisotop	dried over molecular sieves (3 Å), degassed (three freeze-pump-thaw cycles) and stored in glove box
$CDCl_3$	Eurisotop	dried over molecular sieves (3 Å), degassed (three freeze-pump-thaw cycles) and stored in glove box

Table S1. continued.

Substance	Origin	Purification
C_6D_6	Eurisotop	dried over molecular sieves (3 Å), degassed (three freeze-pump-thaw cycles) and stored in glove box
toluene-d_8	Eurisotop	dried over molecular sieves (3 Å), degassed (three freeze-pump-thaw cycles) and stored in glove box
NEt_3	old stock	freshly distilled and stored over molecular sieves
tBu_2PCl	Thermo Scientific	stored over molecular sieves (3 Å)
iPr_2PCl	Acros Organics	stored over molecular sieves (3 Å)
Ph_2PCl	TCI	stored over molecular sieves (3 Å)
$[Ir(COD)Cl]_2$	Sigma Aldrich	
$[Ir(COE)_2Cl]_2$	Strem Chemicals	
pyridine	local trade	distilled over KOH stored over molecular sieves (3 Å)
$BF_3 \cdot EtO_2$	Alfa Aesar	
cyclooctane	Sigma Aldrich	stirred over concentrated H_2SO_4 for 2 h distilled under vacuum on molecular sieves
tert-butyl ethylene	TCI	degassed and stored over molecular sieves

NMR spectra were recorded on Bruker spectrometers (AV300, AV400, or Fourier300) and were referenced internally to the deuterated solvent (^{13}C: CD_2Cl_2 δ_{ref} = 53.8 ppm, $CDCl_3$ δ_{ref} = 77.2 ppm, C_6D_6 δ_{ref} = 128.1 ppm, toluene-d_8 δ_{ref} = 20.4 ppm), to protic impurities in the deuterated solvent (^1H: $CHDCl_2$ δ_{ref} = 5.32 ppm, $CDCl_3$ δ_{ref} = 7.26, C_6HD_5 δ_{ref} = 7.16 ppm, tol-d_7 $\delta_{ref,1}$ = 2.09 ppm), or externally (^{31}P: 85% H_3PO_4 δ_{ref} = 0 ppm). All measurements were carried out at ambient temperature unless denoted otherwise.

IR spectra of crystalline samples were recorded on a Bruker Alpha II FT-IR spectrometer equipped with an ATR unit at ambient temperature under anaerobic conditions.

Elemental analyses were obtained using a Leco TruSpec Micro CHNS analyser. V_2O_5 was used as an oxidiser for CHNS analysis of Ir complexes, circumventing possible Ir-carbide formation.

Melting points were determined using a Mettler-Toledo MP 70 Melt at a heating rate of 5 °C/min. Clearing points are reported uncorrected.

Mass spectra were recorded on a Thermo Electron MAT 95-XP sector field mass spectrometer using crystalline samples.

2 Crystallographic Details

X-ray Structure Determination: X-ray quality crystals were selected in Fomblin YR-1800 perfluoroether (Alfa Aesar) at low temperature. Diffraction data were collected at 123(2) K on a Bruker Kappa APEX II Duo diffractometer using Mo-K_{α} radiation **2-*i*Pr2-*i*Pr**, **2-*t*Bu**, **3-*i*Pr** and **3-Ph** or Cu-K_{α} radiation **4**. The structures were solved by iterative (SHELXT)[1] or direct methods (SHELXS-97)[2] and refined by full matrix least square techniques against F^2 (SHELXL-2014).[3] Semi-empirical absorption corrections were applied (SADABS or TWINABS(**3-*i*Pr**)/Bruker).[4] The non-hydrogen atoms were refined anisotropically. The hydrogen atoms, except the hydrides, were placed into theoretical positions and were refined by using the riding model. Contributions of solvent molecules were removed in **2-*t*Bu** and **3-Ph** from the diffraction data with PLATON / SQUEEZE.[5] DIAMOND (Crystal Impact GbR) was used for structure representations. **3-*i*Pr** was refined as a 2-component twin.

Crystallographic data (excluding structure factors) for the structures reported in this paper have been deposited at the Cambridge Crystallographic Data Centre. Copies of the data can be obtained free of charge on application to CCDC, 12 Union Road, Cambridge, CB21EZ, UK (fax: int. code + (1223) 336-033; e-mail: deposit@ccdc.cam.ac.uk

Table S2. Crystallographic details.

Compound	**2-*i*Pr**	**2-*t*Bu**	**4**
Chem. Formula	$C_{36}H_{64}Cl_2P_4S_4Ir_2 \cdot 2\ CH_2Cl_2$	$C_{22}H_{39}ClIrP_2S_2$	$C_{42}H_{35}ClIrP_3S_3 \cdot 0.5\ C_6H_6$
Formula weight [g/mol]	1374.18	657.24	995.49
Colour	colourless	red	red
Crystal system	triclinic	monoclinic	triclinic
Space group	$P\bar{1}$	$P2_1/c$	$P\bar{1}$
a [Å]	9.2654(10)	16.9551(9)	10.3443(3)
b [Å]	12.1056(14)	7.9802(4)	12.5535(4)
c [Å]	13.1927(15)	21.5807(11)	15.6148(4)
α [°]	114.974(4)	90	79.549(2)
β [°]	106.744(4)	94.181(2)	86.0080(10)
γ [°]	96.813(4)	90	82.805(2)
V [Å^3]	1234.3(2)	2912.2(3)	1976.07(10)
Z	1	4	2
$\rho_{calcd.}$ [g/cm^3]	1.849	1.499	1.673
μ [mm^{-1}]	6.037	4.936	10.046
T [K]	150(2)	150(2)	150(2)
Measured reflections	46559	105824	36859
Independent reflections	4859	9007	6990
Reflections with $I > 2\sigma(I)$	4753	7799	6398
R_{int}	0.0236	0.0386	0.0443
F(000)	676	1308	990
$R_1(R[F^2>2\sigma(F^2)])$	0.0136	0.0226	0.0251
$wR_2(F^2)$	0.0342	0.0561	0.0609
GooF	1.101	1.028	1.025
No. of Parameters	256	402	489
CCDC #	2173068	2173069	2173066

Table S2 continued.

Compound	**3-*i*Pr**	**3-Ph**
Chem. Formula	$C_{23}H_{37}ClIrNP_2S_2$	$C_{35}H_{29}ClIrNP_2S_2$
Formula weight [g/mol]	681.24	817.30
Colour	yellow	yellow
Crystal system	monoclinic	monoclinic
Space group	$P2_1/c$	$P2_1/c$
a [Å]	10.6393(6)	9.5040(10)
b [Å]	14.5060(8)	16.0049(18)
c [Å]	17.4341(10)	21.892(2)
α [°]	90	90
β [°]	96.740(3)	99.492(3)
γ [°]	90	90
V [Å^3]	2672.1(3)	3284.4(6)
Z	4	4
$\rho_{calcd.}$ [g/cm^3]	1.693	1.653
μ [mm^{-1}]	5.384	4.397
T [K]	150(2)	150(2)
Measured reflections	5844	93158
Independent reflections	5844	7552
Reflections with $I > 2\sigma(I)$	5754	6203
R_{int}	-	0.0828
F(000)	1352	1608
$R_1(R[F^2>2\sigma(F^2)])$	0.0339	0.0318
w$R_2(F^2)$	0.0840	0.0693
GooF	1.128	1.089
No. of Parameters	284	383
CCDC #	2173065	2173067

3 Syntheses of starting materials

3.1 General procedure for syntheses of bis(thiophosphinito) pincer ligands

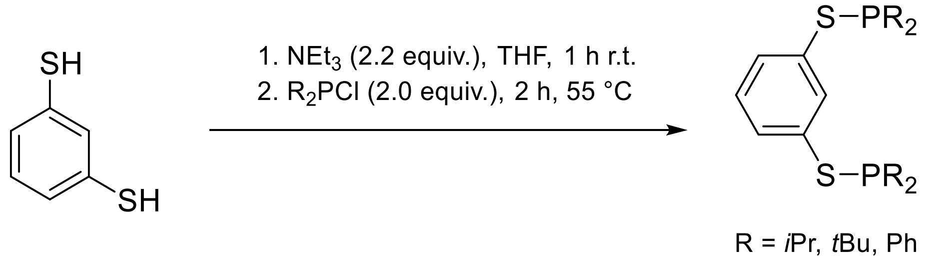

The ligand synthesis was slightly modified from the original protocol.[6]

THF (40 mL) was placed in a 100-mL three necked round bottom flask equipped with a Dimroth condenser, vacuum inlet tube, stirring bar and over pressure valve. Then 1,3-benzenedithiol (1.0 equiv.) was added *via* a syringe, which gave a clear colourless solution. Afterwards NEt_3 (2.2 equiv.) was weighed in a syringe and added to the reaction mixture, which yielded a clear, colourless solution. This solution was stirred at room temperature for 1 h. Subsequently, the corresponding chlorophosphine R_2PCl (2.0 equiv.) was added to the reaction mixture, which immediately caused precipitation of the salt $(HNEt_3)Cl$. *Please note: In case the stir bar stops addition of another portion of THF (5–10 mL) to dilute the reaction suspension and ensure proper mixing might be needed!* The reaction was stirred for additional 2 h at 55 °C (oil bath). The solvent was removed completely *in vacuo* ($1x10^{-3}$ mbar) and the white residue was dried for approximately 10 min at room temperature. The white residue was washed three times with 10 mL of *n*-hexane, the supernatant was filtered off each time by cannula filtration, yielding a colourless filtrate and a white residue. Finally, all volatile components from the *n*-hexane filtrate were removed *in vacuo* ($1x10^{-3}$ mbar) and the residue was dried *in vacuo* (1×10^{-3} mbar) for 30 min at 40 °C (water bath). The products are mostly obtained as viscous oils (R = *i*Pr, Ph), which in some cases solidify (R = ^{t}Bu).

3.1.1 Synthesis of ^{iPr}PSCSP^{iPr} (1-*i*Pr)

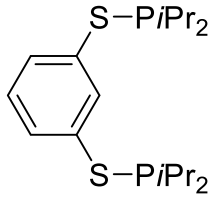

Following the general procedure (*c.f.*: 3.1), 1,3-benzenedithiol (572 mg, 4.02 mmol) was dissolved in THF. Then NEt_3 (904 mg, 1.24 mL, 8.93 mmol) was added to the THF solution. After the mixture was stirred for 1 h at room temperature, $i$$Pr_2PCl$ (1.28 g, 8.36 mmol, 1.33 mL) was added and the resulting suspension was stirred for additional 2 h at 55 °C (oil bath).
Isolated yield: 1.40 g (3.74 mmol, 93%).

Mp. not determined. **CHN** calc. (found) in %: C57.73 (57.50), H 8.61 (8.46), S 17.12 (17.27). **^{1}H NMR** (C_6D_6, 300 MHz, 298.5 K): δ = 1.03 (dd, $J_{H–H}$ = 7.15 Hz; 12 H, PCH(CH_3)$_2$), 1.14 (dd, $J_{H–H}$ = 6.8 Hz, 12 H, PCH(CH_3)$_2$), 1.83 (dsept, $J_{H–H}$ = 7.0 Hz, 4 H, PCH(CH$_3$)$_2$), 6.88 (t, $J_{H–H}$ = 7.80 Hz, 1 H, ArH$_{para}$), 7.39 (m, 2 H, ArH$_{meta}$), 8.11 (m, 1 H, ArH$_{ipso}$) ppm. **^{13}C NMR** (C_6D_6, 75 MHz, 298.8 K): δ = 18.9 (d, $J_{C–P}$ = 8.3 Hz ,PCH(CH_3)$_2$), 19.8 (d, $J_{C–P}$ = 19.4 Hz PCH(CH_3)$_2$), 26.2 (d, $J_{C–P}$ = 21.6 Hz ,PCH(CH_3)$_2$), 129.1 (s, arom. C), 129.3 (s, arom. C), 134.3 (t, $J_{C–P}$ = 9.2 Hz, arom. C), 138.0 (d, $J_{C–P}$ = 14.5 Hz., arom. C) ppm. **^{31}P{^{1}H} NMR** (C_6D_6, 122 MHz, 298.5 K): δ = 65.8 (s) ppm. **MS** (HR-EI, 70 eV, rel. int. > 10%) *m/z* calcd. (found): 374.14152 (374.14156).

3.1.2 Synthesis of ^{tBu}PSCSP^{tBu} (1-*t*Bu)

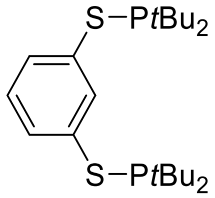

Following the general procedure (*c.f.*: 3.1), 1,3-benzenedithiol (680 mg, 4.78 mmol) was dissolved in THF. Then NEt_3 (1.21 g, 1.66 mL,12.0 mmol) was added to the THF solution. After the mixture was stirred for 1 h at room temperature, $^tBu_2PCl$ (1.73 g, 1.82 mL, 9.58 mmol) was added and the resulting suspension was stirred for additional 2 h at 55 °C (oil bath).
Yield: 1.94 g (4.51 mmol, 94%).

Mp. 84.0 – 86.7 °C. **CHN** calc. (found) in %: C 61.36 (61.67), H 9.36 (9.25), S 14.89 (14.59). **^{1}H NMR** (C_6D_6, 300 MHz, 298 K): δ = 1.22 (d, J_{P-H} = 11.9 Hz, 36 H, PC(CH_3)$_3$), 6.91 (t, J_{H-H} = 7.8 Hz, 1 H, ArH$_{para}$), 7.49 (m, 2 H, ArH$_{meta}$), 8.30 (m, 1 H, ArH$_{ipso}$) ppm. **^{31}P{^{1}H}**

NMR (C_6D_6, 122 MHz, 298 K): δ = 82.9 (s) ppm. **$^{13}C\{^1H\}$ NMR** (C_6D_6, 75 MHz, 298.8 K): δ = 29.8 (d, $J_{C\text{–}P}$ = 15.4 Hz , $PCH(CH_3)_3$), 35.4 (d, $J_{C\text{–}P}$ = 30.9 Hz $PCH(CH_3)_3$), 128.8 (dd, arom. C), 129.2 (s, arom. C), 133.6 (t, $J_{P\text{-}C}$ = 9.6 Hz, arom. C), 138.9 (d, $J_{P\text{-}C}$ = 15.8 Hz, arom. C) ppm. **MS** (HR-EI, 70 eV, rel. int. > 10%) *m/z* calcd. (found): 430.20412 (430.20421).

3.1.3 Synthesis of $^{Ph}PSCSP^{Ph}$ (1-Ph)

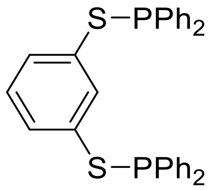

Following the general procedure (*c.f.*: 3.1), 1,3-benzenedithiol (375 mg, 2.64 mmol) was dissolved in THF (40 mL). Then NEt_3 (0.96 g, 1.31 mL, 9.45 mmol) was added to the THF solution. After the mixture was stirred for 1 h at room temperature, Ph_2PCl (1.16 g, 0.94 mL, 5.28 mmol) was added and the resulting suspension was stirred for additional 2 h at 55 °C (oil bath).
Yield: 1.28 g (2.51 mmol, 95%).

Mp. not determined. **^1H NMR** (C_6D_6, 300 MHz, 298 K): δ = 6.71 (t, $J_{H\text{-}H}$ = 7.85, 1 H, ArH_{para}), 6.99 – 7.02 (m, 4 H, PCC(*p-H*), 7.02 – 7.07 (m, 8 H, PCC(*m-H*)) ,7.31 (d, $J_{H\text{-}H}$ = 7.87 Hz, 2 H, ArH_{meta}), 7.54 – 7.60 (m, 8 H, PCC(*o-H*)) ppm. **$^{31}P\{^1H\}$ NMR** (C_6D_6, 122 MHz, 298 K): δ = 32.2 (s) ppm.

4 Synthesis of Ir PSCSP pincer complexes

4.1 Direct synthesis of 2-*i*Pr under an atmosphere of H_2

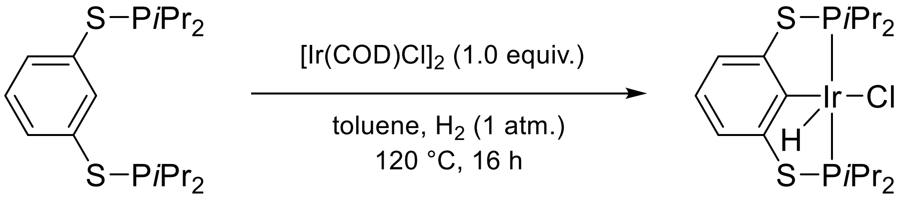

The ligand **1-*i*Pr** (315 mg, 0.84 mmol) and Ir precursor $[Ir(COD)Cl]_2$ (282 mg, 0.42 mmol) were weighed in a 50-mL Schlenk flask in the glovebox. The reaction vessel was brought outside, and the starting materials were dissolved in toluene (10 mL) at room temperature, which yielded a red-orange, clear solution after some vigorous stirring. Afterwards, the solution was degassed (3 freeze-pump-thaw-cycles) and purged with H_2 at room temperature. Then, the reaction mixture was stirred for 19 h at 120 °C (oil bath). A colour intensification of the reaction solution from red orange to dark red was observed after circa 5 min at 120 °C (oil bath). Subsequently, after the reaction ended, the solvent was completely removed *in vacuo* (10^{-3} mbar) and the resulting reddish residue was dried for 1 h under reduced pressure (10^{-3} mbar) at 40°C (water bath). The red residue was dissolved in 8 mL of dichloromethane, then cannula filtrated, yielding a clear, read filtrate and a black solid. The resulting red filtrate was concentrated to incipient crystallisation under reduced pressure (10^{-3} mbar) at 45 °C (water bath). Thereupon, the solution was stored at −40 °C overnight, yielding red orange crystals. A second fraction of crystals was obtained from the mother liquor.
Isolated yield: 218 mg (0.36 mmol, 39%).

Mp. 191 °C (decomp.). **CHN** calc. (found) in %: C 35.90 (35.63), H 5.36 (5.58), S 10.65 (10.59). **^{1}H NMR** ($CDCl_3$, 300 MHz, 298 K): δ = −37.52 (bs, 1 H, Ir-*H*), 1.21 – 1.43 (m, 24 H, $PCH(CH_3)_2$), 2.59 (bsept, 2 H, $PCH(CH_3)_2$), 3.04 (bsept, 2 H, $PCH(CH_3)_2$), 6.67 (bt, $J_{H\text{-}H}$ = 7.64 Hz, 1 H, ArH_{para}), 7.02 (bd, $J_{H\text{–}H}$ = 7.72 Hz, 2 H, ArH_{meta}) ppm. **^{31}P{^{1}H} NMR** ($CDCl_3$, 122 MHz, 298 K): δ = 88.5 (s) ppm. **^{13}C{^{1}H} NMR:** Spectrum not evaluable because of equilibrium between monomer and dimer at room temperature (also for highly concentrated NMR samples: 25 mg in 600 µL CD_2Cl_2). **IR** (ATR, 32 scans, cm^{-1}): $\tilde{\nu}$ = 2265.2 (Ir-H). **MS** (CI pos., *iso*-butane) *m/z* (%): 568 $[C_{18}H_{32}IrP_2S_2+H^+]$, 603 $[M^+ + H^+]$, 658 [M^+ + *iso*-butane].
Single crystals suitable for X-ray diffraction can be grown from saturated dichloromethane solution at −40 °C.

4.2 Synthesis of 2-*i*Pr from 3-*i*Pr

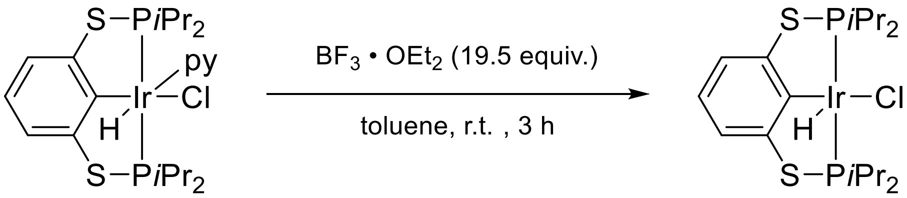

Complex **3-*i*Pr** (16.9 mg, 0.02 mmol) was weighed in a 25-mL Schlenk flask in the glovebox. Afterwards, it was dissolved in toluene (6 mL) outside the glovebox, which gave a clear, yellow solution. Then, $BF_3 \cdot Et_2O$ (55.7 mg, 0.39 mmol, 19.5 equiv.) was added to the reaction solution, which resulted in an instantaneous colour change from yellow to red. The solution was stirred for 3 h at room temperature. The solvent was completely removed *in vacuo* (10^{-3} mbar) at 44 °C (water bath) yielding a pale, off white residue. Subsequently, the residue was washed with 2 x 3 mL of dichloromethane and cannula filtrated each time, which gave a red clear filtrate. Afterwards, the filtrate was concentrated under reduced pressure and kept at −40 °C over night, yielding a microcrystalline residue from which the liquid supernatant was removed completely with a cannula frit. The product was unambiguously identified as the complex **2-*i*Pr** by ^{1}H and $^{31}P\{^{1}H\}$ NMR spectroscopy (*c.f.*: Figure S20, Figure S21).

4.3 Direct synthesis of 2-*t*Bu under an atmosphere of H_2

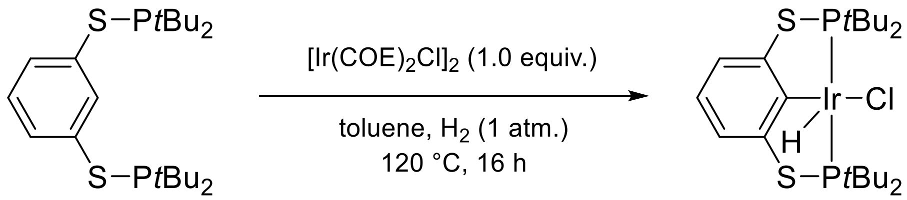

The ligand **1-*t*Bu** (146 mg, 0.34 mmol) and Ir precursor $[Ir(COE)_2Cl]_2]$ (153 mg, 0.17 mmol) were weighed in a 50-mL Schlenk flask in the glovebox. The reaction vessel was brought outside, and the starting material was dissolved in toluene (12 mL) at room temperature, which yielded an orange, clear solution after some vigorous stirring. Afterwards, the solution was degassed (1 freeze-pump-thaw-cycle) and purged with H_2 at room temperature. Then, the reaction mixture was stirred for 22 h at 120 °C (oil bath). The reaction mixture appeared dark red on the next day. After the reaction ended, the solvent was completely removed *in vacuo* (10^{-3} mbar) and the resulting black residue was dried for 30 min under reduced pressure (10^{-3} mbar) at 55°C (water bath). The black residue was washed with 3 x 10 mL of *n*-hexane and cannula filtrated, which yields a red filtrate and a black insoluble residue. All volatiles were removed from the filtrate under reduced pressure (10^{-3} mbar) at 50 °C (water bath). Finally, the obtained red

residue was dried *in vacuo* for 30 min at 50 °C (water bath), which can then be used without further purification.
Isolated yield: 144 mg (0.22 mmol, 65%). *Note: The isolated yield decreased to 53%, when using [Ir(COD)Cl]$_2$ instead of [Ir(COE)$_2$Cl]$_2$.*.

Mp. 179 °C (decomp.). **CHN** calc. (found) in %: C 40.14 (36.43), H 6.12 (7.06), S 9.74 (5.39).[a] **^{1}H NMR** (C_6D_6, 300 MHz, 298 K): δ = −41.84 (t, 1 H, $J_{P\text{-}H}$ = 12.6 Hz, Ir-*H*), 1.38 (dd, $J_{H\text{-}P}$ = 7.7 Hz, 18 H, PC(C*H*$_3$)$_3$),1.45 (dd, $J_{H\text{-}P}$ = 7.7 Hz, 18 H, PC(C*H*$_3$)$_3$), 6.53 (t, $J_{H\text{-}H}$ = 7.7 Hz, 1H, ArH$_{para}$), 7.15 (d, $J_{H\text{-}H}$ = 7.7 Hz, 2 H, ArH$_{meta}$) ppm. **^{31}P{^{1}H} NMR** (C_6D_6, 121 MHz, 298 K): δ = 94.3 (d, $J_{P\text{-}P}$ = 7 Hz) ppm. **^{13}C{^{1}H} NMR** (C_6D_6, 75.5 MHz,, 2048 scans): δ = 29.4 (t, $J_{C\text{-}P}$ = 3 Hz, PC(*C*H$_3$)$_3$), 29.9 (t, $J_{C\text{-}P}$ = 3 Hz, PC(CH$_3$)$_3$), 39.7 (t, $J_{C\text{-}P}$ = 9 Hz, PC(CH$_3$)$_3$), 42.8 (t, $J_{C\text{-}P}$ = 9 Hz, PC(CH$_3$)$_3$), 118.7 (t, $J_{C\text{-}P}$ = 5 Hz, ArC$_{meta}$), 123.7 (s, ArC$_{para}$), 128.4 (s, ArC$_{ortho}$), 129.2 (s, ArC$_{ipso}$) ppm. **IR** (ATR, 32 scans, cm^{-1}): $\tilde{\nu}$ = 1933.0 (Ir-H). **MS** (CI+, *iso*-butane): 431 [^{tBu}PSCSP]$^+$, 623 [^{tBu}PSCSPIr(H)]$^+$, 658 [M$^+$], 715 [^{tBu}PSCSPIr(H)(Cl) + *iso*-butane]$^+$.
Single crystals suitable for X-ray diffraction can be grown from saturated toluene solution at −30 °C.

4.4 Synthesis of 2-*t*Bu under reflux in mesitylene

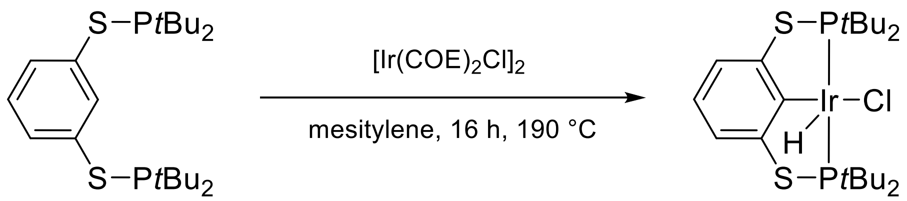

In a 25 mL three necked round bottom flask with gas inlet tube and Dimroth condenser, [Ir(COE)$_2$Cl]$_2$ (1.00 g, 1.12 mmol) and ligand **1-*t*Bu** (960 mg, 2.23 mmol) were placed in the glovebox. After the reaction apparatus was brought outside the box, it was connected to the Schlenk line and equipped with an over pressure valve. Subsequently, the starting materials were dissolved in mesitylene (15 mL) giving an orange, turbid solution. Then, the reaction mixture was stirred over night for ca. 18 h at 190 °C (oil bath). After approximately 10 min a colour intensification from orange to dark red could be observed. A brown, turbid reaction mixture was observed the next day from which the solvent was completely removed *in vacuo* (10^{-3} mbar). The obtained brown residue was dried for at least 1 h at 50 °C (water bath) under vacuum (10^{-3} mbar). The residue was washed with 4 x 15 mL of *n*-hexane, yielding a brown insoluble residue and a red, clear filtrate. Removal of solvent from the filtrate gave a red brown residue. This

[a] Despite several attempts, no valid results for elemental analysis were obtained.

residue was washed twice with small (1 mL) portions of cold (ice bath) *n*-pentane to furnish the desired Ir complex.
Isolated yield: 271 mg (0.41 mmol, 18%).

For analytical data: *c.f.* 4.3.

4.5 Synthesis of 4

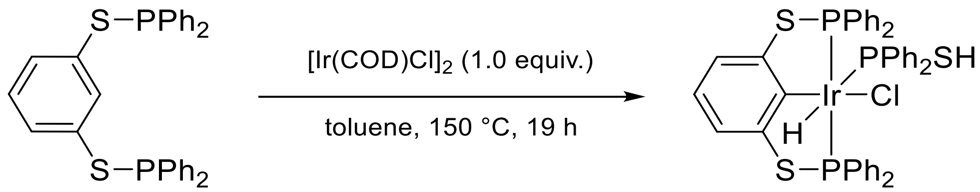

In a 25-mL Schlenk flask **1-Ph** (153 mg, 0.30 mmol) and $[Ir(COD)Cl]_2$ (100 mg, 0.15 mmol) were placed in the glovebox. The starting materials were dissolved in 10 mL of toluene. The orange solution was heated to reflux (oil bath, 150 °C) for 19 h and then cooled to room temperature. The solvent was removed *in vacuo* (10^{-3} mbar) and the resulting brown residue was dried for at least 30 min.
Isolated yield: Not determined, since experiment was poorly reproducible.

Mp. 223 °C (decomp.). **CHN** calc. (found) in %: C 52.74 (51.63), H 3.69 (3.25), S 10.06 (4.73).[b] **^{1}H NMR** (C_6D_6, 300 MHz, 298 K): δ = −9.07 (dt, $J_{P\text{-}H/trans}$ = 189 Hz, $J_{P\text{-}H/cis}$ = 17 Hz, 1 H, Ir-*H*), 1.37 (broad s, 1 H, S*H*), 6.74 – 6.84 (m, 10 H, Ar*H*), 6.85 – 6.95 (m, 9 H, Ar*H*), 7.21 (d, *J* = 7.7 Hz, 2 H, ArH_{meta}), 7.29 – 7.40 (m, 4 H, Ar*H*), 8.01 – 8.19 (m, 8 H, Ar*H*) ppm. **^{31}P{^{1}H} NMR** ($CDCl_3$, 121 MHz, 298 K): δ = 27.3 (d, $J_{P\text{–}P}$ = 17 Hz, 2 P, *cis-P*), 57.9 (m, 1 P, *trans-P*) ppm. **^{31}P NMR** ($CDCl_3$, 121 MHz, 298 K): δ = 27.3 (s, 2 P, *cis-P*), 57.9 (d, $J_{P\text{–}H}$ = 189 Hz, 1 P, *trans-P*) ppm. **^{13}C{^{1}H} NMR** (tol-d_8, 101 MHz, 297 K): δ = 119.3 (t, $J_{C\text{-}P}$ = 7 Hz, 2 C, ArC_{meta}), 124.0 (s, 1 C, ArC_{para}), 127.5 (d, $J_{C\text{-}P}$ = 10 Hz, 4 C, Ar*C*), 128.0 (d, $J_{C\text{-}P}$ = 5 Hz, 6 C, Ar*C*), 128.1 (s, 4 C, Ar*C*), 128.5 (s, 5 C, Ar*C*), 130.1 (bs, 6 C, Ar*C*), 132.8 (d, $J_{C\text{-}P}$ = 13 Hz, 4 C, Ar*C*), 133.0 (t, $J_{C\text{-}P}$ = 6 Hz, 9 C, Ar*C*), 150.6 (t, 1 C, ArC_{ipso}) ppm. **IR** (ATR, 32 scans, cm^{-1}): $\tilde{\nu}$ = 2098.3 (Ir-H), 2325.0 (S-H).
Single crystals suitable for X-ray diffraction can be grown from saturated benzene solution over night at 8 °C.

[b]Despite several attempts, no valid results for elemental analysis were obtained.

4.6 Synthesis of 3 -*i*Pr

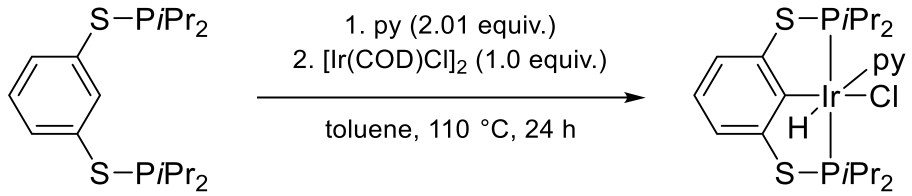

The synthesis was carried out after a slightly modified literature procedure.[7]

In a three-necked round bottom flask with a Dimroth condenser with over pressure valve on top and gas inlet tube, was placed $[Ir(COD)Cl]_2$ (202 mg, 0.30 mmol) in the glove box. The ligand **1-*i*Pr** (223 mg, 0.60 mmol) was weighed in a separate 25-mL Schlenk tube in the glovebox. The glassware was brought outside the glove box and the Ir precursor and the ligand were dissolved in toluene (10 mL and 6 mL, respectively), which yielded clear, red and colourless solutions, respectively. Subsequently, pyridine (108 mg, 110 µL,1.37 mmol) was added to the Ir precursor. The solution immediately turned yellow after base addition. *Note: The order of base addition is crucial! Otherwise, only ill-defined reaction mixtures were obtained.* The ligand solution was cannula transferred to the reaction solution, Causing an immediate colour change to red orange. The condenser was equipped with an over pressure valve prior to refluxing the solution under an atmosphere of argon for 24 h at 110 °C (oil bath). The following day, the yellow orange reaction mixture was cooled to room temperature and the solvent was completely removed *in vacuo* (10^{-3} mbar). The yellow orange residue was dried for 30 min at room temperature. Then the crude product was dissolved in 10 mL of dichloromethane. The resulting yellow orange solution was filtered over a plug of celite. The clear orange filtrate was concentrated *in vacuo* and layered with *n*-pentane. Yellow crystals were grown from this solution at −30 °C over night. The supernatant was removed and was layered again with *n*-pentane. This yielded a second fraction of crystals.

Isolated yield: 181 mg (0.27 mmol, 44%).

Mp. 208.6 °C (decomp.). **CHN** calc. (found) in %: C 40.55 (37.23), H 5.47 (6.87), N 2.06 (0.74), S 9.41 (5.87).[c] **^{1}H NMR** (C_6D_6, 400 MHz, 297 K): δ = −20.41 (t, $J_{H\text{-}P}$ = 16.7 Hz, 1 H, Ir-*H*), 0.87 (dd, $J_{H\text{-}H}$ = 7.0 Hz, $J_{H\text{-}P}$ = 7.0 Hz, 6 H, PCH(CH_3)$_2$), 0.92 (dd, $J_{H\text{-}H}$ = 7.1 Hz, $J_{H\text{-}P}$ = 7.1 Hz, 6 H ,PCH(CH_3)$_2$), 1.26 (dd, $J_{H\text{-}H}$ = 6.9 Hz, $J_{H\text{-}P}$ = 6.9 Hz, 6 H, PCH(CH_3)$_2$), 1.49 (dd, $J_{H\text{-}H}$ = 6.9 Hz, $J_{H\text{-}P}$ = 6.9 Hz,6 H, , PCH(CH_3)$_2$), 2.34 (sept, $J_{H\text{-}H}$ = 7.1 Hz, $J_{H\text{-}P}$ = 7.1 Hz, 2 H, PC*H*(CH_3)$_2$), 2.44 (sept, $J_{H\text{-}H}$ = 6.9 Hz, $J_{H\text{-}P}$ = 6.9 Hz, 2 H, PC*H*(CH_3)$_2$), 6.38 (broad s, 2 H,

[c] Despite several attempts, no satisfactory results for elemental analyses were obtained for the recrystallised product.

pyH$_{meta}$), 6.66 (t, $J_{H\text{-}H}$ = 7.7 Hz, 1 H, ArH$_{para}$), 6.72 (broad t, $J_{H\text{-}H}$ = 7.6 Hz, 1 H, pyH$_{para}$), 7.25 (d, $J_{H\text{-}H}$ = 7.7 Hz, 2 H, ArH$_{meta}$), pyH$_{ortho}$ very broad signals at 8.32 and 10.26 ppm (hindered rotation about the Ir-N-axis). **^{31}P{^{1}H} NMR** (C_6D_6, 162 MHz, 297 K): δ = 66.8 (d, $J_{P\text{-}P}$ = 14 Hz) ppm. **^{13}C{^{1}H} NMR** (C_6D_6, 101 MHz, 298 K): δ = 18.2 (s, PCH(CH_3)$_2$), 18.3 (s, PCH(CH_3)$_2$), 18.6 (s, PCH(CH_3)$_2$), 19.2 (s, PCH(CH_3)$_2$), 28.4 (t, $J_{C\text{-}P}$ = 11 Hz, PCH(CH_3)$_2$), 30.1 (t, $J_{C\text{-}P}$ = 14 Hz, PCH(CH_3)$_2$), 119.7 (t, $J_{C\text{-}P}$ = 5 Hz, ArC$_{meta}$), 123.5 (s, ArC$_{para}$), 124.6 (broad s, pyC$_{meta}$);136.5 (s, pyC$_{para}$), 150.9 (s, ArC$_{ortho}$), 152.4 (s, pyC$_{ortho}$) ppm (ArC$_{ipso}$ carbon could not be detected). **IR** (ATR, 32 scans, cm^{-1}): $\tilde{\nu}$(Ir-H) = 2219.9. **MS** (CI+, *iso*-butane): 567 [(^{iPr}PSCSP)Ir(H)]$^+$, 602 [(^{iPr}PSCSP)Ir(H)(Cl)]$^+$, 646 [(^{iPr}PSCSP)Ir(Cl)]$^+$, 682 [M$^+$ + H]$^+$.

4.7 Synthesis of 3-*i*Pr from 2-*i*Pr

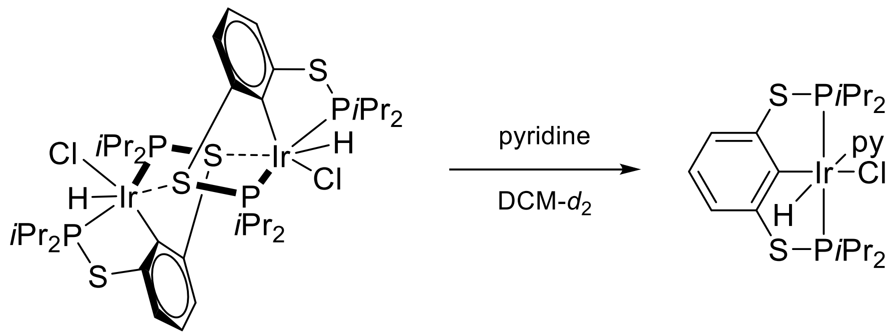

To a solution of **2-*i*Pr** in deuterated dichloromethane (0.4 mL) in a J-Young NMR tube was added pyridine (0.2 mL). An immediate colour change from red to yellow was observed. NMR spectroscopy of the yellow solution revealed formation of the known pyridine complex **3-*i*Pr** (*c.f.* Figure S31, Figure S32).

4.8 Synthesis of 3-Ph

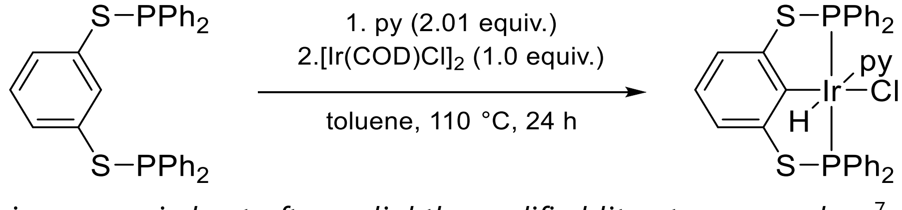

The synthesis was carried out after a slightly modified literature procedure.[7]

In a three-necked round bottom flask with a Dimroth condenser with over pressure valve on top and gas inlet tube, was placed [Ir(COD)Cl]$_2$ (219 mg, 0.33 mmol) in the glove box. The ligand **1-Ph** (332 mg, 0.65 mmol) was weighed in a 25-mL Schlenk tube in the glovebox. The glassware was brought outside the glove box and the Ir precursor and the ligand were dissolved in toluene (10 mL and 6 mL, respectively), which yielded clear, red and colourless solutions, respectively. Subsequently, pyridine (62 mg, 63 µL,

0.8 mmol) was added to the Ir precursor. The solution immediately turned yellow after base addition. *Note: The order of base addition is crucial! Otherwise, only ill-defined reaction mixtures were obtained.* The ligand solution was cannula transferred to the reaction solution, causing an immediate colour change to red orange. The condenser was equipped with an over pressure valve prior to refluxing the solution under an atmosphere of argon for 24 h at 110 °C (oil bath). After approximately 15 min a colour intensification from red orange to dark red was observed. Moreover, a precipitate on the wall of the reaction vessel was observed after 1 h. The following day, the orange reaction mixture was cooled to room temperature and the solvent was completely removed *in vacuo* (10^{-3} mbar). The orange crude product was dried for 30 min at room temperature and dissolved in 7 mL of dichloromethane. The resulting orange solution was cannula filtered, giving a clear orange solution, which was concentrated *in vacuo* (10^{-3} mbar) and stored at −30 °C. After 48 h orange crystals suitable for single crystal X-Ray diffraction analysis could be isolated.
Isolated yield: 255 mg (0.31 mmol, 48%).

Mp. 210 °C (decomp.). **CHN** calc. (found) in %: C 51.43 (51.56), H 3.58 (3.73), N 1.71 (1.41), S 7.84 (7.64). **^{1}H NMR** (CD_2Cl_2, 300 MHz, 302 K): δ = −19.30 (t, $J_{H\text{-}P}$ = 15.2 Hz, 1 H, Ir-*H*), 5.33 (s, CH_2Cl_2 from crystal), 6.60 (t, 2 H, $J_{H\text{-}H}$ = 6.5 Hz, pyH$_{meta}$), 6.78 (t, $J_{H\text{-}H}$ = 7.7 Hz, 1 H, ArH$_{para}$), 6.98 – 7.06 (m, 5 H, Ph*H*), 7.13 (d, $J_{H\text{-}H}$ = 7.7 Hz, 2 H, ArH$_{meta}$), 7.28 (t, $J_{H\text{-}H}$= 7.6 Hz, 1 H, pyH$_{para}$),7.35 – 7.44 (m, 5 H, Ph*H*), 7.47 – 7.53 (m, 6 H, Ph*H*), 7.94 (broad d, $J_{H\text{-}H}$ = 5.4 Hz, 2 H, pyH$_{ortho}$), 8.05 – 8.14 (m, 4 H, Ph*H*) ppm. **^{31}P{^{1}H} NMR** (CD_2Cl_2, 122 MHz, 302 K): δ = 40.4 (s) ppm. **^{13}C{^{1}H} NMR** (CD_2Cl_2, 75.5 MHz, 302 K): δ = 119.6 (t, ArC$_{meta}$), 123.4 (s, ArC$_{para}$), 124.7 (s, pyC$_{meta}$), 127.9 (t, $J_{C\text{-}P}$ = 5 Hz, Ph*C*), 128.8 (t, $J_{C\text{-}P}$ = 6 Hz, Ph*C*), 130.1(s, PhC$_{quart}$), 131.4 (s, Ph*C*), 132.1 (t, $J_{C\text{-}P}$ = 6 Hz, Ph*C*), 134.5 (t, $J_{C\text{-}P}$ = 7 Hz, Ph*C*),135.6 (s, pyC$_{para}$),150.5 (s, ArC$_{ortho}$), 151.0 (s, pyC$_{ortho}$), 156.8 (s, ArC$_{ipso}$) ppm. **IR** (ATR, 32 scans, cm^{-1}): $\tilde{\nu}$ = 2189.0 (Ir-H). **MS** (CI+, *iso*-butane): 80 [py + H]$^{+}$, 567 [^{Ph}PSCSP + *iso*-butane]$^{+}$, molecular ion peak could not be found.
Single crystals suitable for X-Ray diffraction analysis can be grown from saturated dichloromethane solutions at −30 °C.

4.9 Synthesis of 5

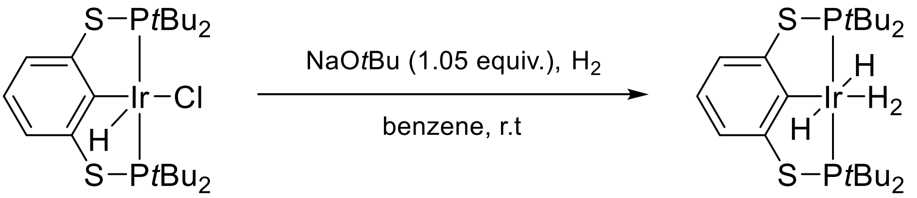

Complex **2-*t*Bu** (18.7 mg, 28.4 µmol) and NaO^{t}Bu (2.9 mg, 29.8 µmol) were weighed in a Young-NMR tube and dissolved in C_6D_6 (0.6 mL). The reaction mixture was degassed (three freeze-pump-thaw cycles) and frozen at −78°C. Afterwards the solution was purged with H_2 gas. The mixture was allowed to warm to room temperature under vigorous shaking. The purging cycle was repeated at least five times. During this a colour change from red to yellow was observed. ^{1}H NMR monitoring of the reaction solution shows a broad singlet at −8.49 ppm, corresponding to complex **5**. Removing the solvent *in vacuo*, results in the formation of **6**.

^{1}H NMR (C_6D_6, 400 MHz, 298 K): δ = −8.49 (br. s, 4 H), 1.32 (t, $J_{P\text{-}H}$ = 7.6 Hz, 36 H, 2x PC(CH_3)$_3$), 6.73 (t, $J_{H\text{-}H}$ = 7.7 Hz, 1 H, ArH$_{para}$), 7.27 (d, $J_{H\text{-}H}$ = 7.7 Hz, 2 H, ArH$_{ortho}$) ppm.
^{31}P{H} NMR (C_6D_6, 122 MHz, 298 K): δ = 106.7 (s) ppm.

4.10 Synthesis of 6

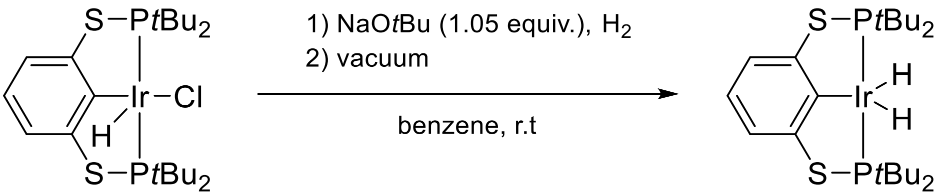

Complex **2-*t*Bu** (60.0 mg, 91.1 µmol) and NaO^{t}Bu (9.20 mg, 95.7 µmol) were weighed in a 50-mL Schlenk flask in the glovebox. The starting material was dissolved in benzene (8 mL) and the solution was degassed (three freeze-pump-thaw cycles). Then the reaction mixture was frozen at −78°C, vacuum was applied, followed by purging with H_2 gas. The mixture was then allowed to warm to room temperature under vigorous stirring. The purging cycle was repeated at least three times. After the reaction, the solvent was removed *in vacuo* (10^{-3} mbar) and the resulting brown residue was extracted with pentane (3 x 6 mL) and cannula filtered, which yields a yellow-brown filtrate. All volatiles were removed from the filtrate under reduced pressure (10^{-3} mbar), the residue was washed with cold pentane (2 x 1.5 mL, −78 °C) and dried *in vacuo*. The product was obtained as a red solid.
Isolated yield: 44.4 mg (71.2 µmol, 78%).

Mp. 174 °C (decomp.). **CHN** calc. (found) in %: C 42.36 (42.76), H 6.62 (6.80), S 10.28 (10.10). **^{1}H NMR** (CD_2Cl_2, 400 MHz, 298 K): δ = −23.2 (t, $J_{P\text{-}H}$ = 13.5 Hz, 2 H, Ir-*H*), 1.40 (t, $J_{P\text{-}H}$ = 7.5 Hz, 36 H, 2x PC(CH_3)$_3$), 6.75 (t, $J_{H\text{-}H}$ = 7.7 Hz, 1 H, ArH_{para}), 7.24 (d, $J_{H\text{-}H}$ = 7.7 Hz, 2 H, ArH_{ortho}) ppm. **^{31}P{H} NMR** (C_6D_6, 122 MHz, 298 K): δ = 126.4 (s) ppm. **^{13}C{^{1}H} NMR** (CD_2Cl_2, 101 MHz, 298 K, 2048 scans): 29.5 (t, $J_{C\text{-}P}$ = 3.2 Hz, PC(CH_3)$_3$), 40.3 (t, $J_{C\text{-}P}$ =9.1 Hz, PC(CH_3)$_3$), 116.5 (t, $J_{C\text{-}P}$ = 5.4 Hz, ArC_{meta}), 125.5 (s, ArC_{para}), 159.9 (t, $J_{C\text{-}P}$ = 9.6 Hz). **IR** (ATR, 32 scans, cm^{-1}): $\tilde{\nu}$ = 1915 cm^{-1} (Ir−H).

T_1 Experiment:

Table S3. Spectroscopic data for Ir hydride complexes **2-*t*Bu**, **5**, and **6**.

complex	^{1}H NMR (400 MHz, C6D6)		
	$\delta_{M\text{-}H}$ [ppm]	$J_{P\text{-}H}$ [Hz]	T_1
2-*t*Bu	−41.8	12.5	1.70 s
5	−8.49	–	318 ms
6	−23.1	13.7	1.03 s

5 Catalytic and thermal stability tests with Ir hydrides

5.1 Catalytic tests in transfer dehydrogenation

All transfer dehydrogenation experiments were carried out according to slightly modified literature procedures.[8, 9]

All catalytic tests were carried out in 50-mL Schlenk tubes closed with Teflon screw caps, heated three times *in vacuo* using a heat gun and cooled under argon atmosphere prior to use. The tubes were placed in cavities of a heated metal block at 200 °C. Starting materials were weighed in the glovebox and transferred into 50-mL Schlenk tubes. After the desired reaction time, the reaction vessel was removed from the aluminium block and cooled under an argon atmosphere. Aliquots of the reaction mixture were taken into the glovebox and analysed by ^{1}H NMR spectroscopy. Three ^{1}H NMR spectra were recorded (all from the same stock solution) to determine the TON at a given time. TONs were calculated from the ratio of the integrals of the olefinic COE and TBE signals. The complex **2-*i*Pr** was found to be unstable at 200 °C in the presence of base, so it was not tested further in transfer dehydrogenation (*c.f.* 5.2).

Complexes **2-*t*Bu** (COA (4.71 g, 42.0 mmol, 3000 equiv.), TBE (3.54 g, 42.1 mmol, 3000 equiv.), cat. (9.7 mg, 15 µmol, 1.1 equiv.), NaOtBu (2.3 mg, 24 µmol, 1.6 equiv.)) and **6** (COA (2.70 g, 24.1 mmol, 3000 equiv.), TBE (2.02 g, 24.0 mmol, 3000 equiv.), cat. (6.3 mg, 10 µmol, 1.0 equiv.), no base used), showed no conversion in transfer dehydrogenation of COA.

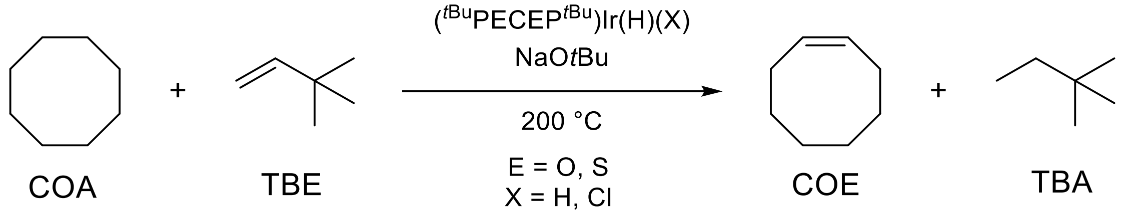

5.2 Thermal stability tests of bis(thiophosphinite) complexes

No conversion could be observed for the bis(thio)phosphinito complex **2-*t*Bu** in several attempts using different reaction conditions (NaO*t*Bu instead of KO*t*Bu, COA:TBE (3:1)). Hence, the thermal stability of **2-*t*Bu** against decomposition at 200 °C in the presence of NaO*t*Bu was tested in an NMR scaled experiment: Complex **2-*t*Bu** (9.0 mg, 14 µmol) and NaO*t*Bu (2.6 mg, 27 µmol) were weighed in a J-Young NMR tube and dissolved in toluene-d_8 (600 µL) in the glovebox, which yielded a red, clear solution. The NMR tube was taken outside the glovebox and was placed in a cavity of a heating block at 200 °C for 2 h 25 min (Figure S1, Figure S2). After 5 min the rection mixture turned black and

turbid.
A similar experiment was carried out for **2-*i*Pr** (10 mg, 8.3 µmol) with NaO*t*Bu (2.4 mg, 24.9 µmol) in toluene-d_8 (600 µL). In contrast to the above-mentioned experiment, a colour intensification from red to dark red was observed immediately after solvent addition. The J-Young NMR tube was taken outside the glovebox and kept in an ultrasonic bath for 10 min to ensure proper mixing of the starting materials. The solution turned purple, after measurement of ^{1}H and ^{31}P{^{1}H} NMR spectra at room temperature, (Figure S3, Figure S4). Afterwards the NMR tube was kept at 200 °C in a cavity of a heating block for 2 h 40 min. After that, the reaction mixture turned also black and turbid (Figure S5, Figure S6).
In contrast to bis(thio)phosphinito Ir complexes, BROOKHARTs complex **7** (10 mg, 16 µmol) showed just partial decomposition at 200 °C after 24 h in the presence of NaO*t*Bu (3.5 mg, 37 µmol) (Figure S7, Figure S8).

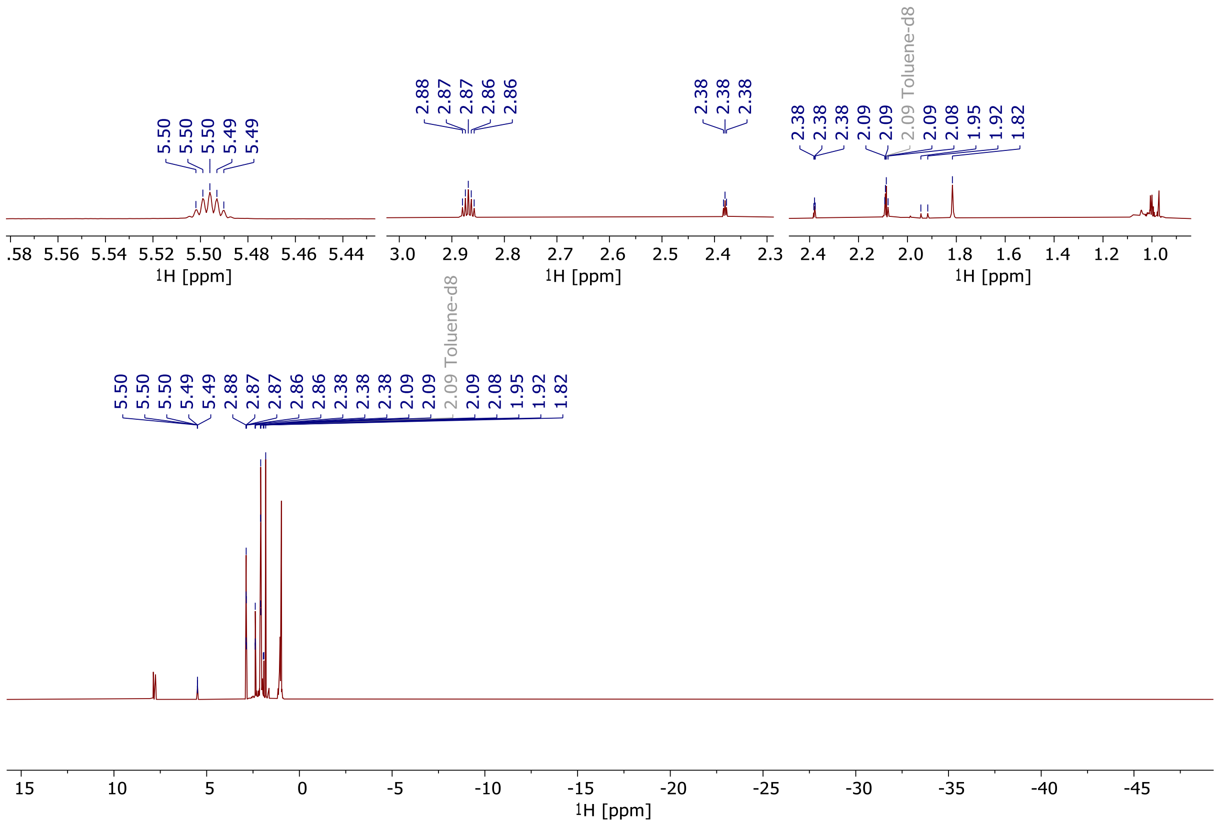

Figure S1. ^{1}H NMR spectrum (toluene-d_8, 400 MHz, 297 K) of **2-*t*Bu** in the presence of NaO*t*Bu at 200 °C after 2 h 25 min.

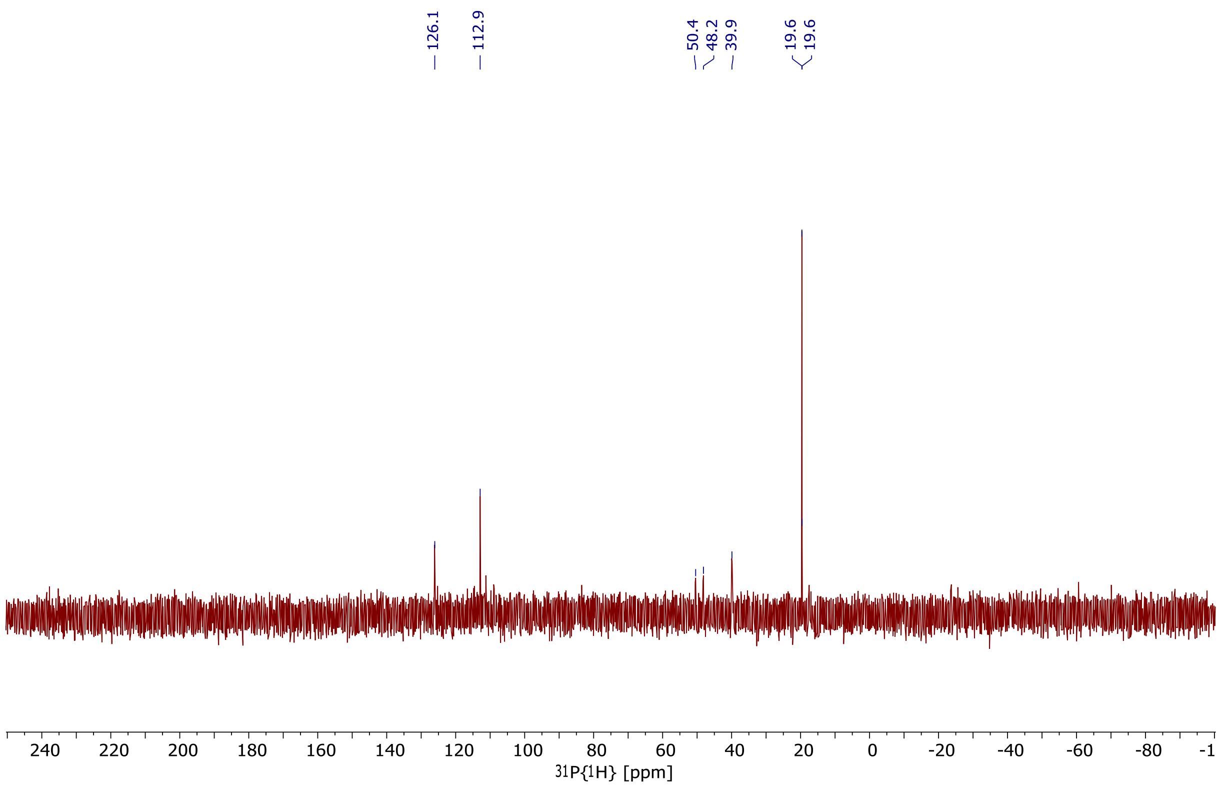

Figure S2. ^{31}P{^{1}H} NMR spectrum (toluene-d_8, 162 MHz, 297 K) of **2-*t*Bu** in the presence of NaO*t*Bu at 200 °C after 2 h 25 min.

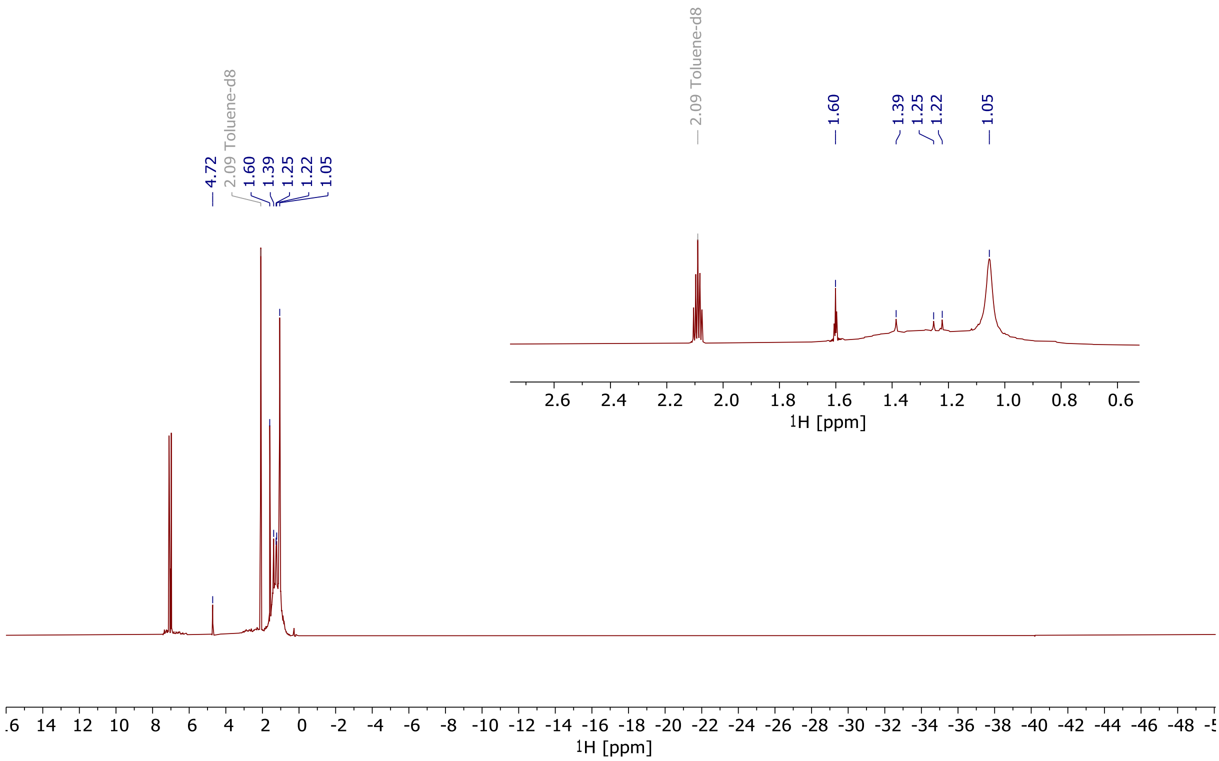

Figure S3. ^{1}H NMR spectrum (toluene-d_8, 300 MHz, 298 K) of **2-*i*Pr** in the presence of NaO*t*Bu at room temperature.

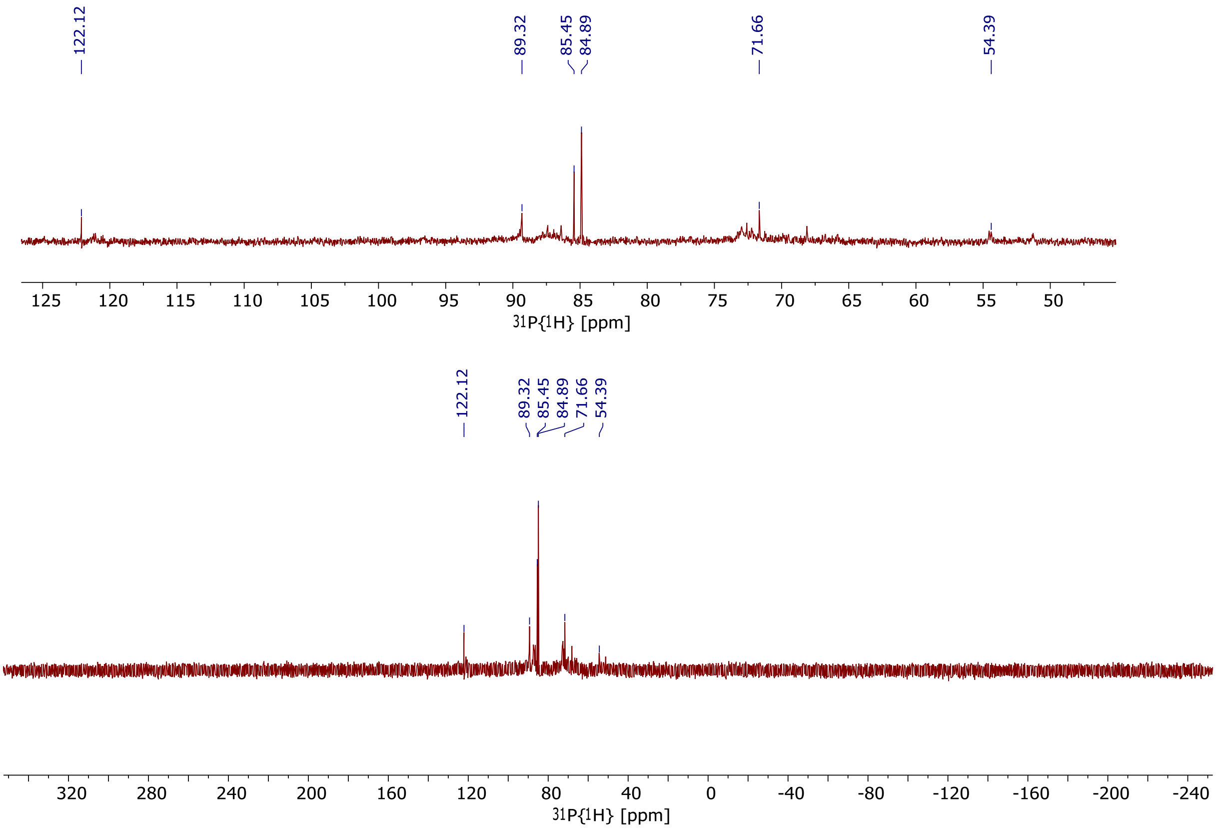

Figure S4. ^{31}P{^{1}H} NMR spectrum (toluene-d_8, 122 MHz, 298 K) of **2-*i*Pr** in the presence of NaO*t*Bu at room temperature.

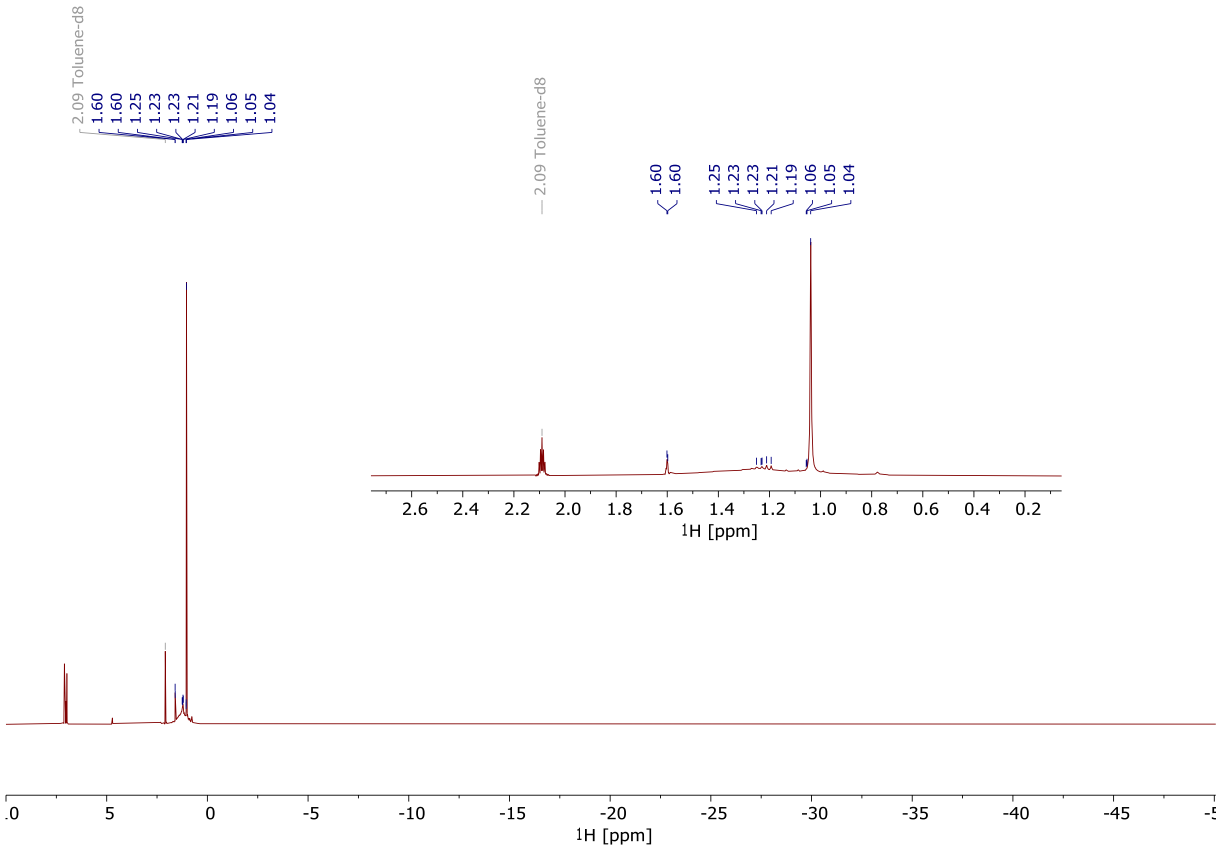

Figure S5. ^{1}H NMR spectrum (toluene-d_8, 400 MHz, 297 K) of **2-*i*Pr** in the presence of NaO*t*Bu at 200 °C after 2 h 40 min.

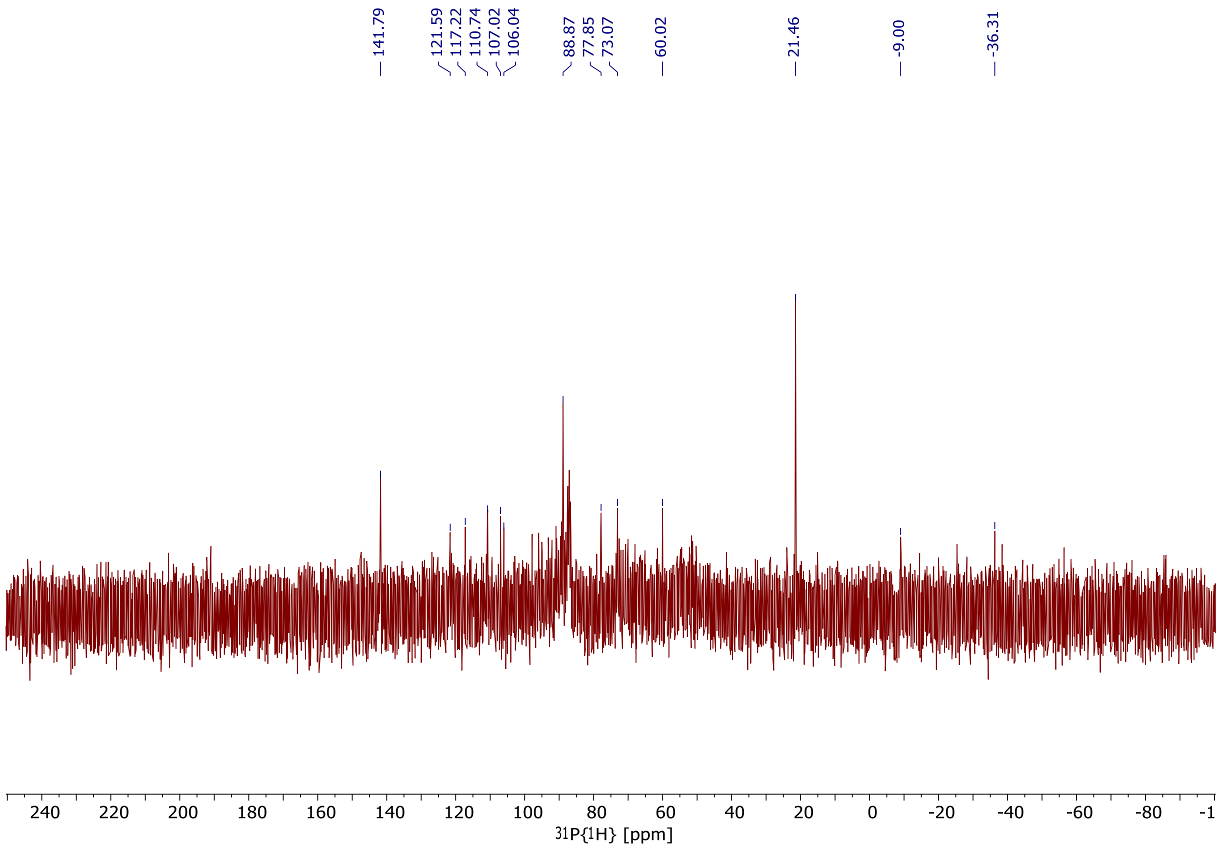

Figure S6. ^{31}P{^{1}H} NMR spectrum (toluene-d_8, 162 MHz, 297 K) of **2-*i*Pr** in the presence of NaO*t*Bu at 200 °C after 2 h 40 min.

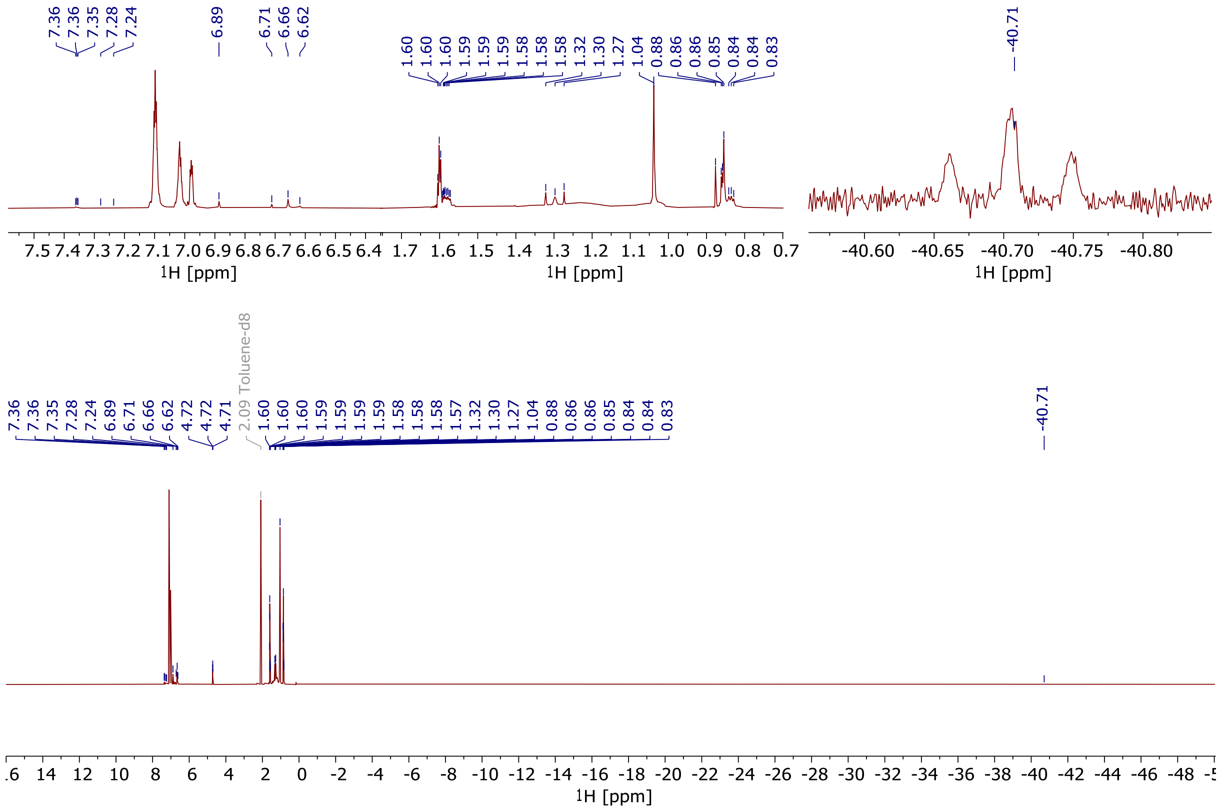

Figure S7. ^{1}H NMR spectrum (toluene-d_8, 300 MHz, 298 K) of complex **7** in the presence of NaO*t*Bu after 24 h at 200 °C.

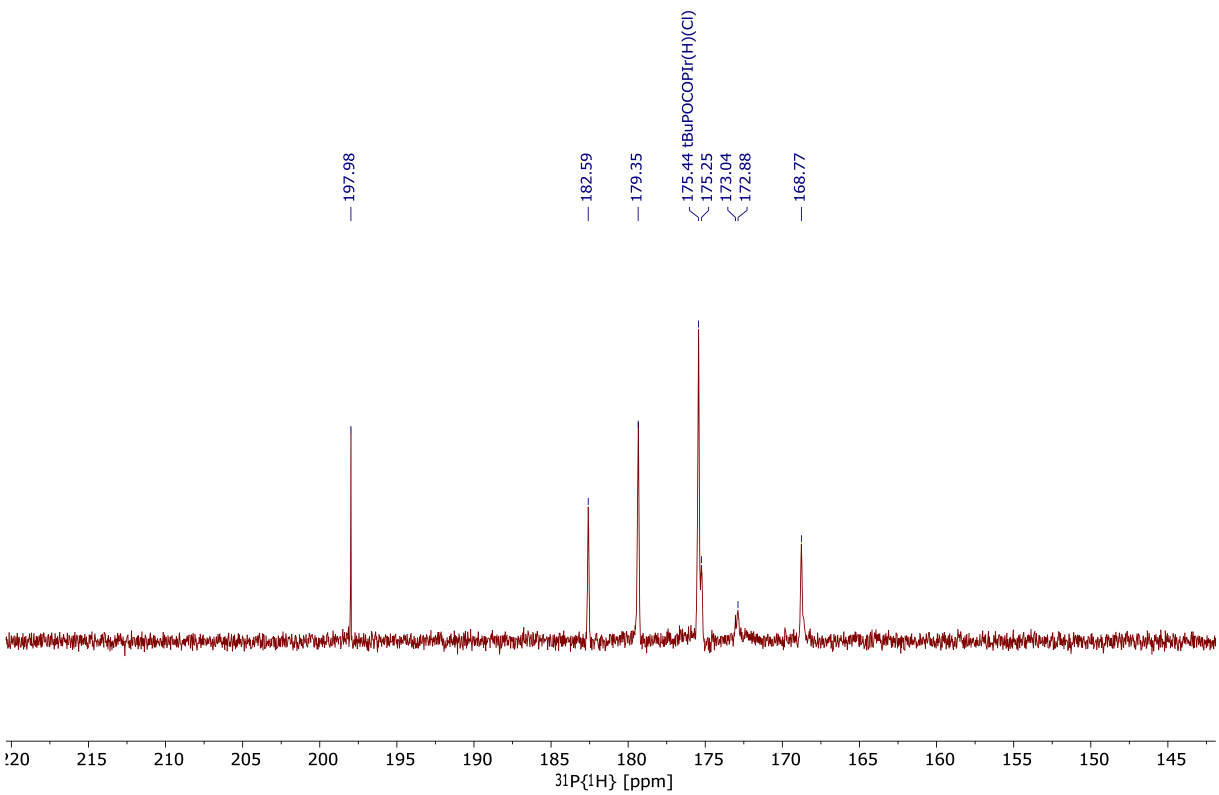

Figure S8. $^{31}P\{^{1}H\}$ NMR spectrum (toluene-d_8, 300 MHz, 122 K) of complex **7** in the presence of NaO*t*Bu after 24 h at 200 °C.

6 NMR Spectra

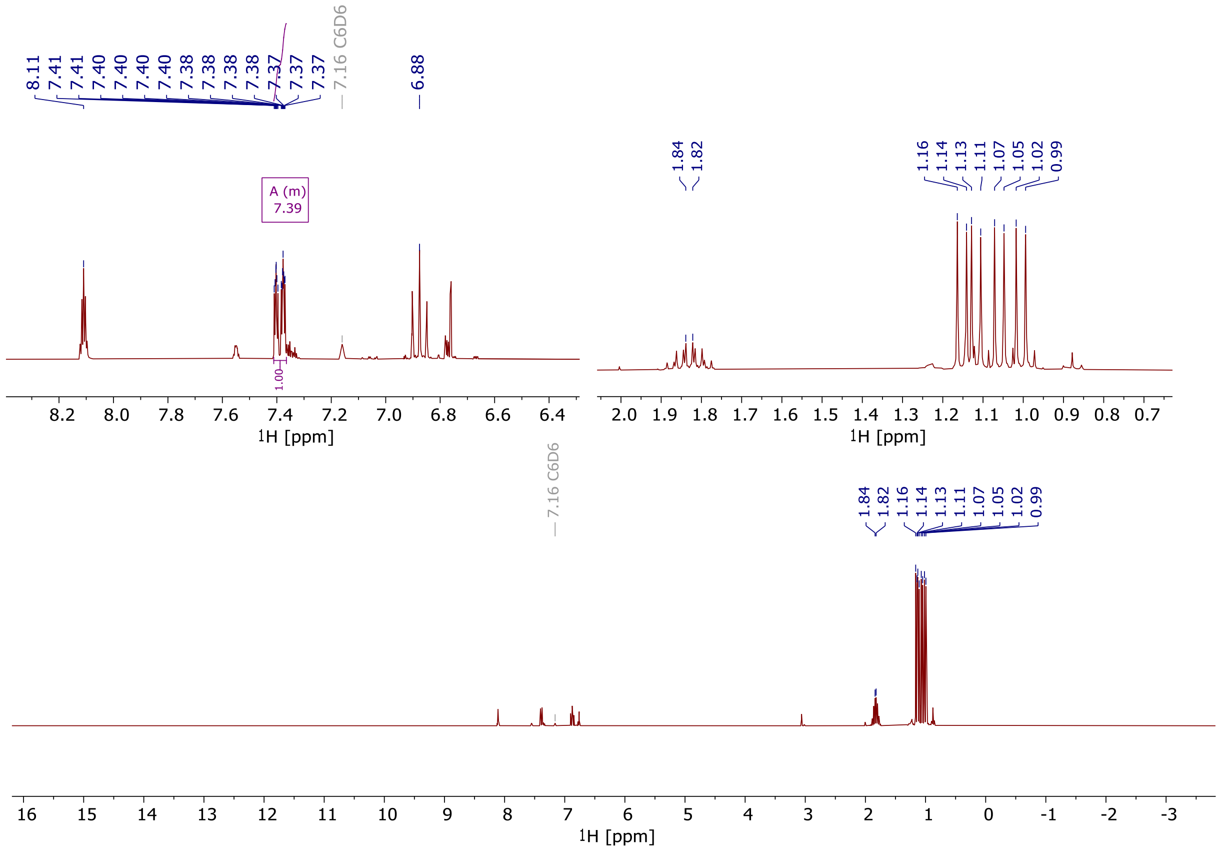

Figure S9. ^{1}H NMR spectrum (benzene-d_6, 300 MHz, 298 K) of ligand **1-*i*Pr**.

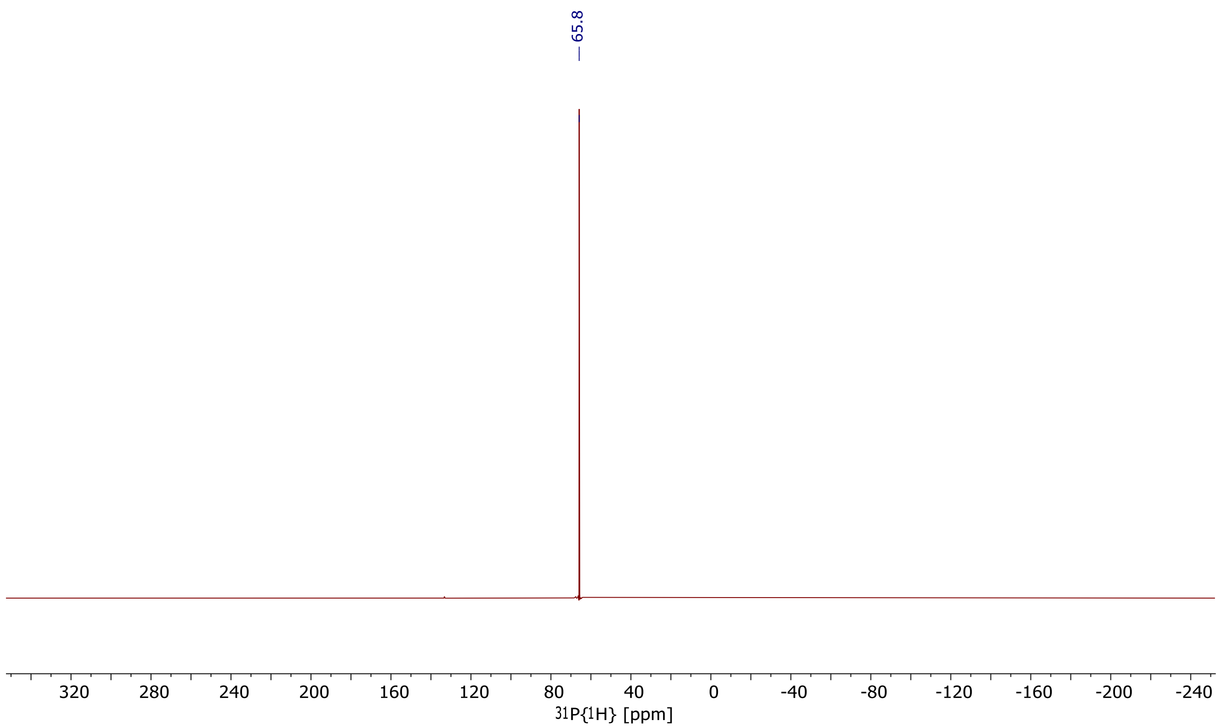

Figure S10. ^{31}P{^{1}H} NMR spectrum (benzene-d_6, 122 MHz, 298 K) of ligand **1-*i*Pr**.

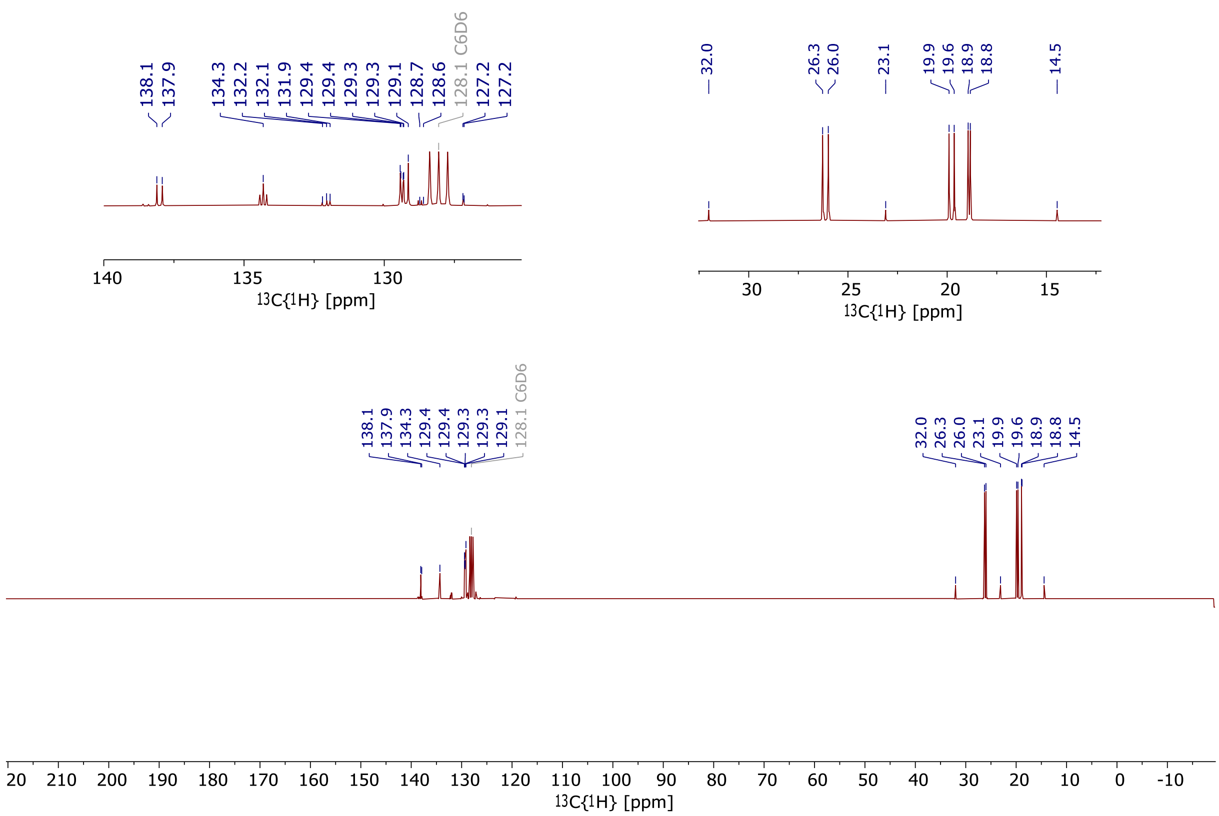

Figure S11. ^{13}C{^{1}H} NMR spectrum (benzene-d_6, 75 MHz, 298 K) of ligand **1-*i*Pr**.

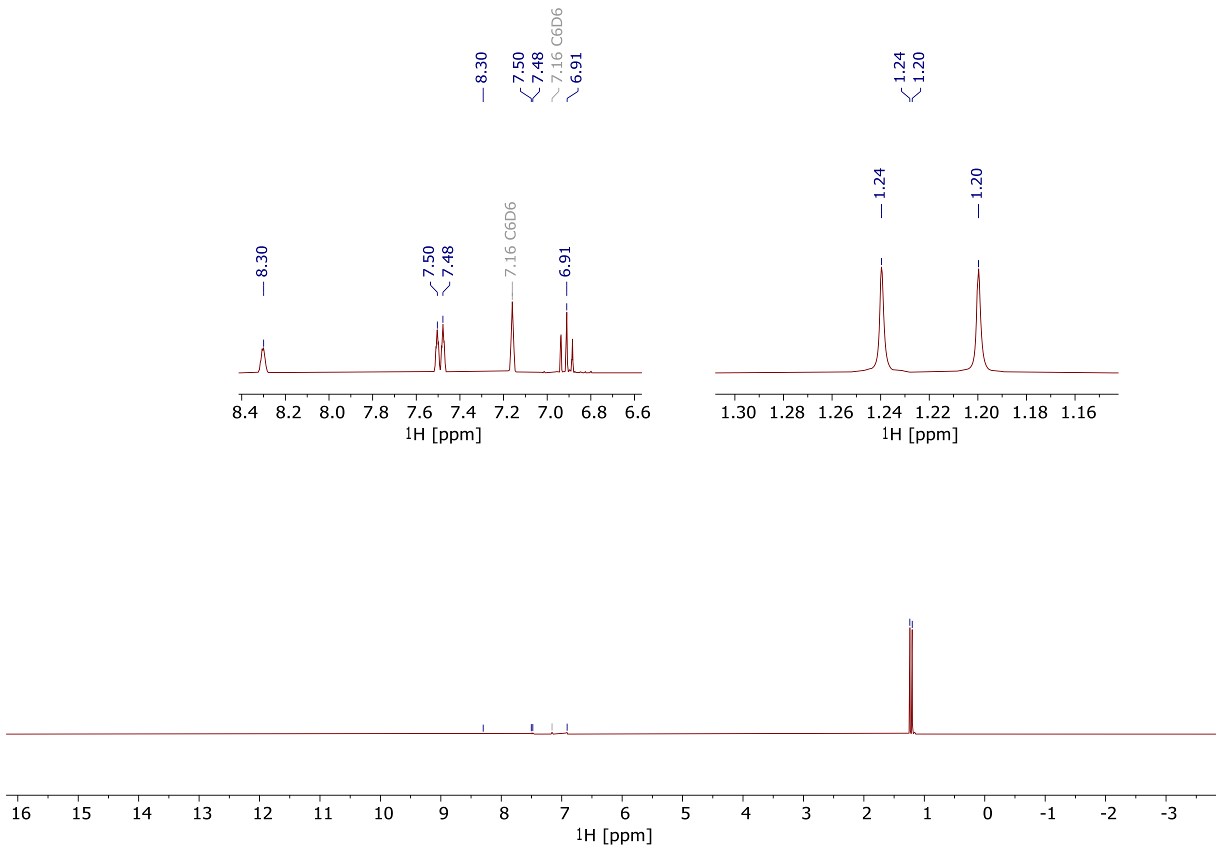

Figure S12. ^{1}H NMR spectrum (benzene-d_6, 300 MHz, 298 K) of ligand **1-*t*Bu**.

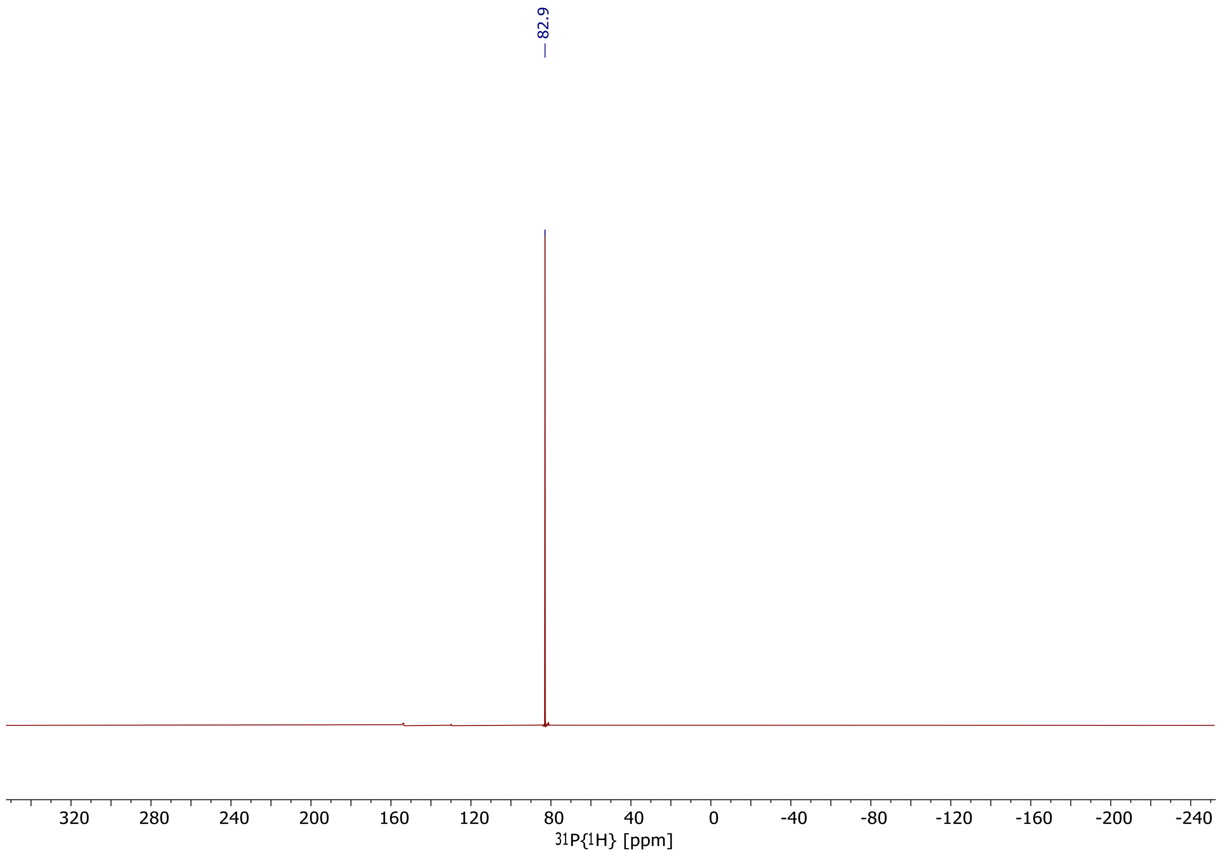

Figure S13. $^{31}P\{^{1}H\}$ NMR spectrum (benzene-d_6, 122 MHz, 298 K) of ligand **1-*t*Bu**.

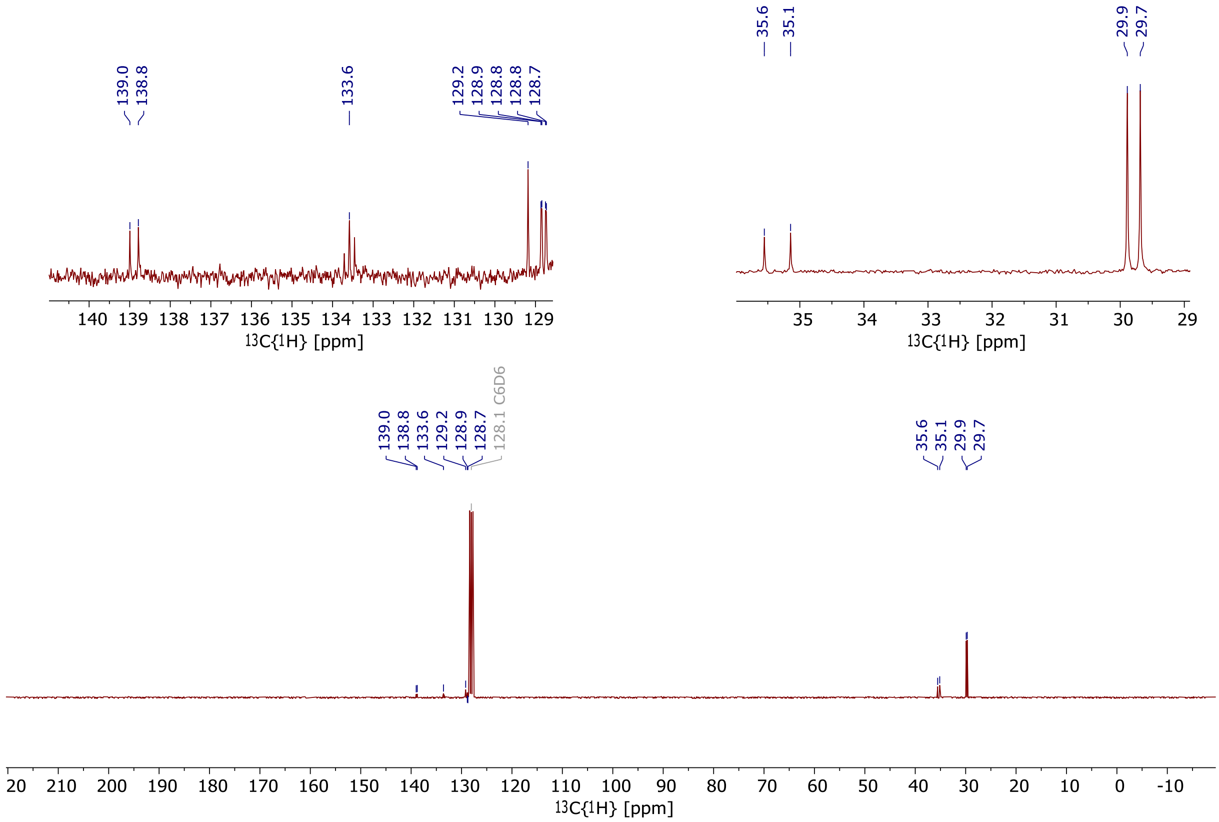

Figure S14. $^{13}C\{^1H\}$ NMR spectrum (benzene-d_6, 75 MHz, 298 K) of ligand **1-*t*Bu**.

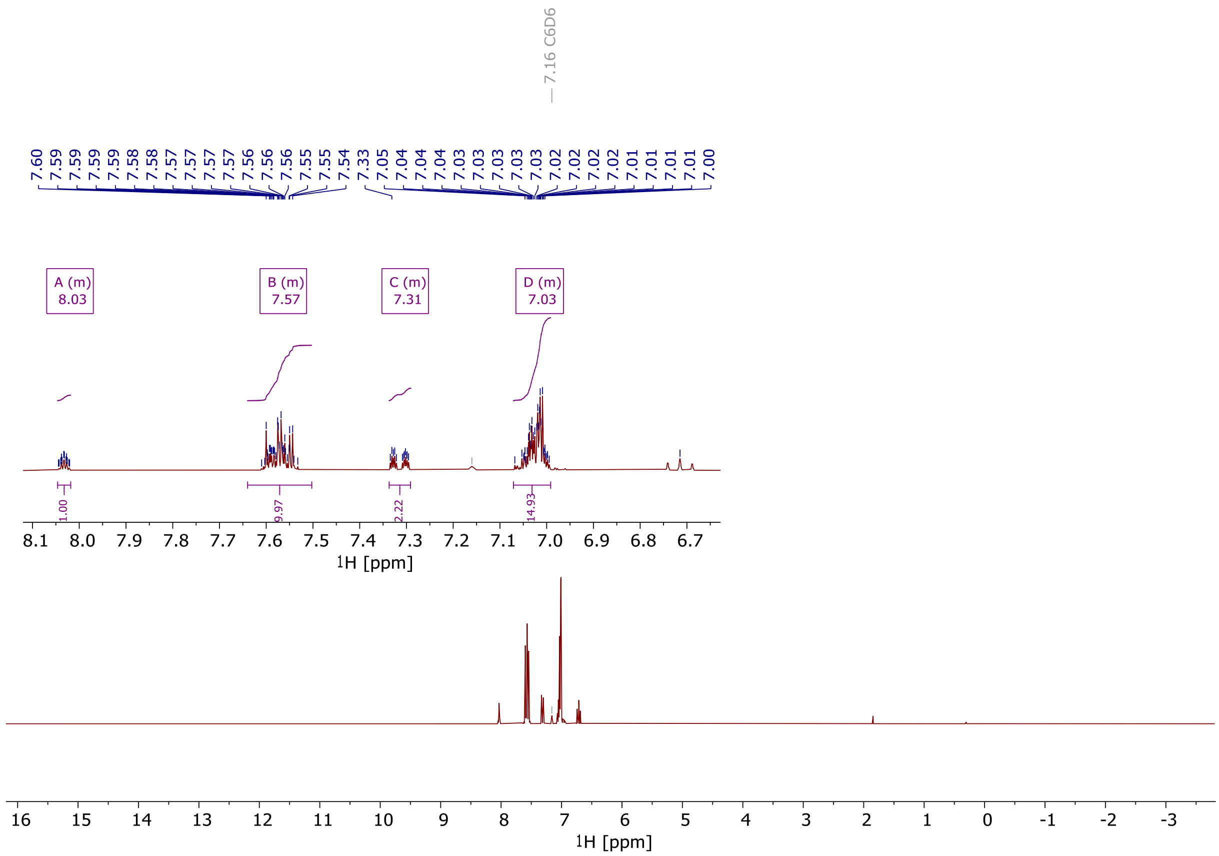

Figure S15. ^1H NMR spectrum (benzene-d_6, 300 MHz, 298 K) of ligand **1-Ph**.

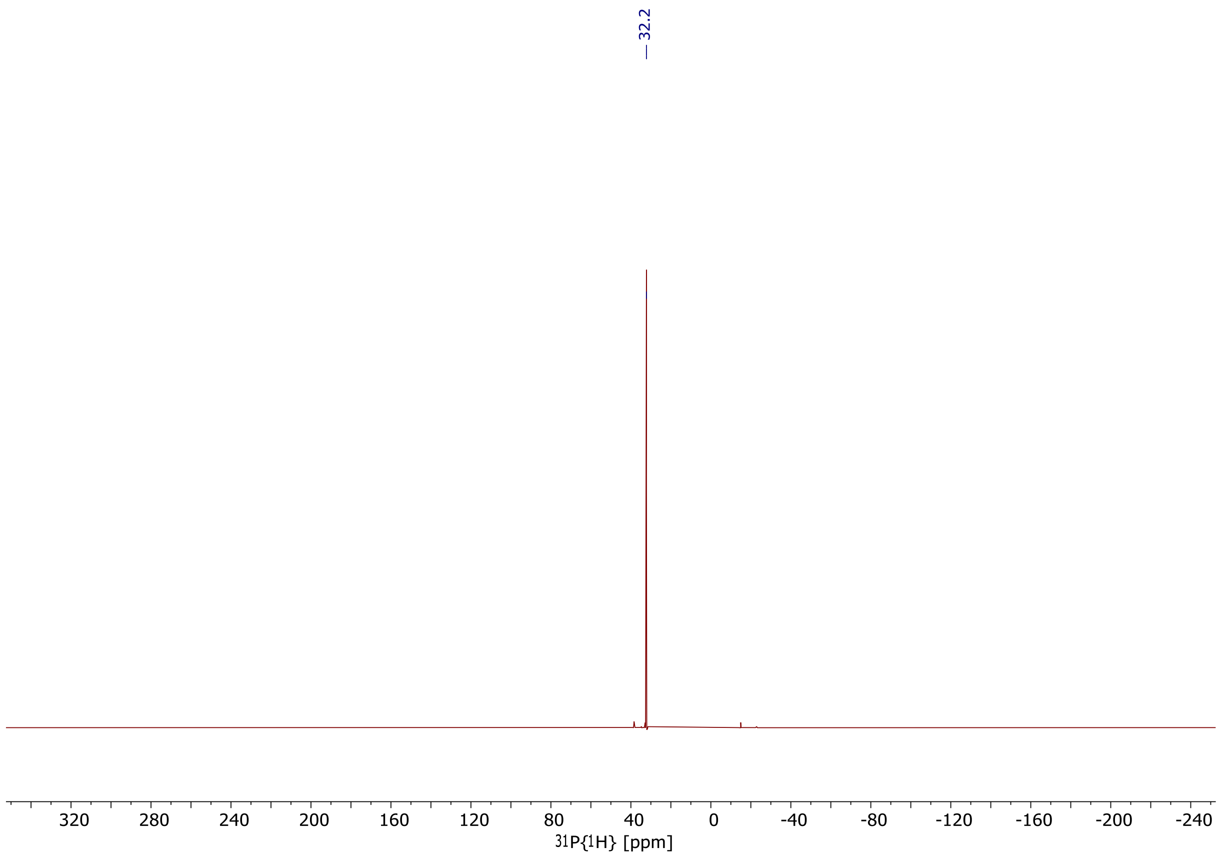

Figure S16. $^{31}P\{^{1}H\}$ NMR spectrum (benzene-d_6, 122 MHz, 298 K) of ligand **1-Ph**.

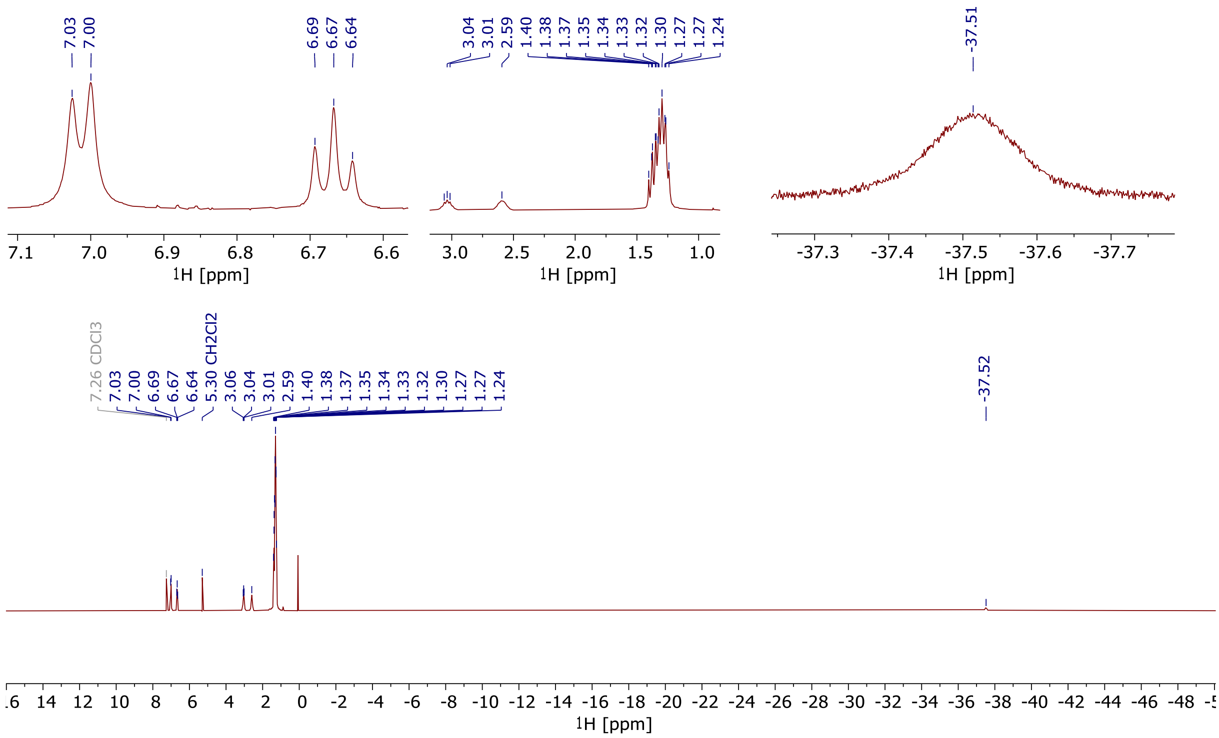

Figure S17. ^{1}H NMR spectrum ($CDCl_3$, 300 MHz, 298 K) of complex **2-*i*Pr**.

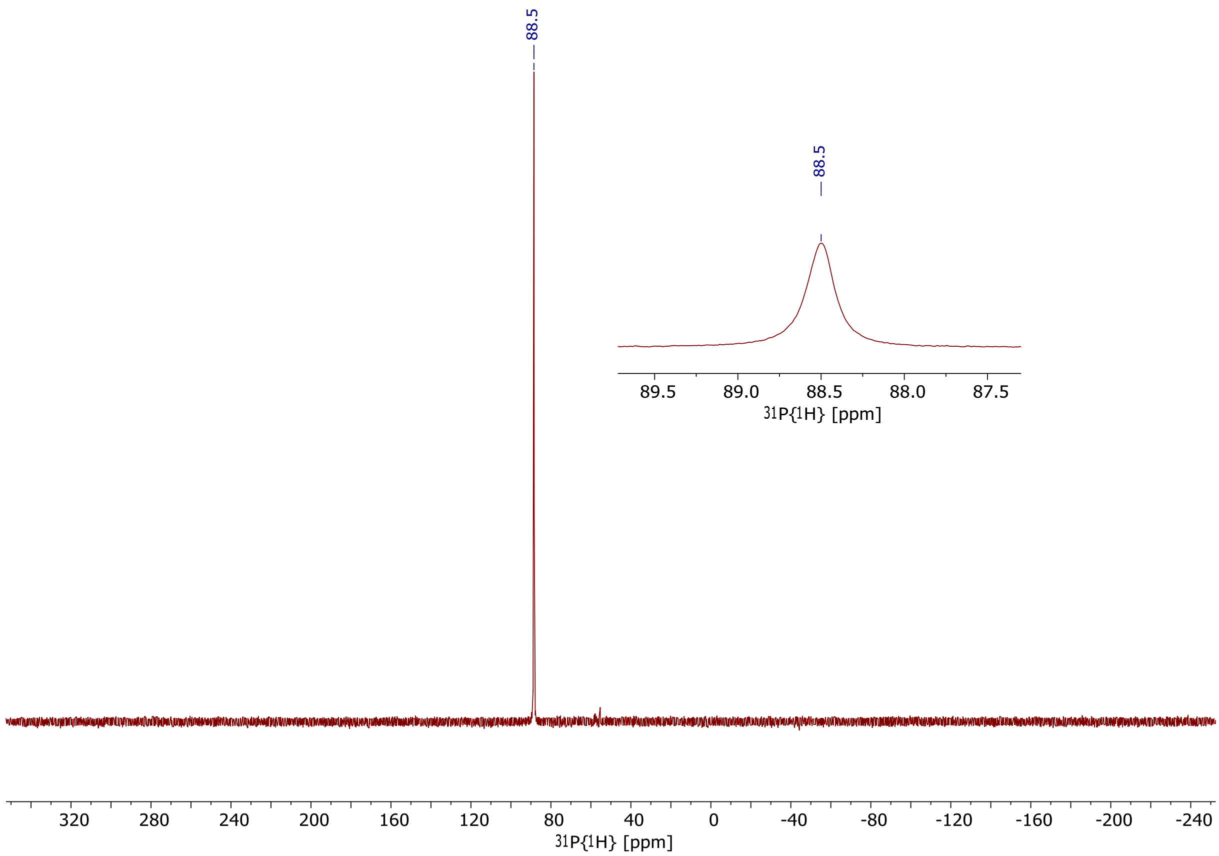

Figure S18. $^{31}P\{^1H\}$ NMR spectrum ($CDCl_3$, 122 MHz, 298 K) of complex **2-*i*Pr**.

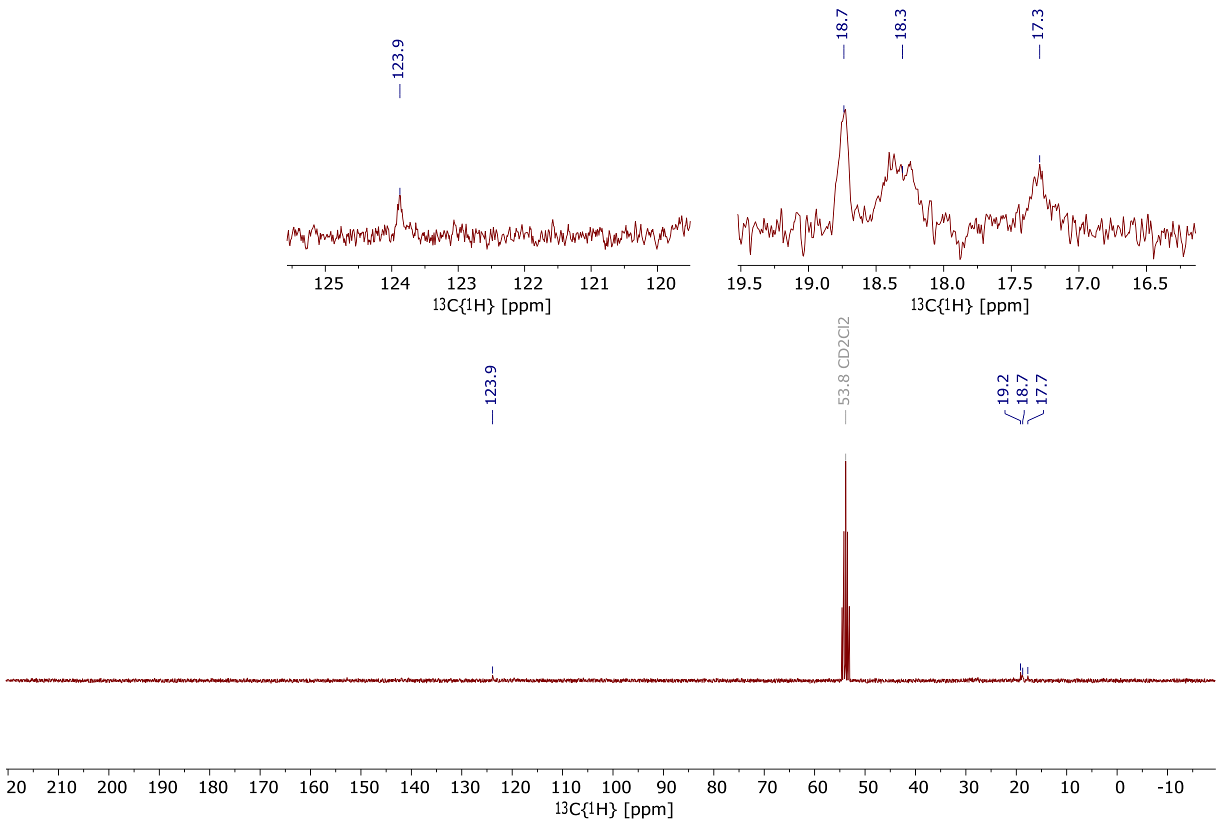

Figure S19. $^{13}C\{^1H\}$ NMR spectrum (CD_2Cl_2, 75 MHz, 298 K) of complex **2-*i*Pr**.

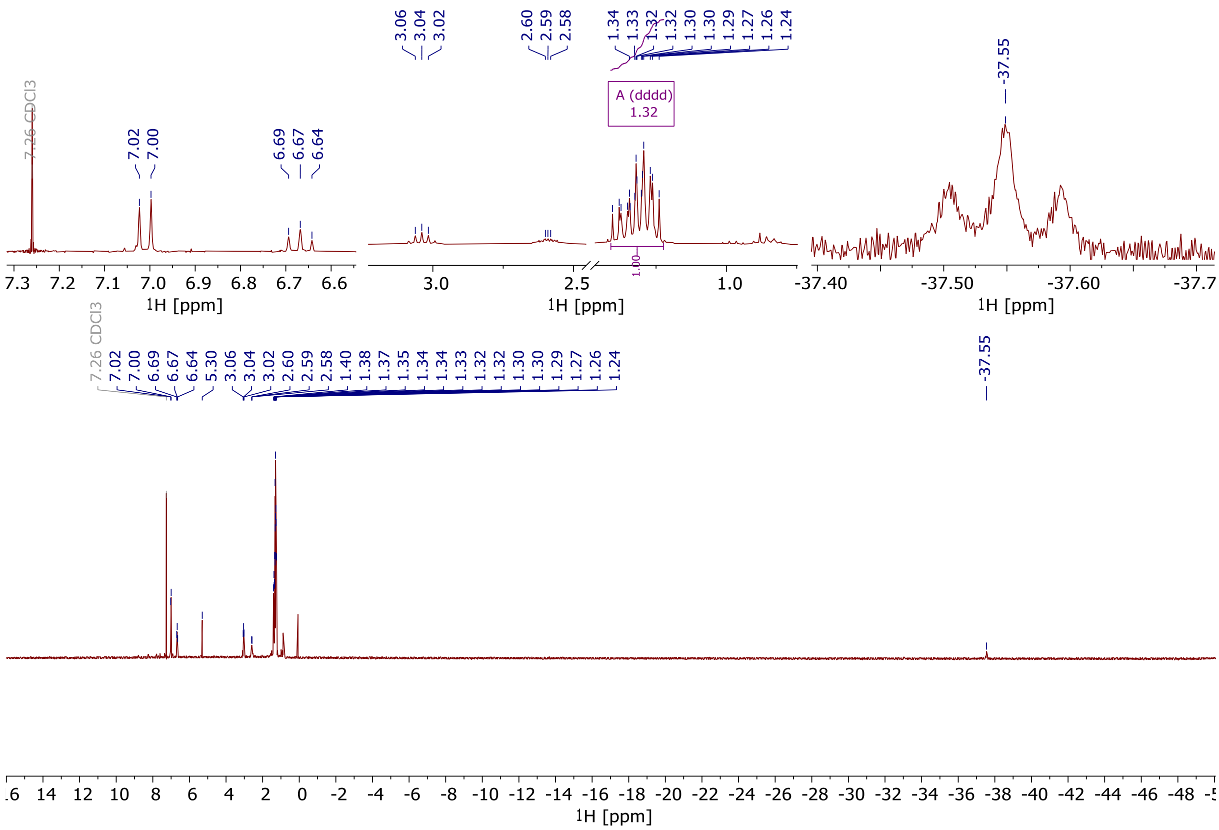

Figure S20. ^{1}H NMR spectrum ($CDCl_3$, 300 MHz, 298 K) of complex **2-*i*Pr** synthesised from pyridine complex **3-*i*Pr**.

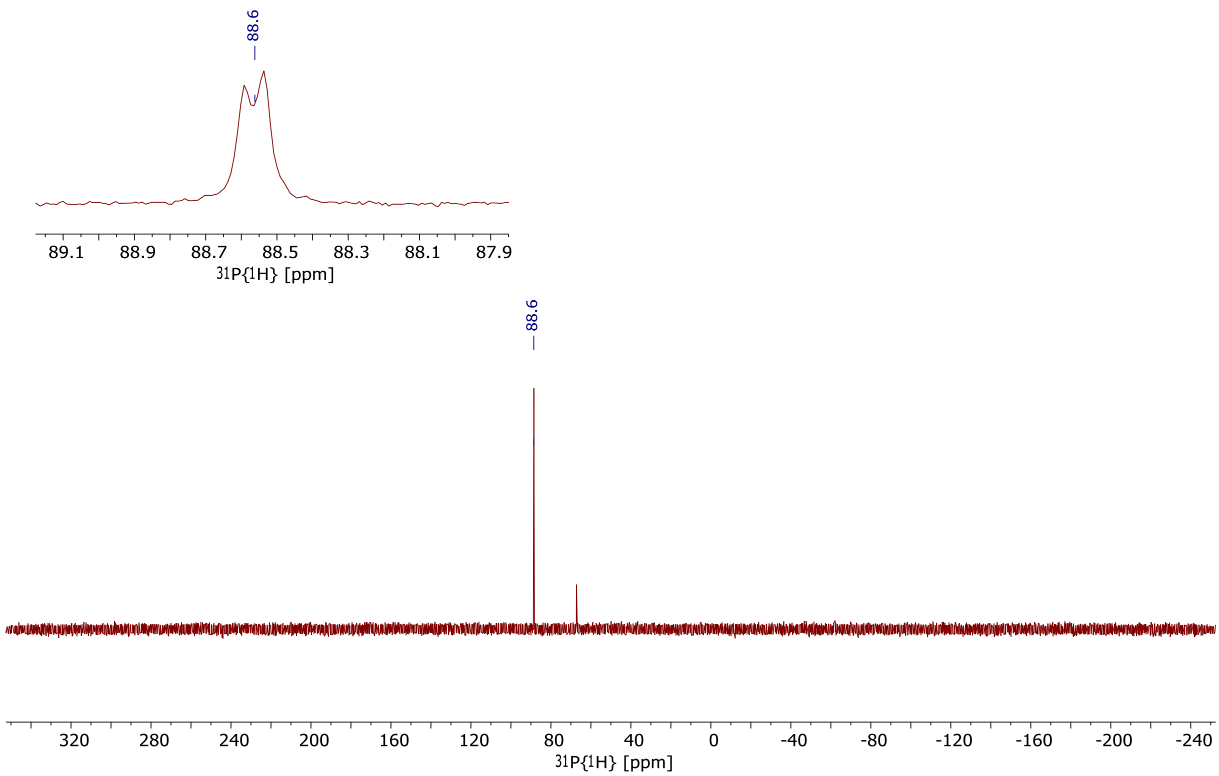

Figure S21. $^{31}P\{^{1}H\}$ NMR spectrum ($CDCl_3$, 122 MHz, 298 K) of complex **2-*i*Pr** synthesised from pyridine complex **3-*i*Pr**.

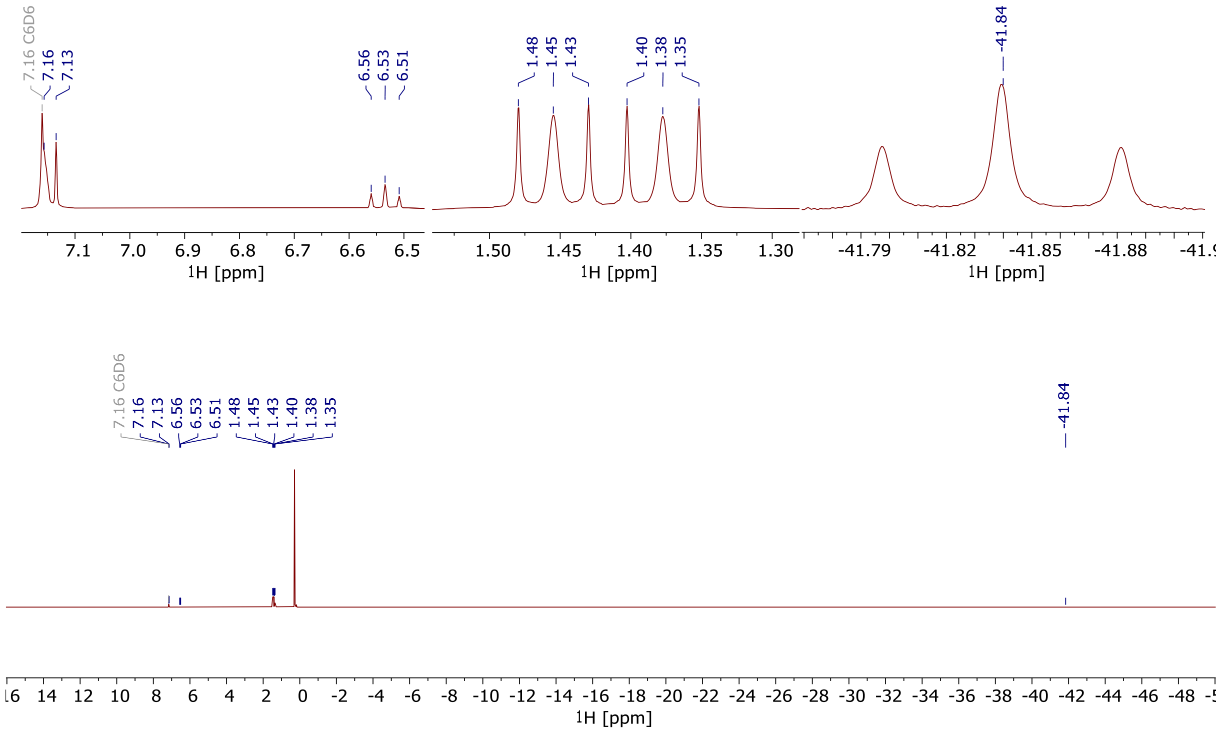

Figure S22. ^{1}H NMR spectrum (C_6D_6, 300 MHz, 298 K) of complex **2-*t*Bu**.

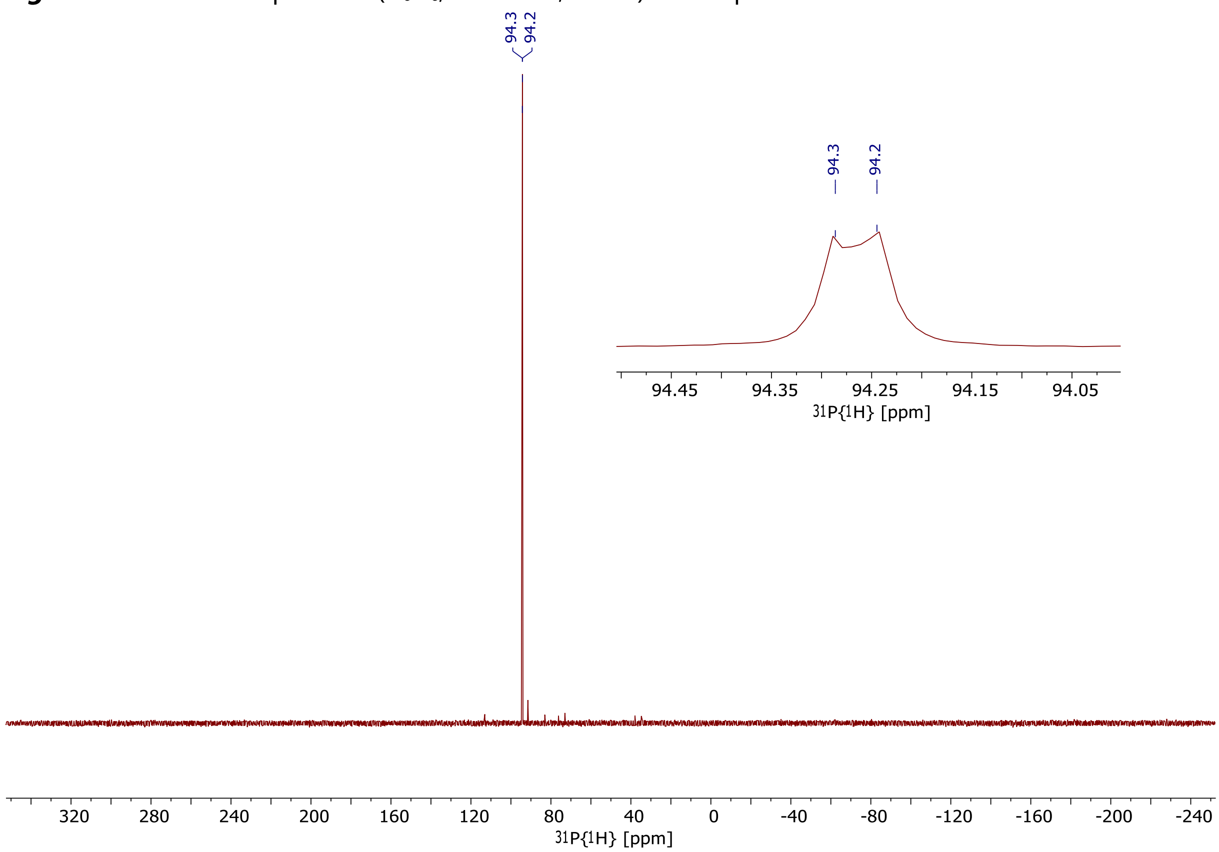

Figure S23. ^{31}P{^{1}H} NMR spectrum (benzene-*d*$_6$, 122 MHz, 298 K) of complex **2-*t*Bu**.

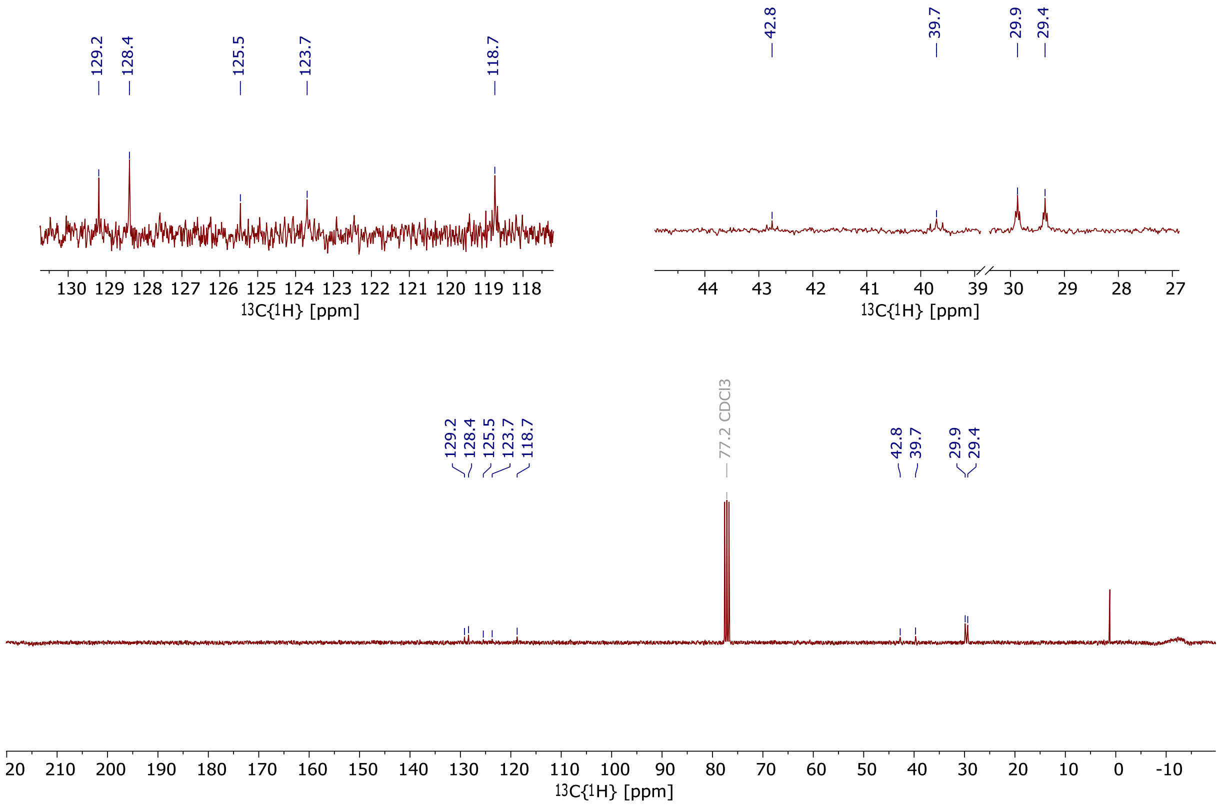

Figure S24. $^{13}C\{^{1}H\}$ NMR spectrum ($CDCl_3$, 122 MHz, 75.5 K) of complex **2-*t*Bu**.

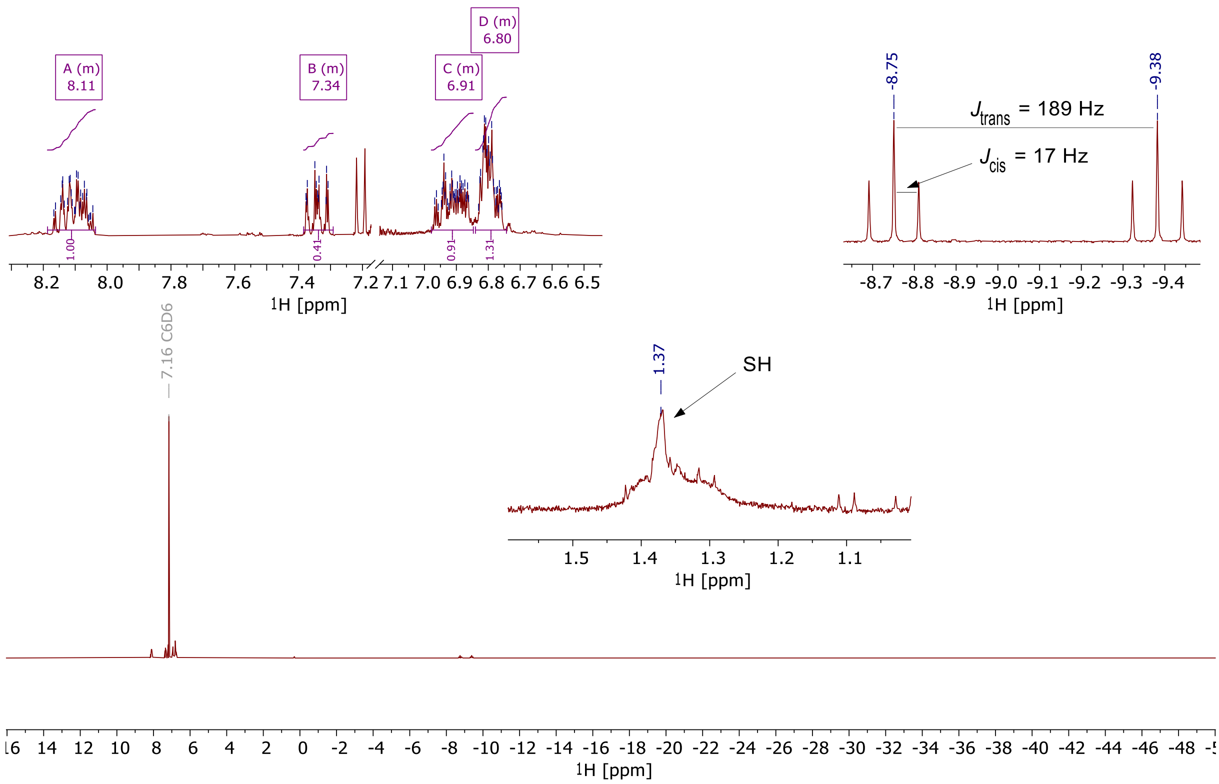

Figure S25. ^{1}H NMR spectrum (benzene-d_6, 300 MHz, 298 K) of complex **4**.

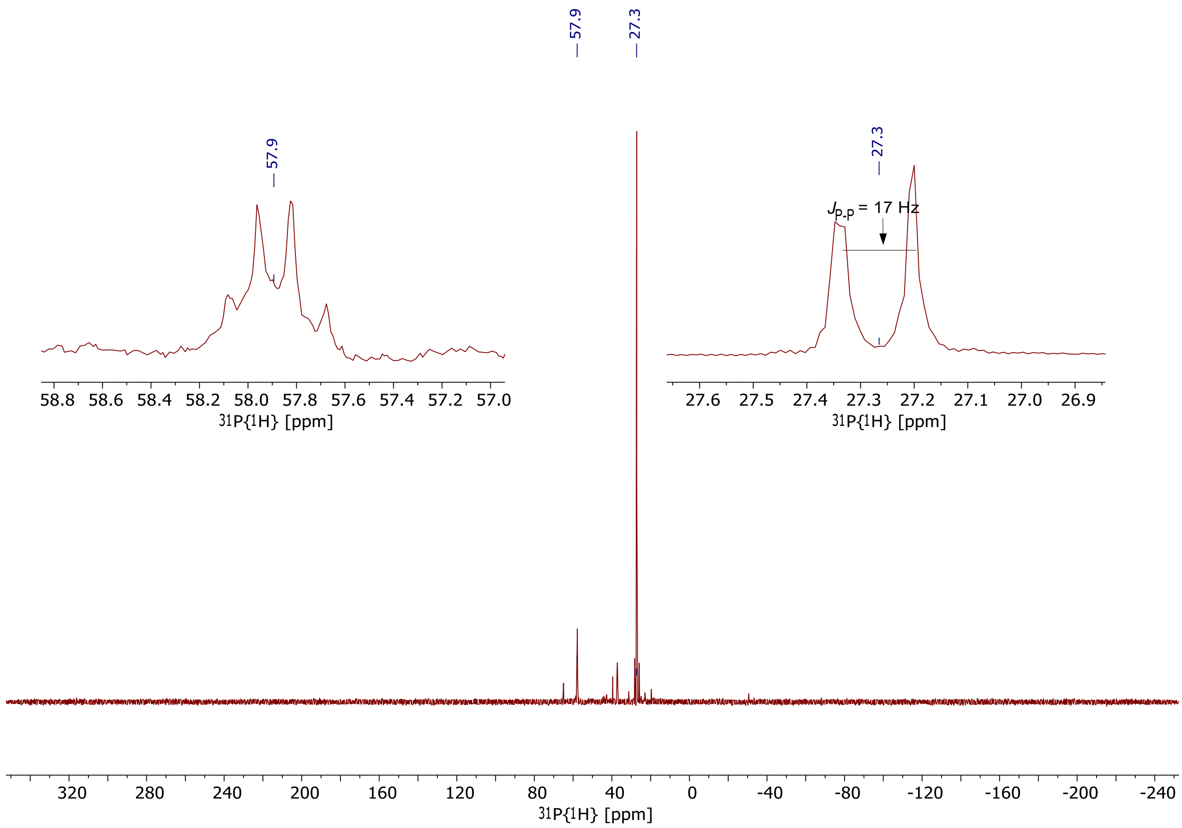

Figure S26. ^{31}P{^{1}H} NMR spectrum ($CDCl_3$, 122 MHz, 298 K) of complex **4**.

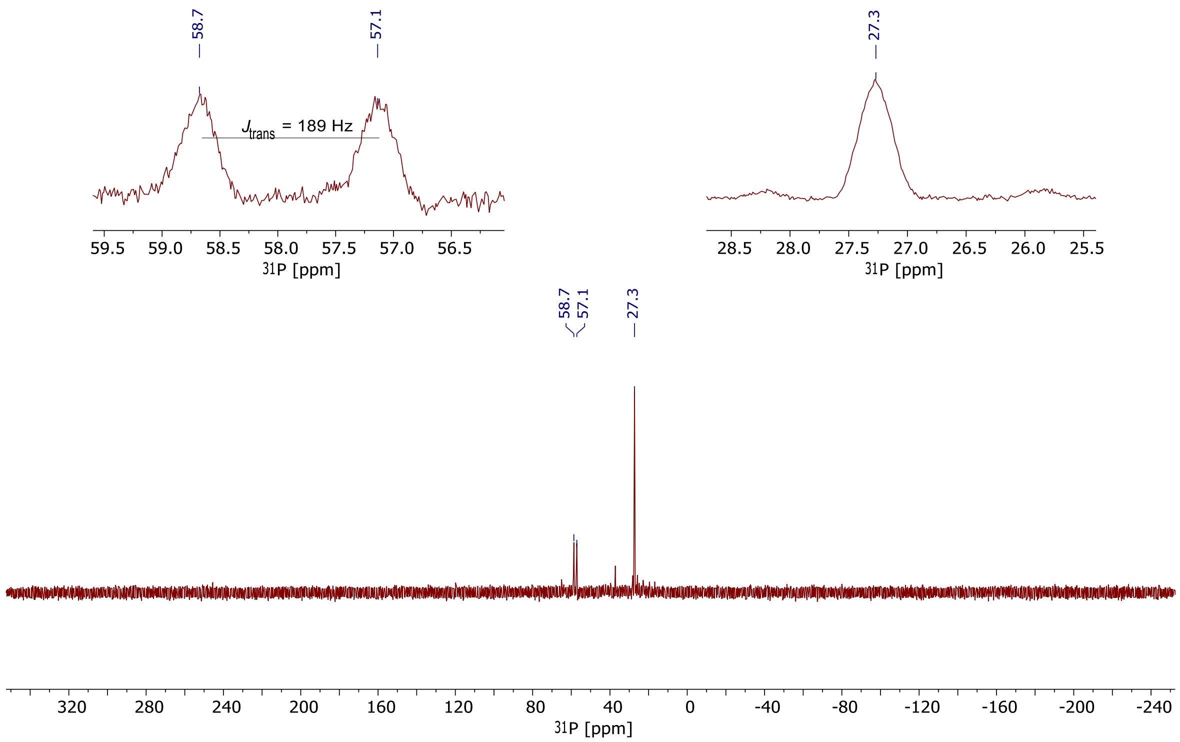

Figure S27. ^{31}P NMR spectrum ($CDCl_3$, 122 MHz, 298 K) of complex **4**. *Note that $J_{PH(cis)}$ and J_{PP} could not be found, likely due to the poor solubility of the complex and the rather large half width of both signals.*

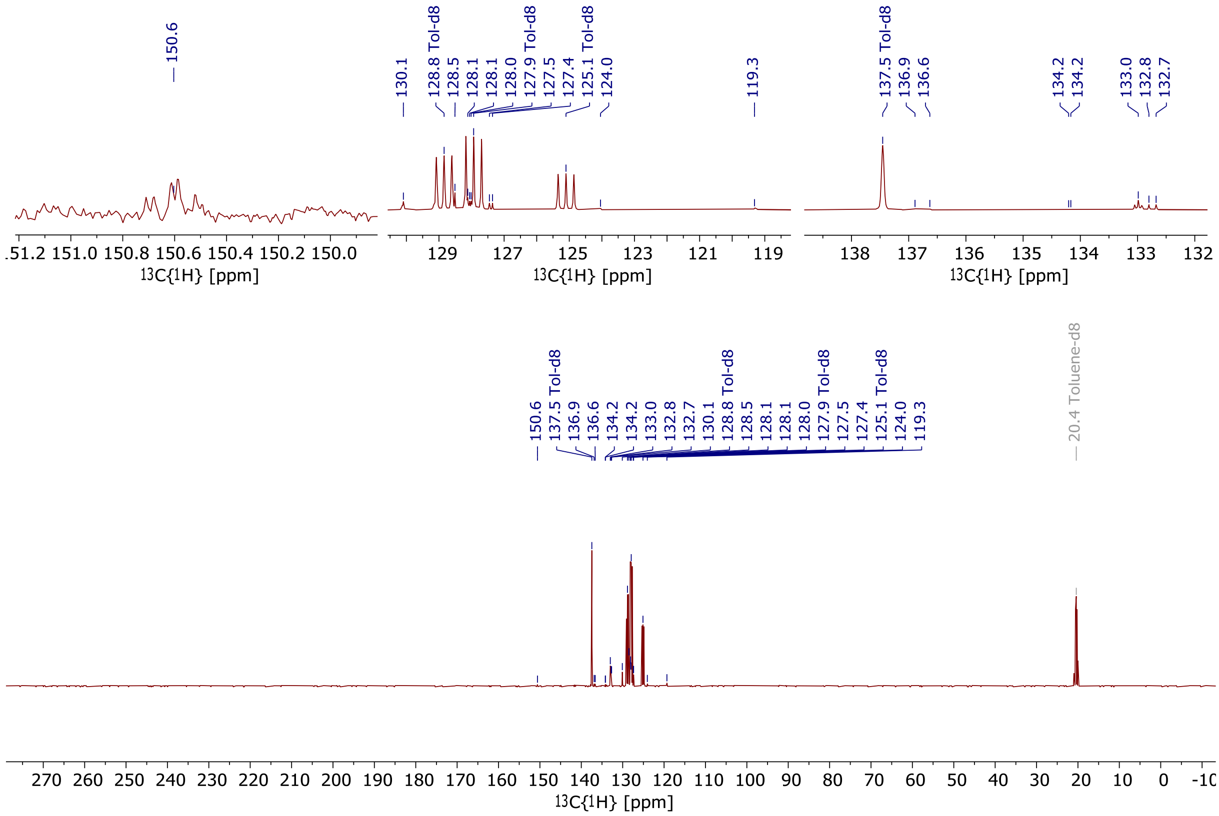

Figure S28. $^{13}C\{^1H\}$ NMR spectrum (toluene-d_8, 101 MHz, 297 K) of complex **4**.

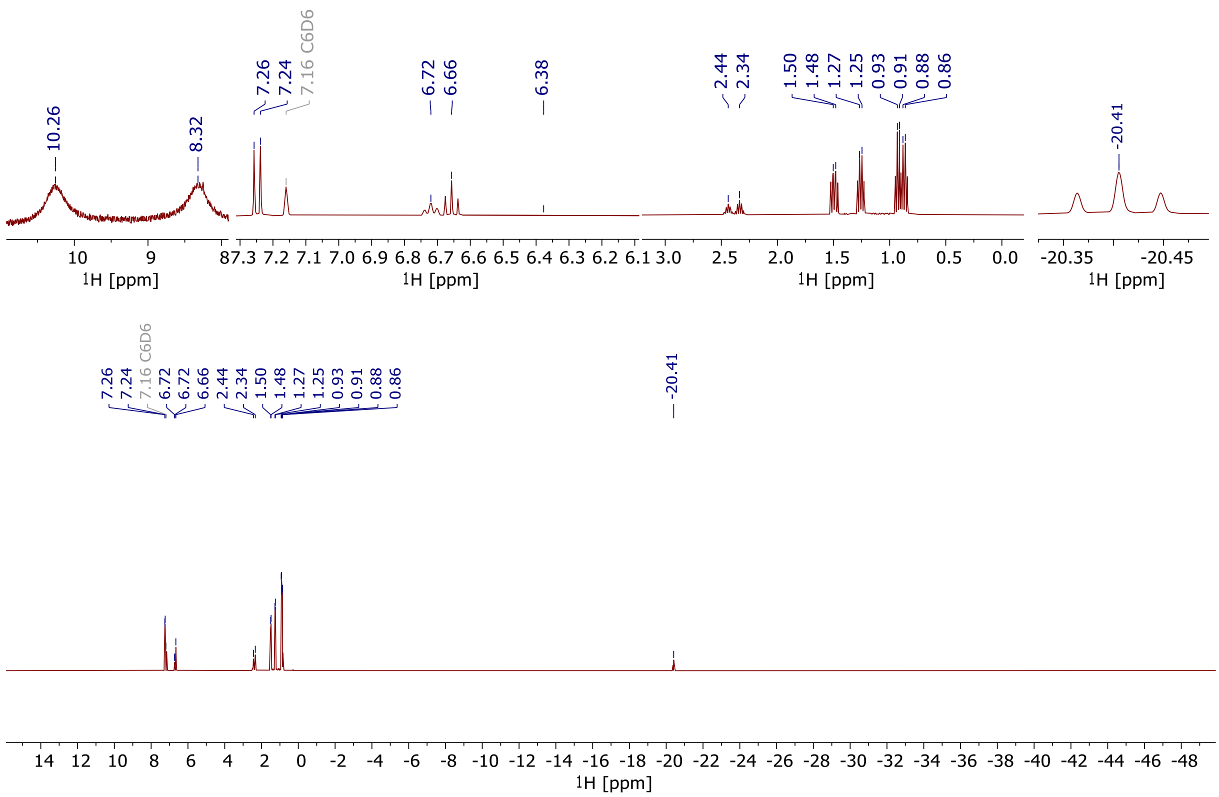

Figure S29. ^1H NMR spectrum (benzene-d_6, 400 MHz, 297 K) of complex **3-*i*Pr**.

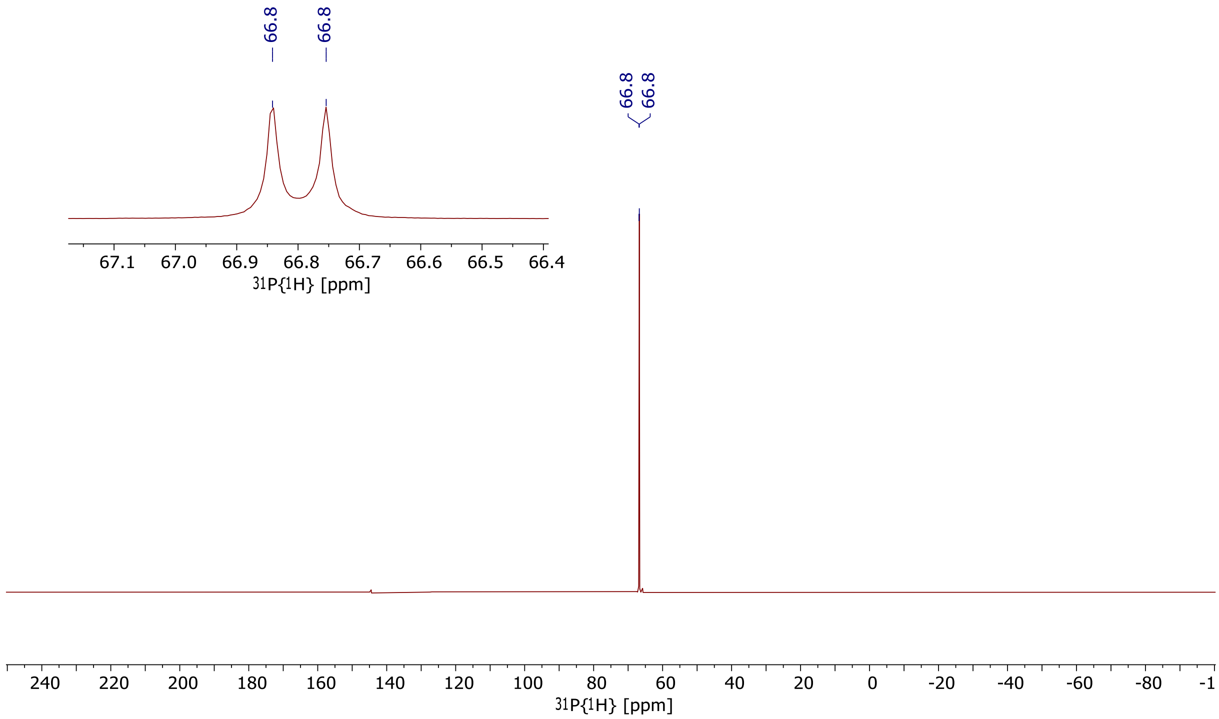

Figure S30. $^{31}P\{^{1}H\}$ NMR spectrum (benzene-d_6, 122 MHz, 298 K) of complex **3-*i*Pr**.

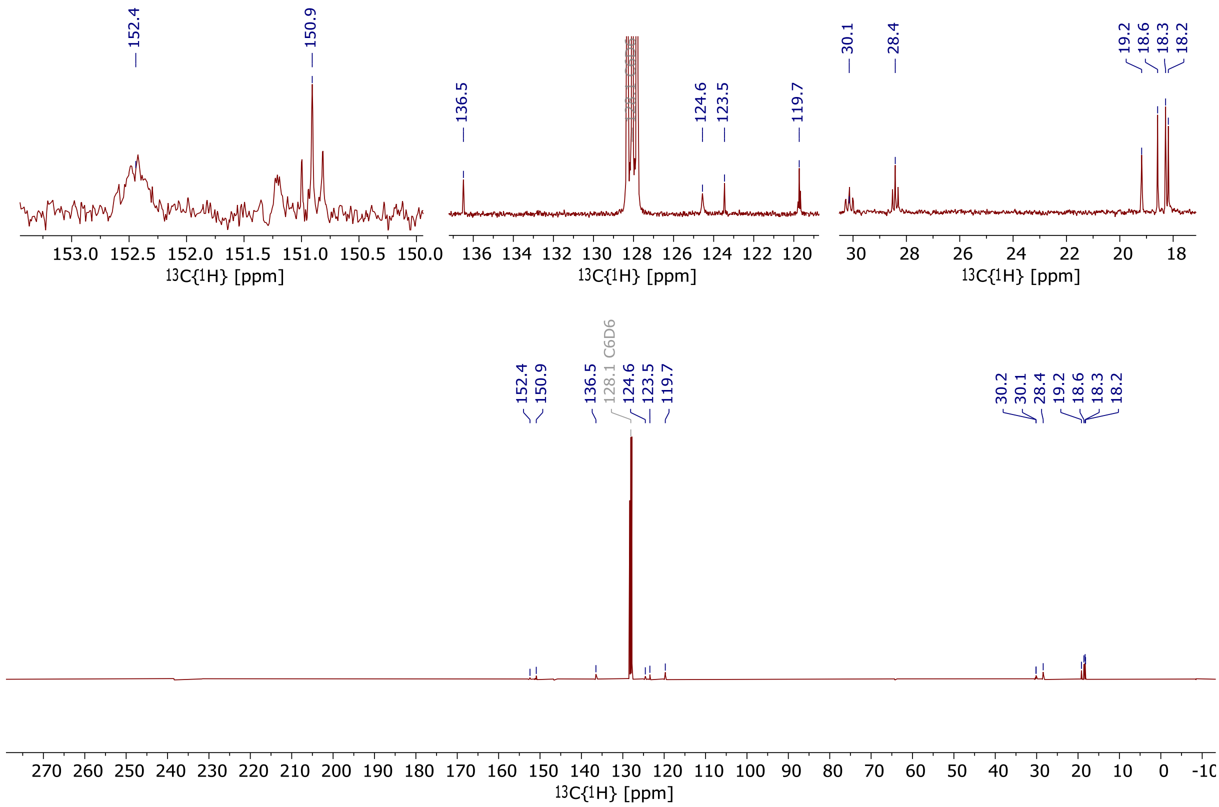

Figure S31. $^{13}C\{^{1}H\}$ NMR spectrum (benzene-d_6, 101 MHz, 298 K) of complex **3-*i*Pr**.

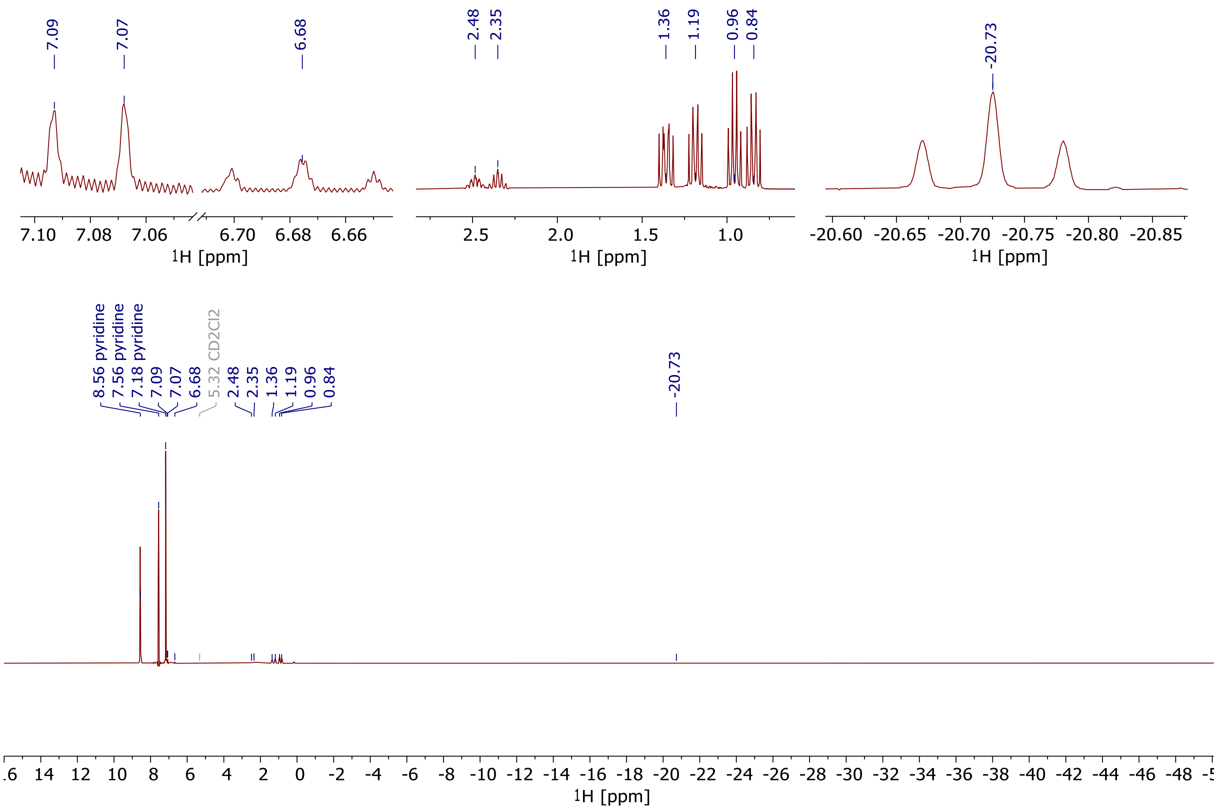

Figure S32. ^{1}H NMR spectrum (CD_2Cl_2, 300 MHz, 298 K) of **3-*i*Pr** formed from **2-*i*Pr**.

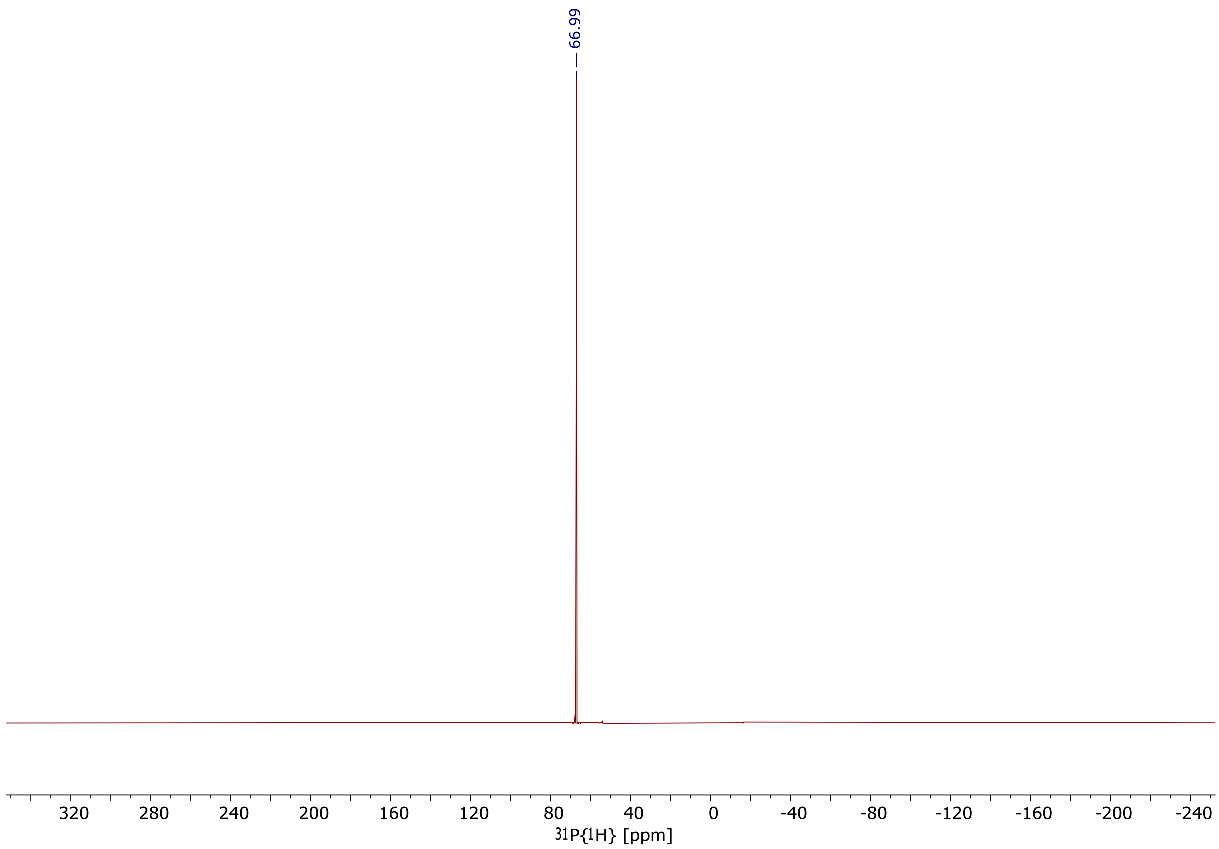

Figure S33. $^{31}P\{^{1}H\}$ NMR spectrum (CD_2Cl_2, 122 MHz,298 K) of **3-*i*Pr** formed from **2-*i*Pr**.

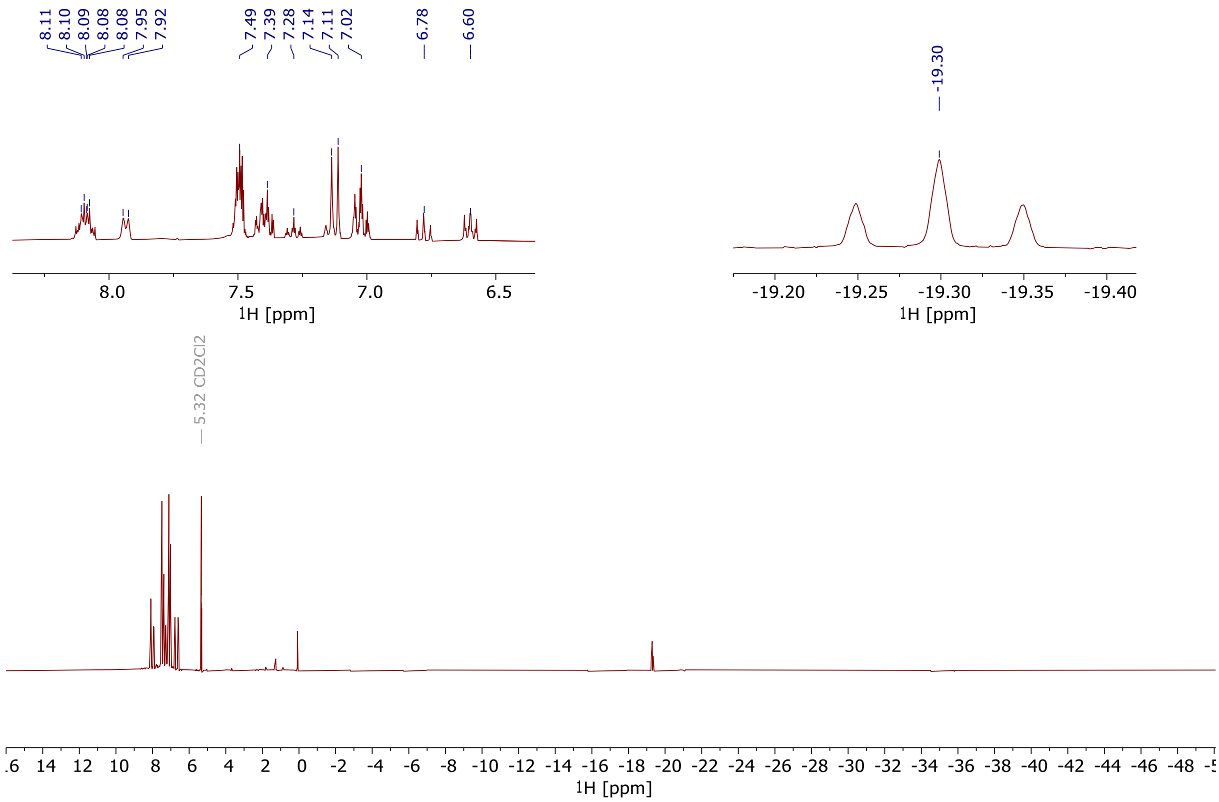

Figure S34. ^{1}H NMR spectrum (CD_2Cl_2, 300 MHz, 302 K) of complex **3-Ph**.

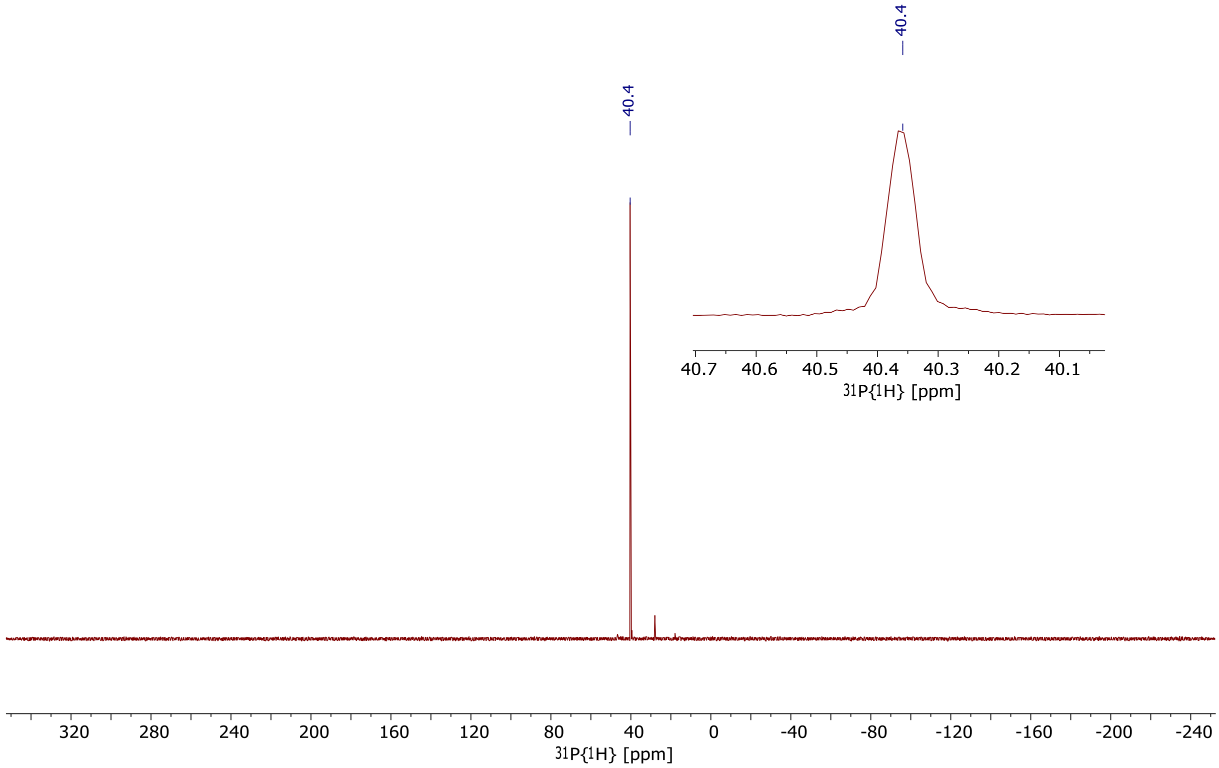

Figure S35. $^{31}P\{^1H\}$ NMR spectrum (CD_2Cl_2, 122 MHz, 302 K) of complex **3-Ph**.

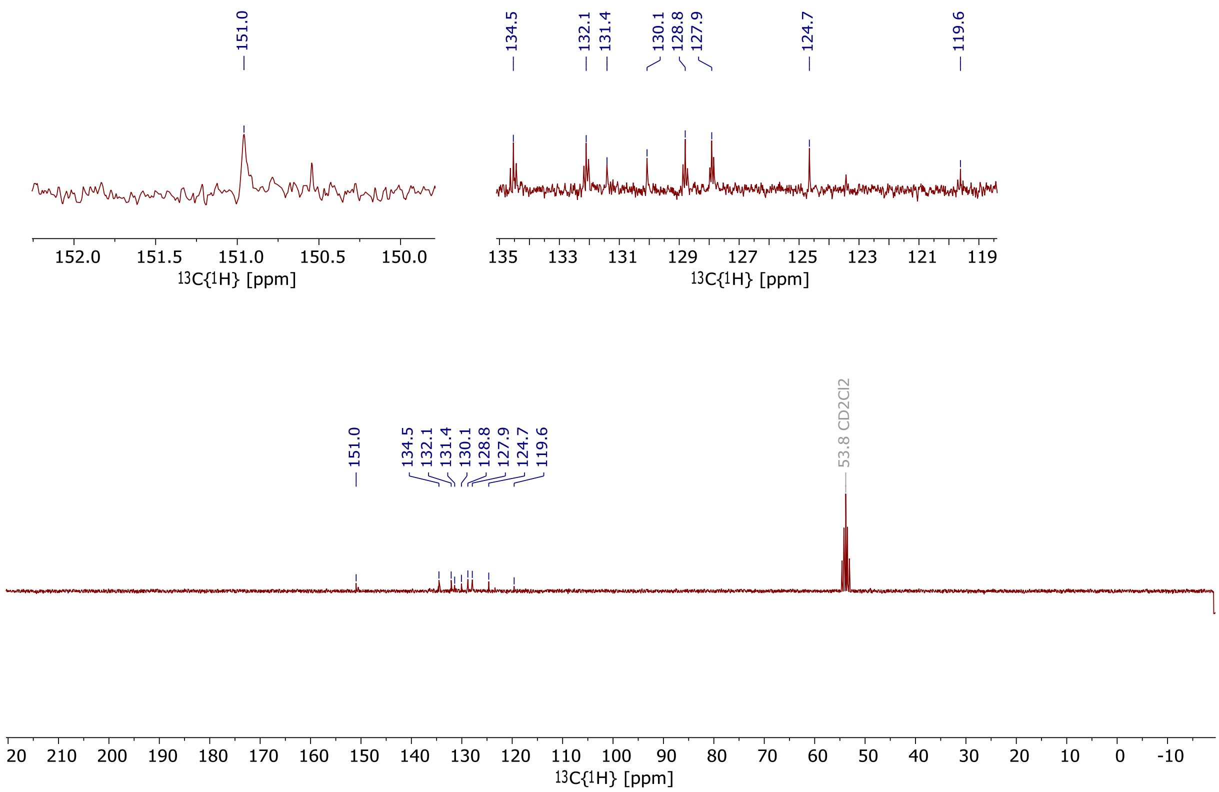

Figure S36. $^{13}C\{^1H\}$ NMR spectrum (CD_2Cl_2, 75 MHz, 302 K) of complex **3-Ph**.

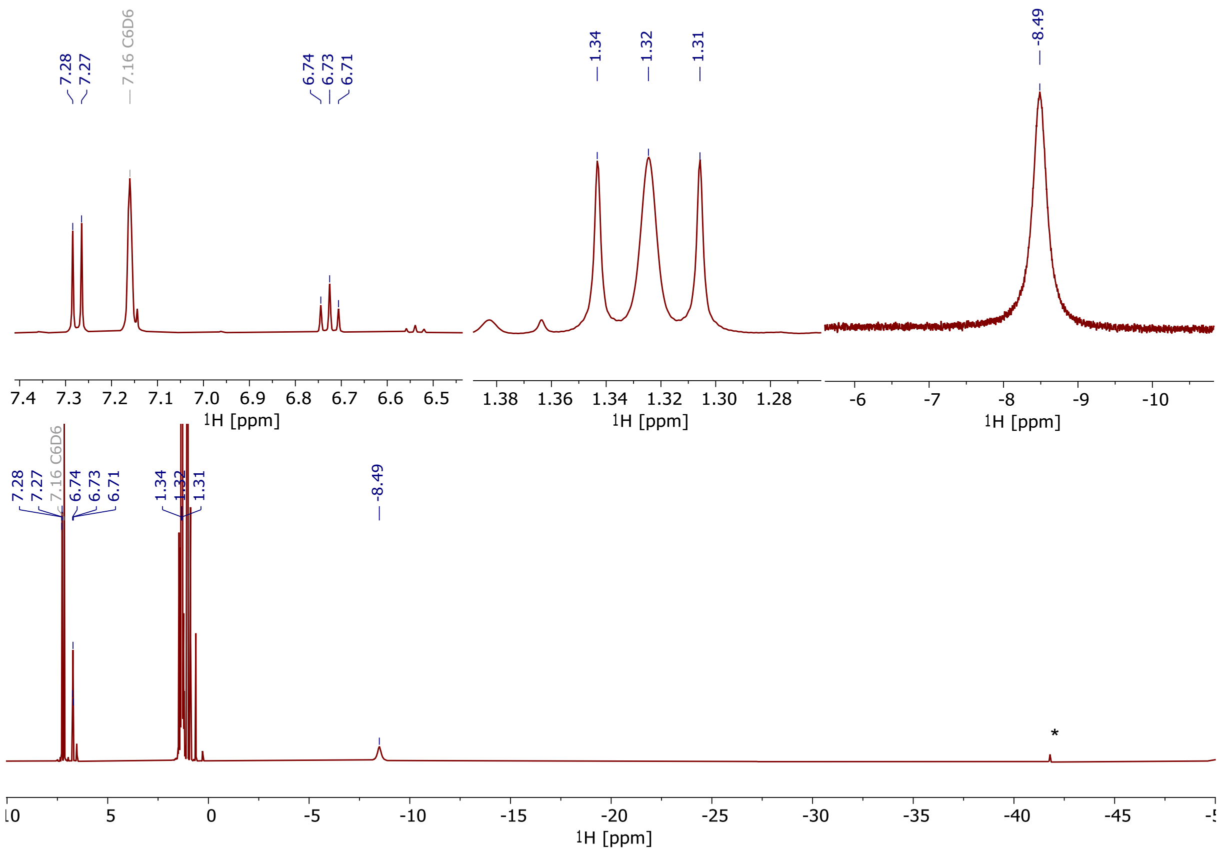

Figure S37. ^{1}H NMR spectrum (C_6D_6, 400 MHz, 298 K) of complex **5**. Residual complex **2-*t*Bu** marked by asterisk.

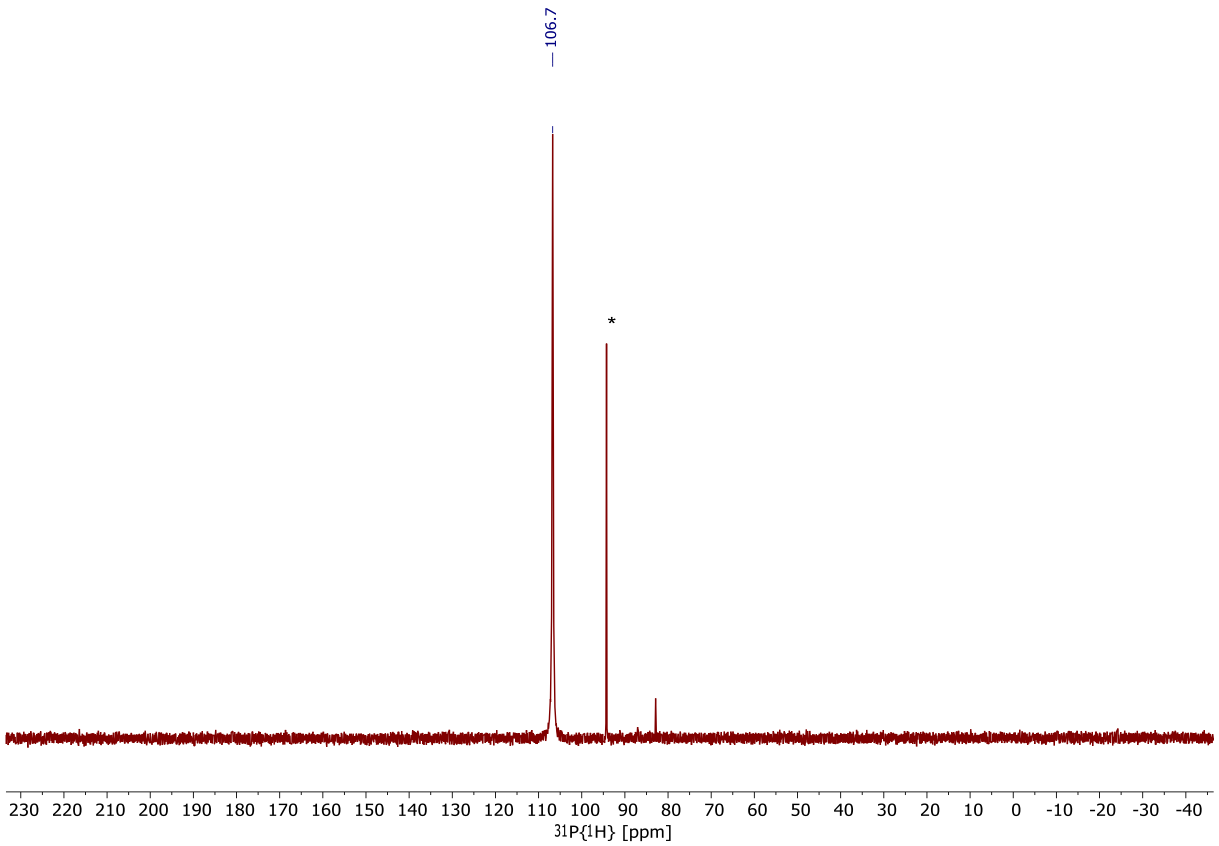

Figure S38. ^{31}P{H} NMR spectrum (C_6D_6, 162 MHz, 298 K) of complex **5**. Residual complex **2-*t*Bu** marked by asterisk.

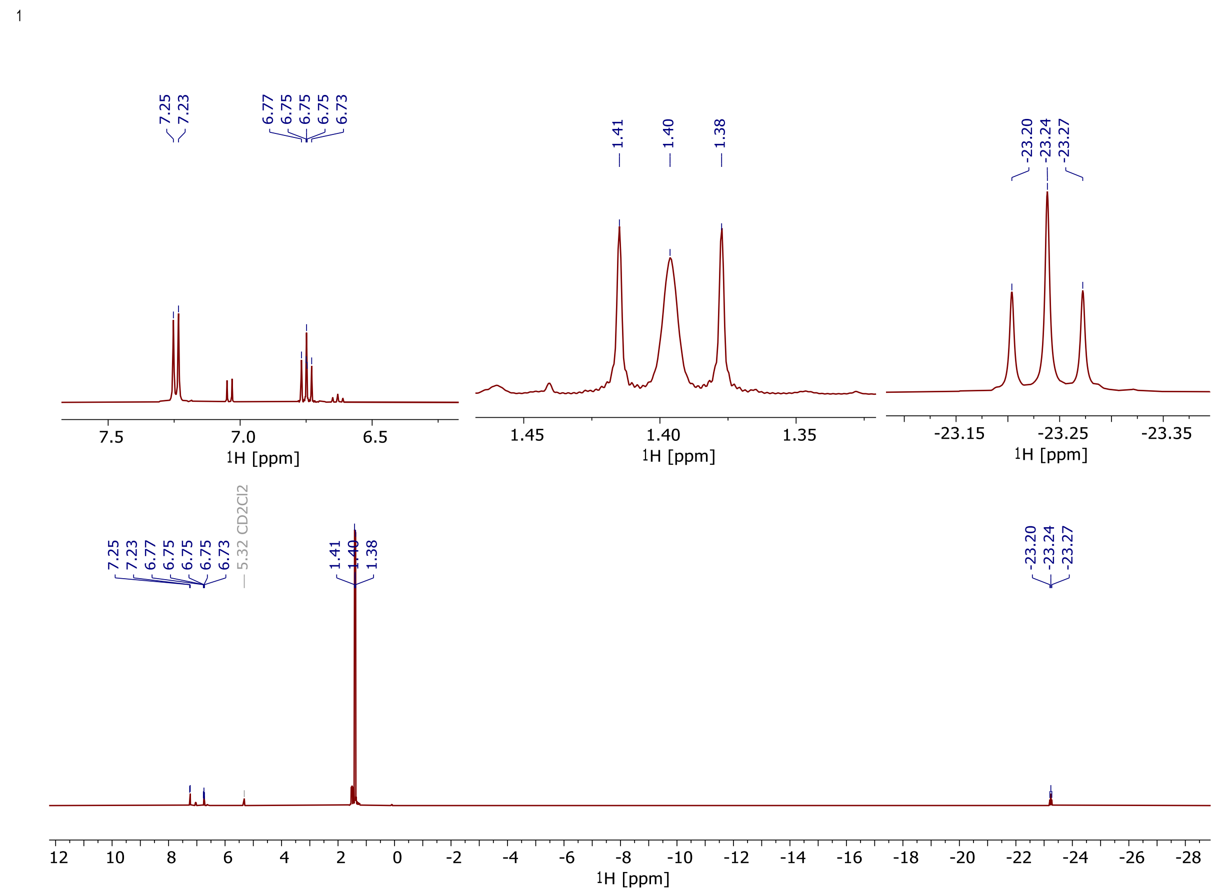

Figure S39. ^{1}H NMR spectrum (CD_2Cl_2, 400 MHz, 298 K) of **6**.

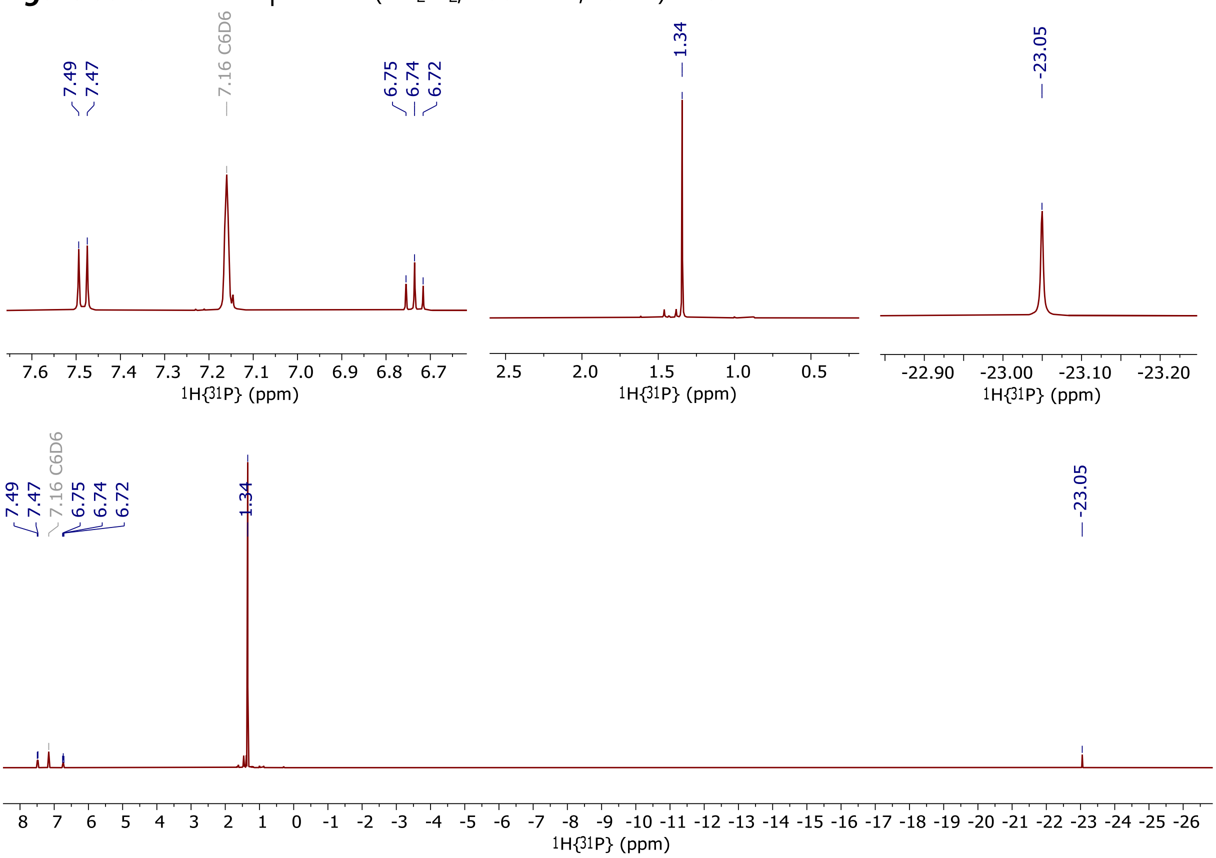

Figure S40. ^{1}H{^{31}P} NMR spectrum (C_6D_6, 400 MHz, 298 K) of **6**.

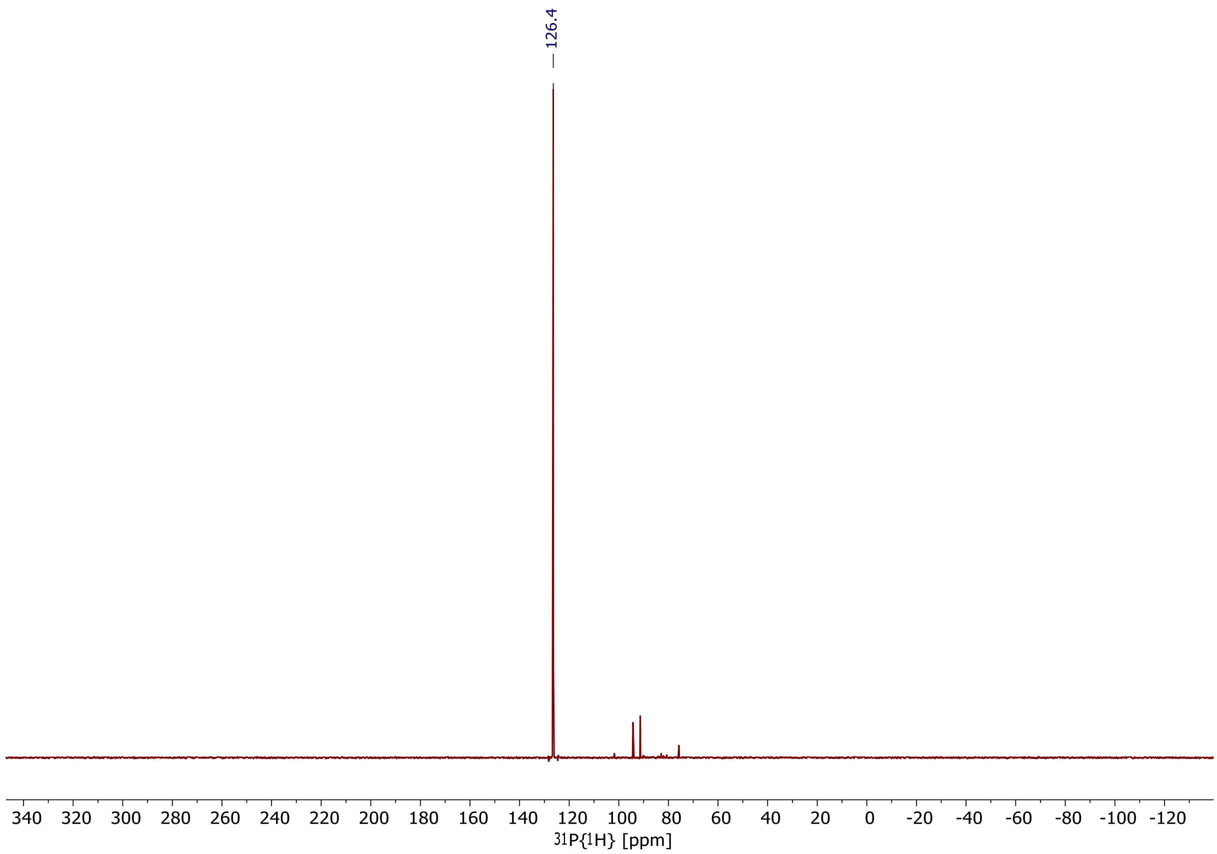

Figure S41. $^{31}P\{^{1}H\}$ NMR spectrum (C_6D_6, 122 MHz, 298 K) of **6**.

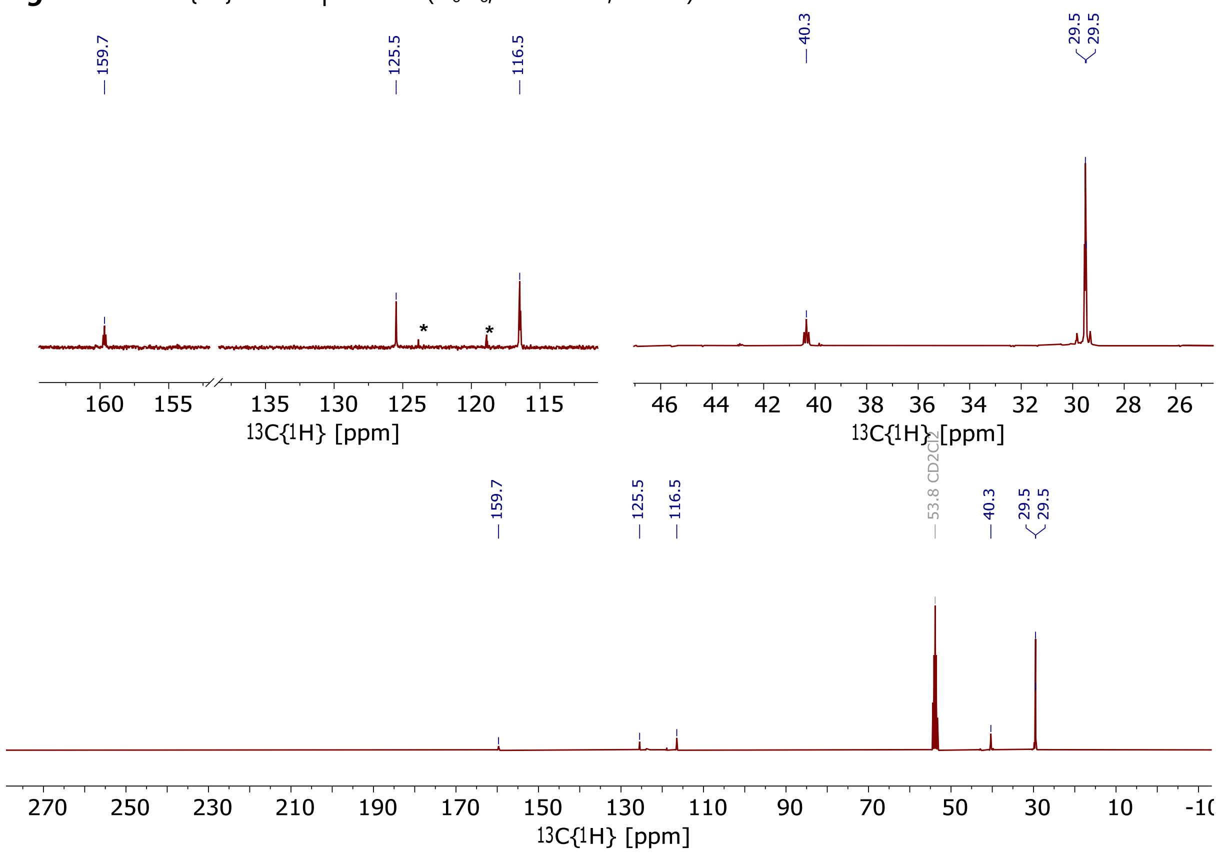

Figure S42. $^{13}C\{^{1}H\}$ NMR spectrum (CD_2Cl_2, 101 MHz, 298 K) of **6**.

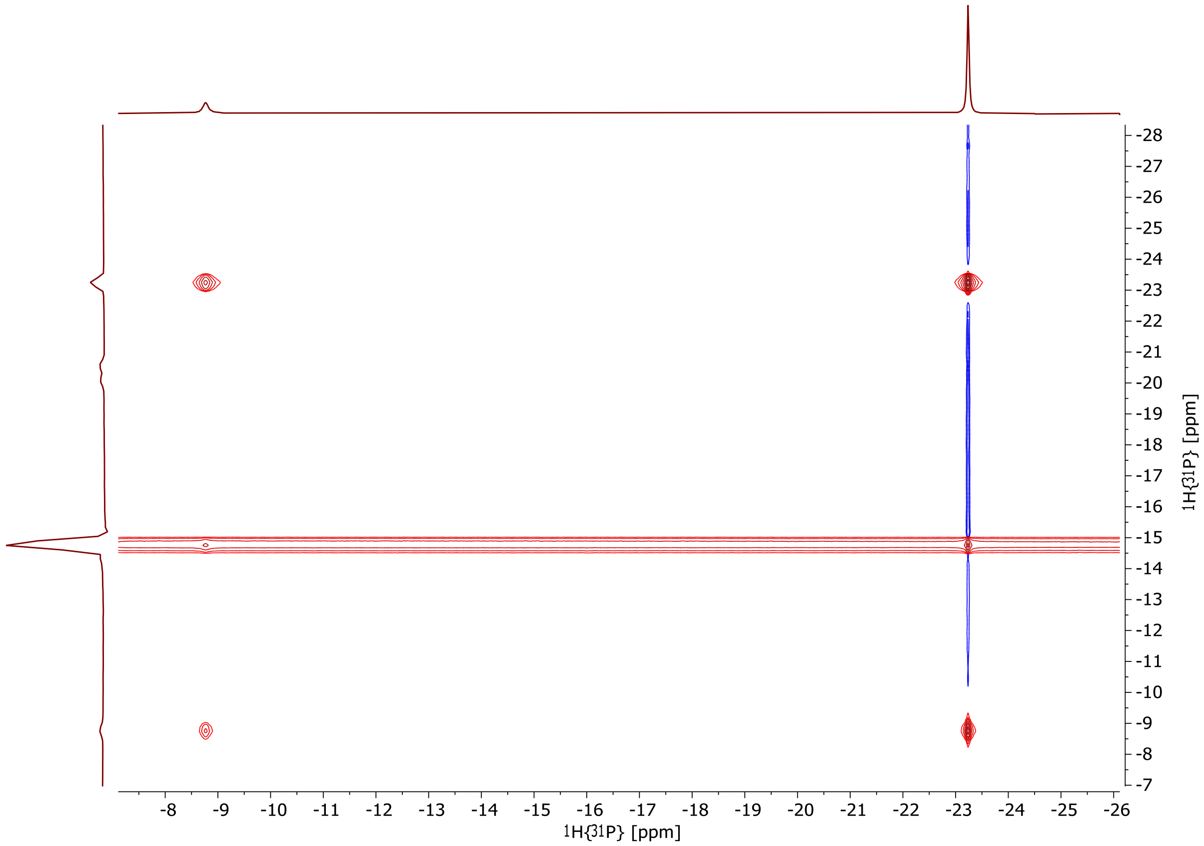

Figure S43. $^{1}H\{^{31}P\}$ NOESY experiment (CD_2Cl_2, 400 MHz,298 K) of **6**.

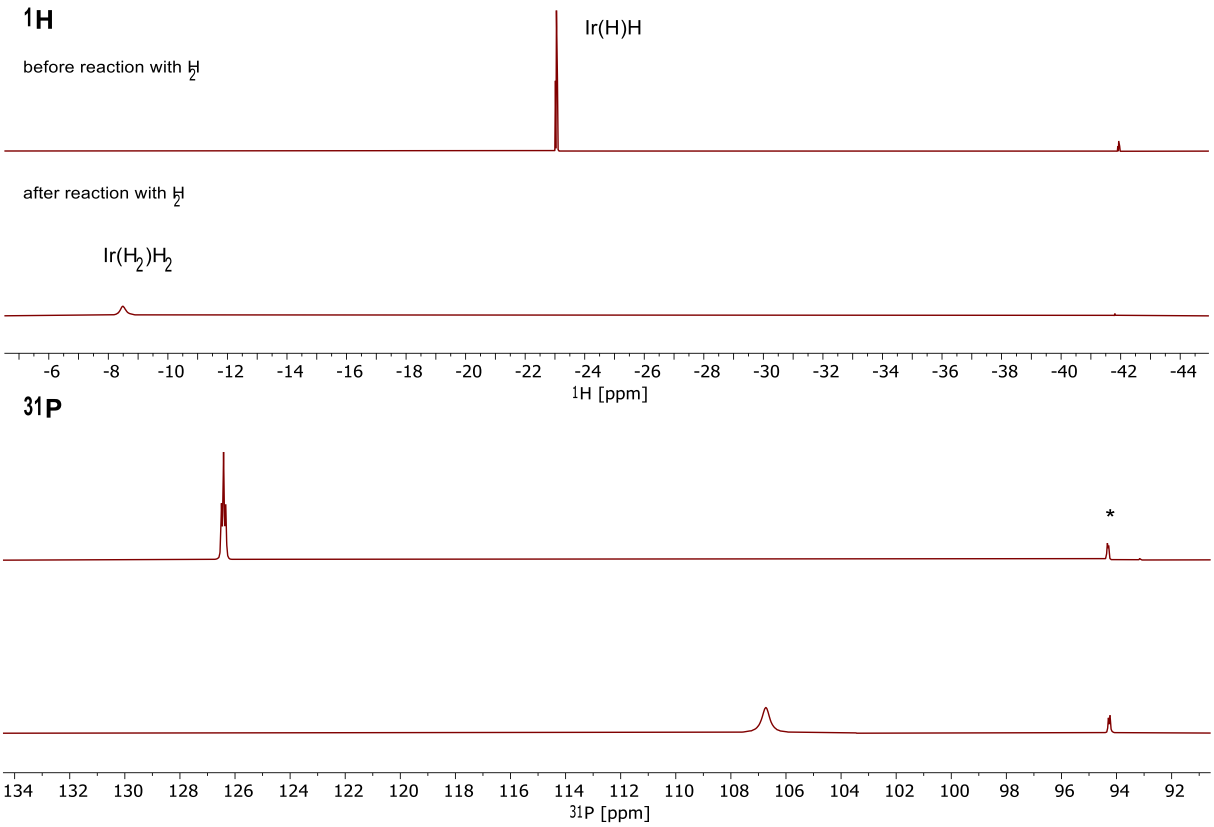

Figure S44. Back reaction of **6** with H_2 to **5**. Top: ^{1}H NMR spectrum (C_6D_6, 400 MHz, 298 K); bottom: ^{31}P NMR spectrum (C_6D_6, 162 MHz, 298 K). Residual complex **2-*t*Bu** marked by asterisk.

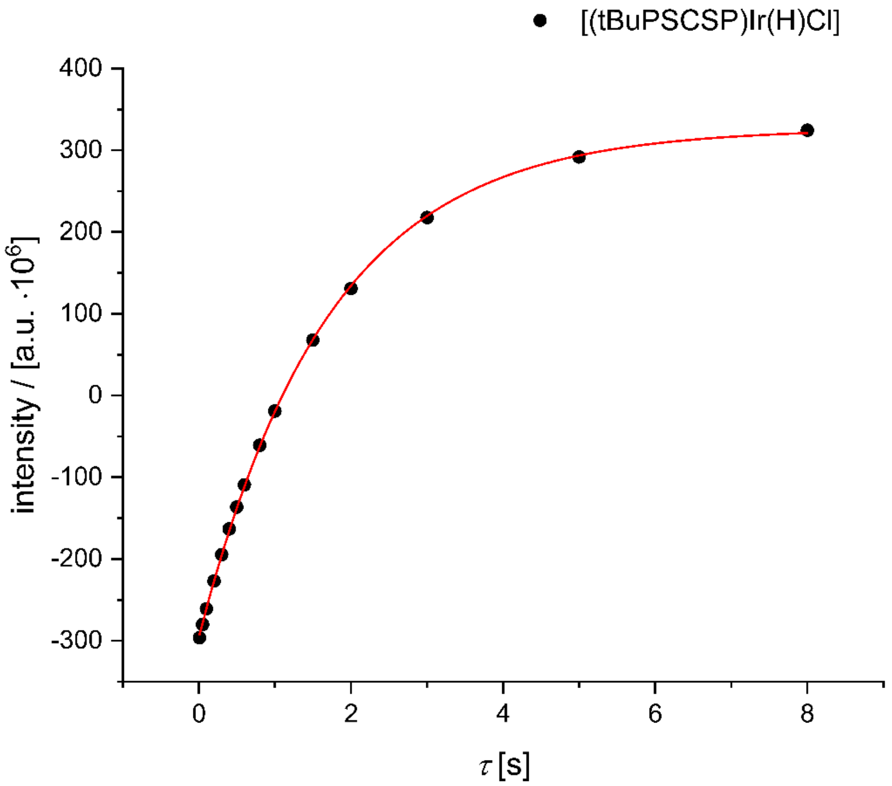

Figure S45. Estimation of the longitudinal relaxation time T_1 for the hydride ligand (−42 ppm) by the inversion recovery sequence of **2-*t*Bu** in C_6D_6 at 298 K.

Table S4. Fitting parameters for inversion recovery experiment of **2-*t*Bu**.

model	
equation	$y = A_1 \cdot \exp(-x/t_1) + y_0$
Draw	intensity
y_0	3.26652E8 ± 1988429.49709
A_1	-6.22841E8 ± 2034886.53094
t_1	1.70358 ± 0.01499
Chi-square reduced	5.47397E12
R-square (COD)	0.99989
corr. *R*-square	0.99987

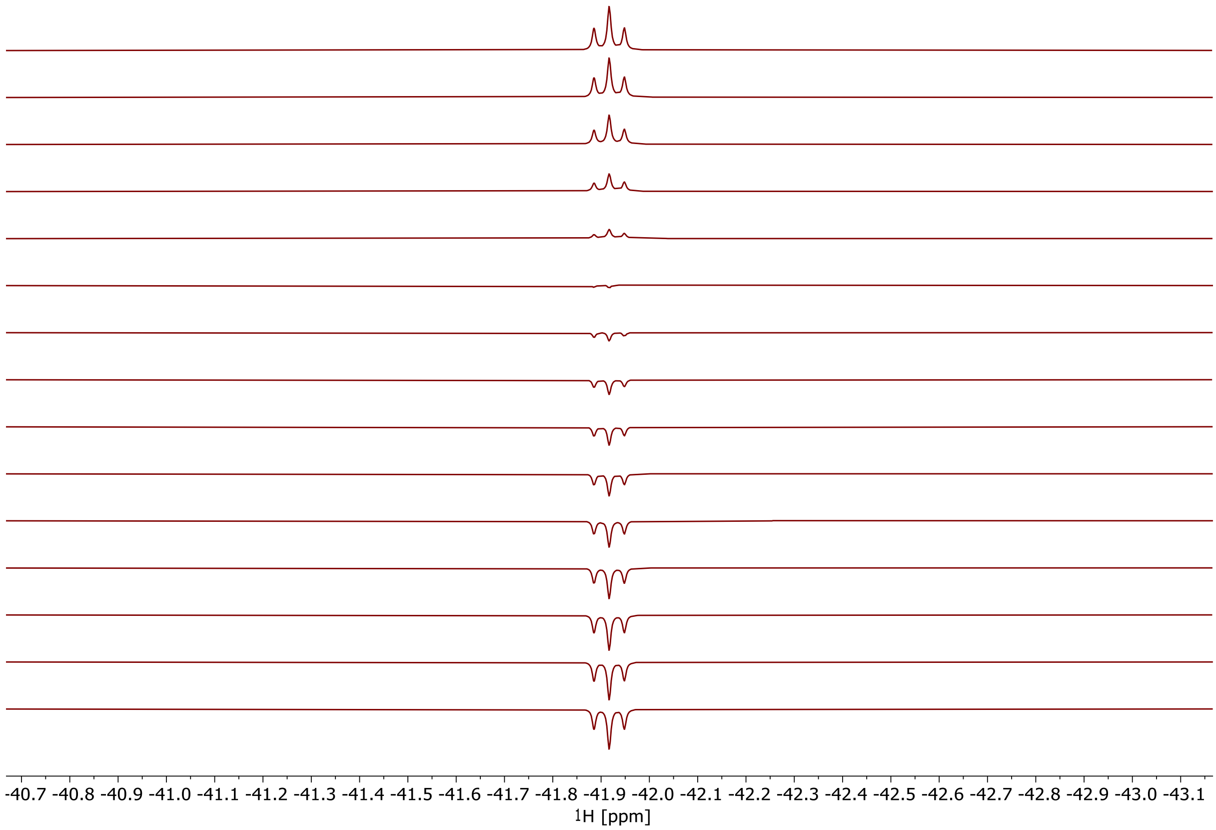

Figure S46. [1]H inversion recovery experiment of hydride signal (−42 ppm) in C_6D_6 at 298 K of **2-*t*Bu**.

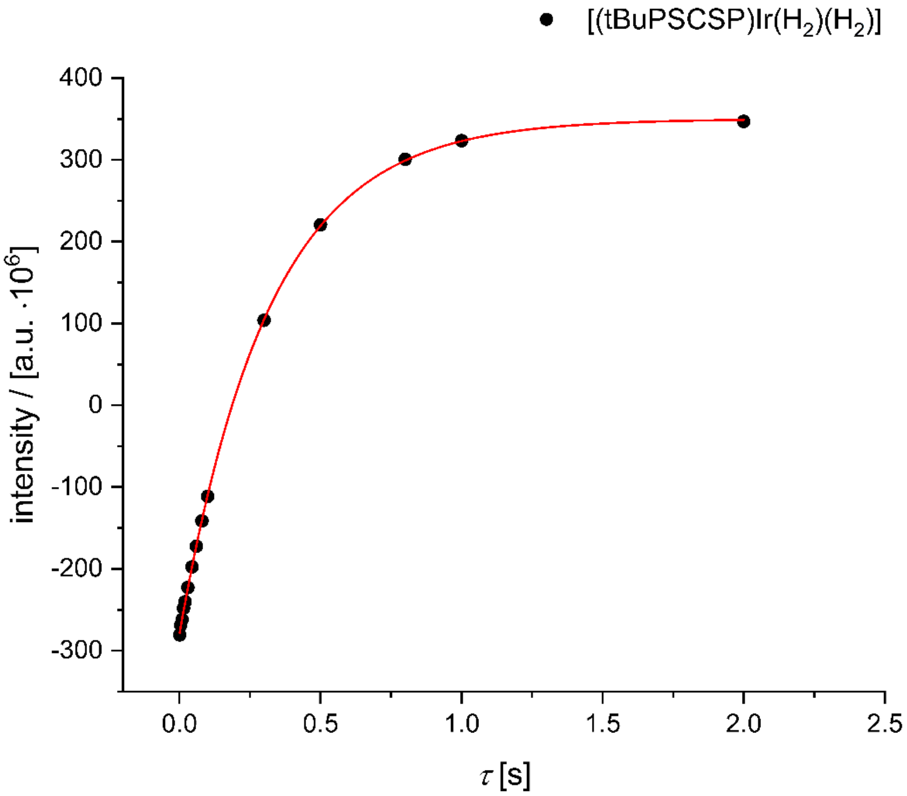

Figure S47. Estimation of the longitudinal relaxation time T_1 for the hydride ligand (−8 ppm) by the inversion recovery sequence of **5** in C_6D_6 at 298 K.

Table S5. Fitting parameters for inversion recovery experiment of **5**.

model	
equation	$y = A_1 \cdot \exp(-x/t_1) + y_0$
Draw	intensity
y_0	3.49932E8 ± 1298738.61657
A_1	-6.3014E8 ± 1314006.57184
t_1	0.31782 ± 0.00222
Chi-square reduced	2.86376E12
R-square (COD)	0.99996
corr. *R*-square	0.99995

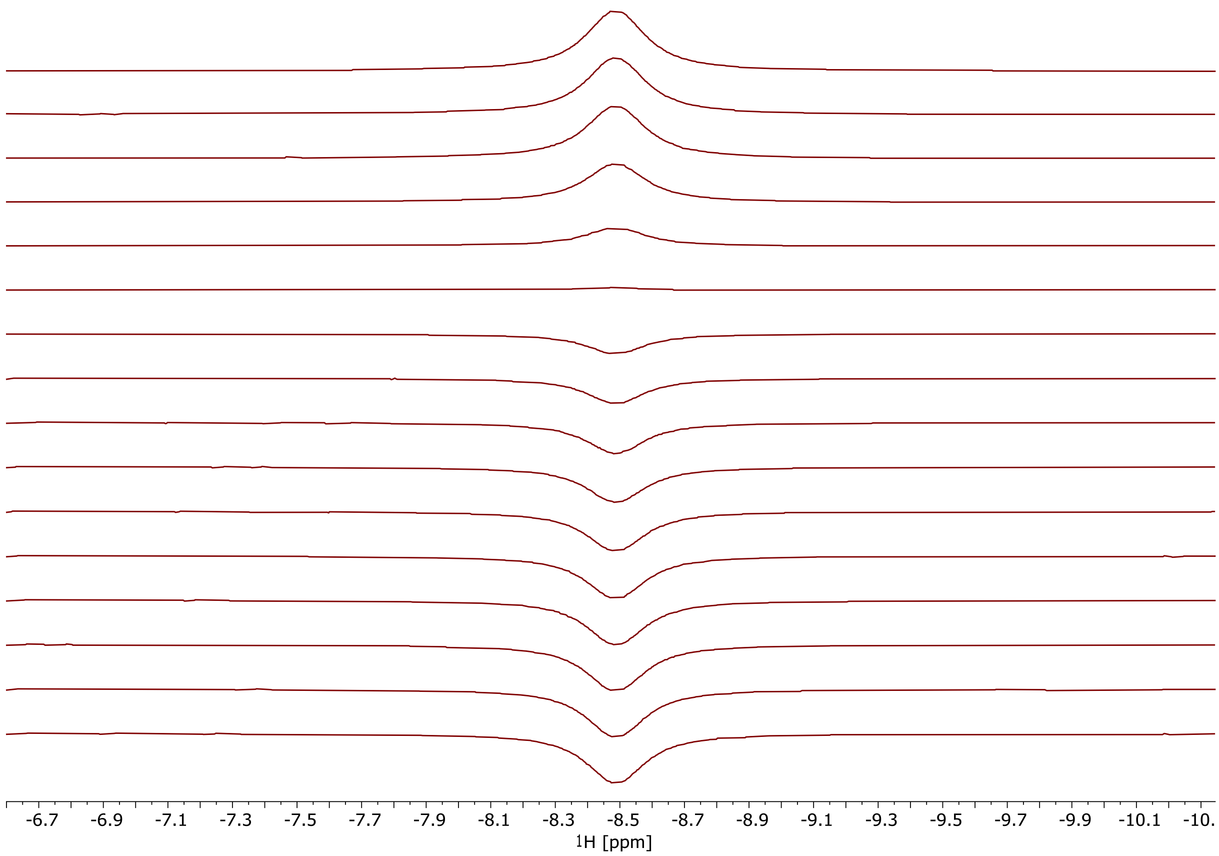

Figure S48. ^1H inversion recovery experiment of hydride signal (−8 ppm) in C_6D_6 at 298 K of **5**.

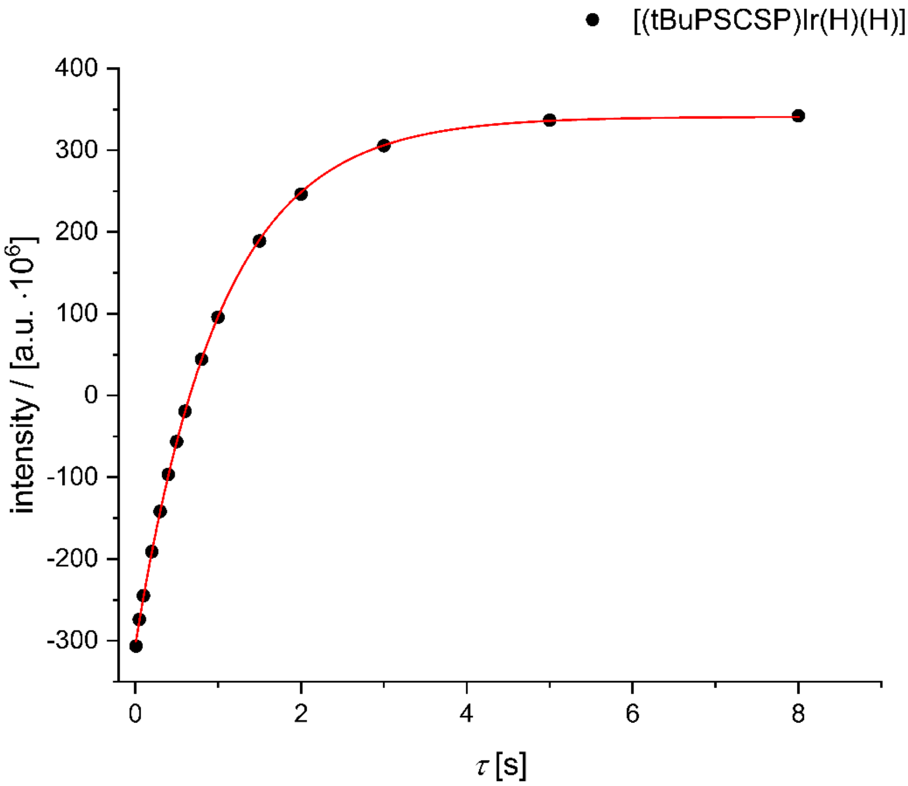

Figure S49. Estimation of the longitudinal relaxation time T_1 for the hydride ligand (−23 ppm) by the inversion recovery sequence of **6** in C_6D_6 at 298 K.

Table S6. Fitting parameters for inversion recovery experiment of **6**.

Model	
equation	$y = A_1 \cdot \exp(-x/t_1) + y_0$
Draw	intensity
y_0	3.40899E8 ± 1452214.22725
A_1	-6.4762E8 ± 1735704.44225
t_1	1.02668 ± 0.00725
Chi-square reduced	5.13561E12
R-square (COD)	0.99992
corr. *R*-square	0.9999

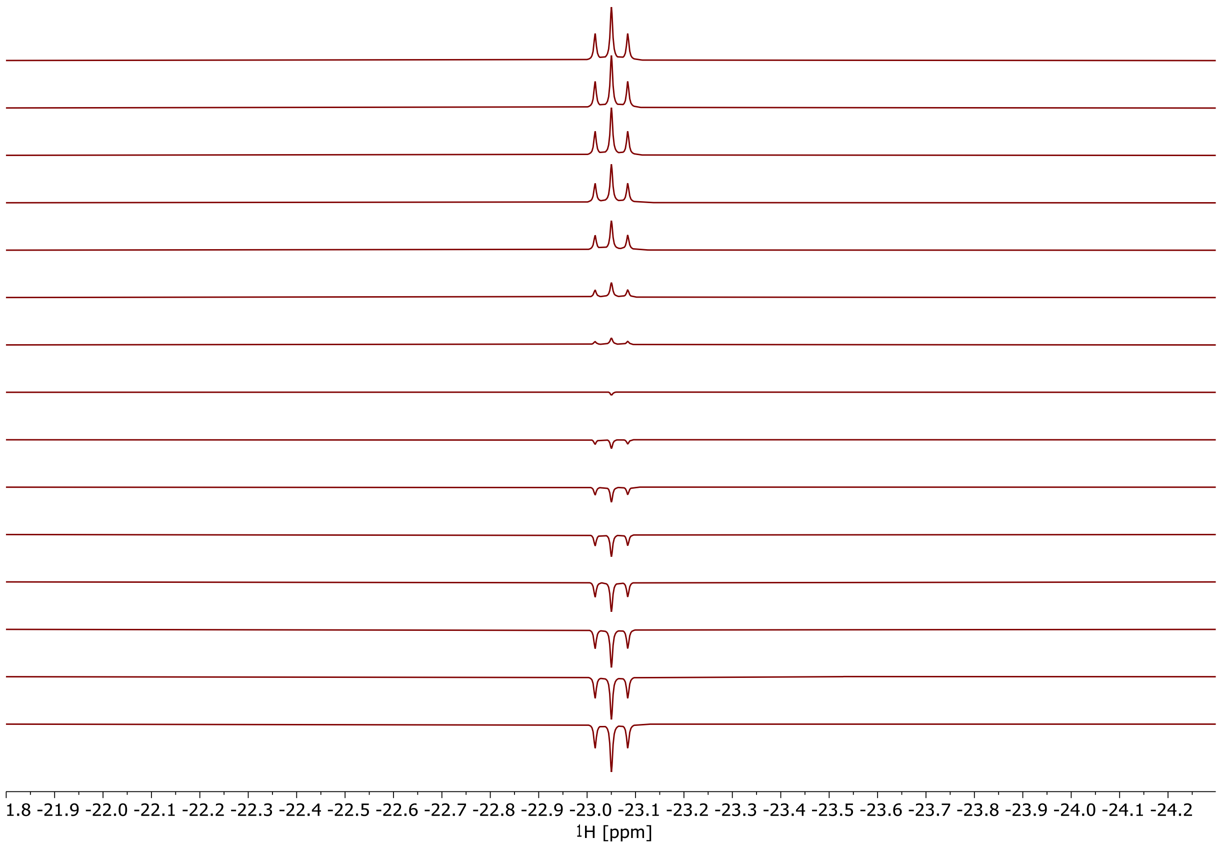

Figure S50. ^{1}H inversion recovery experiment of hydride signal (−23 ppm) in C_6D_6 at 298 K of **6**.

7 IR Spectra

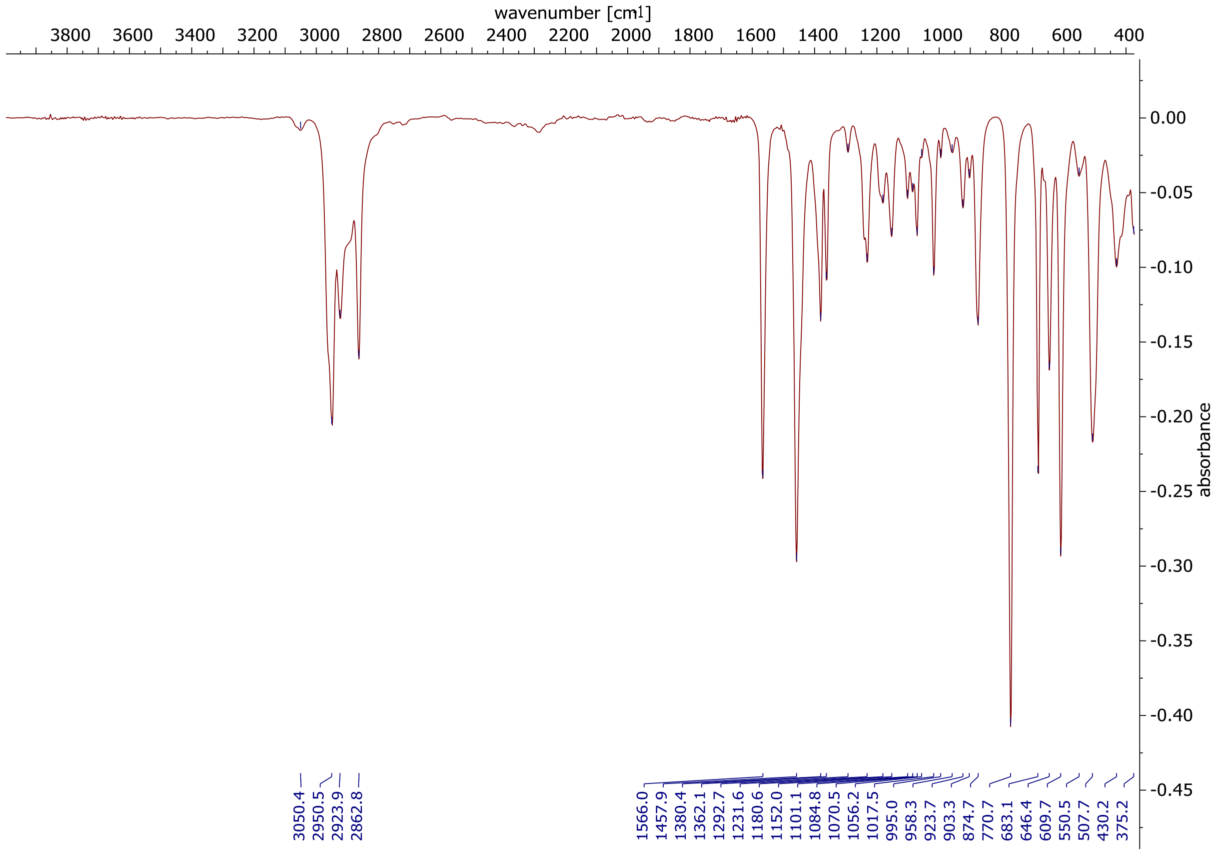

Figure S51. IR spectrum of ligand **1-*i*Pr**.

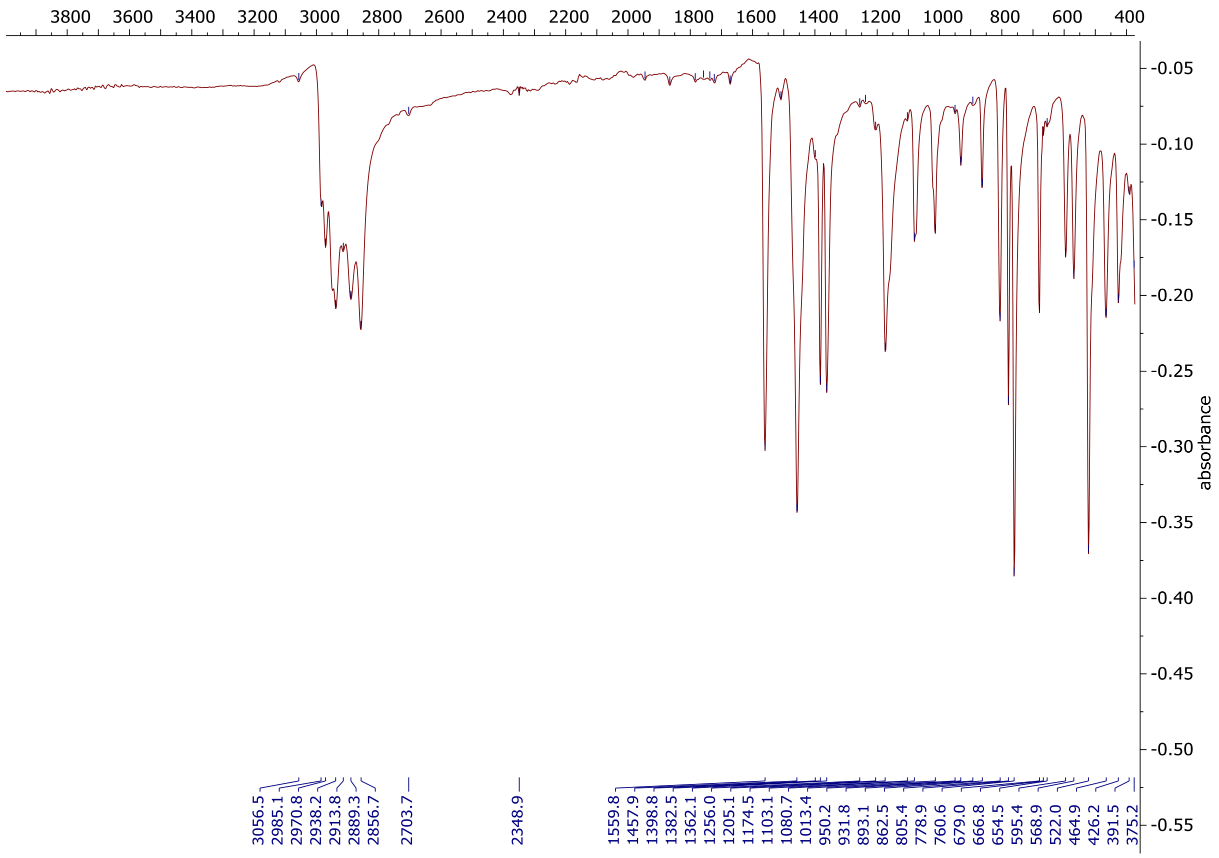

Figure S52. IR spectrum of ligand **1-*t*Bu**.

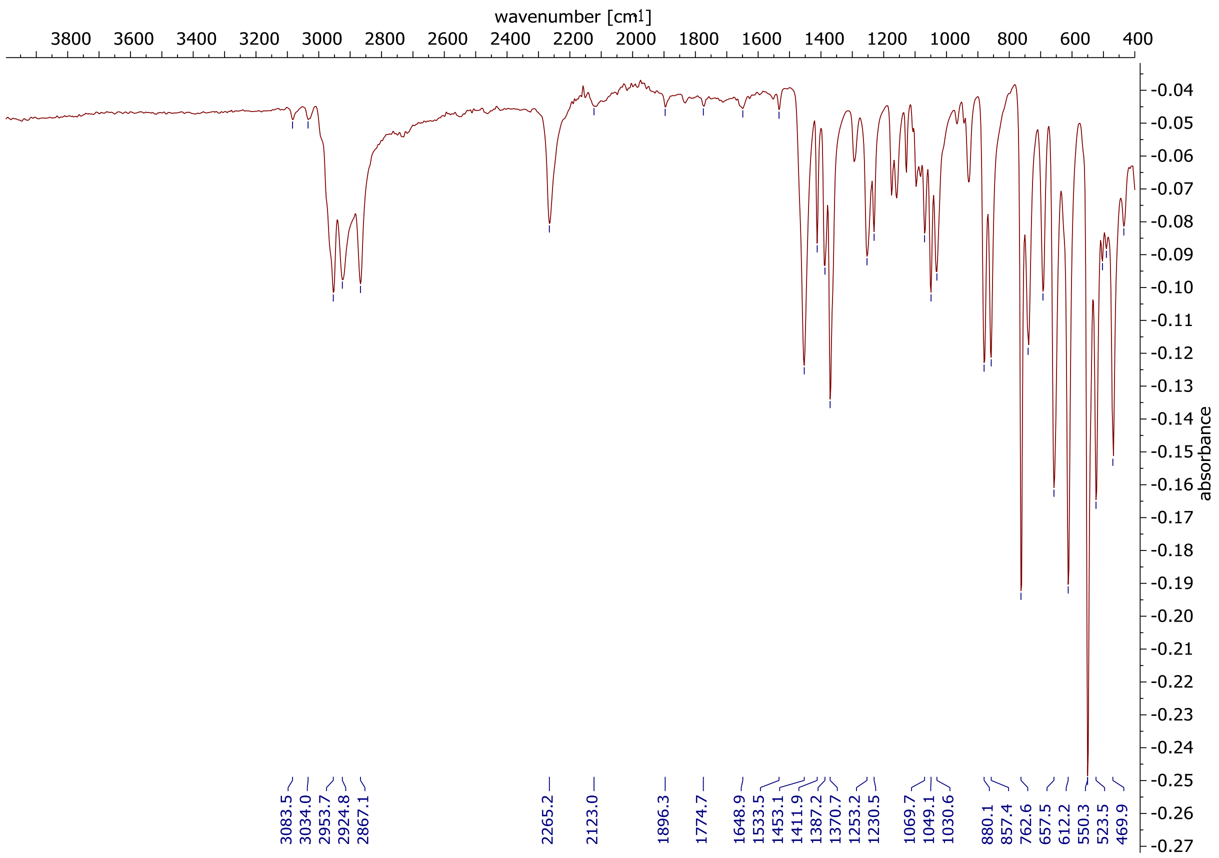

Figure S53. IR spectrum of complex **2-*i*Pr**.

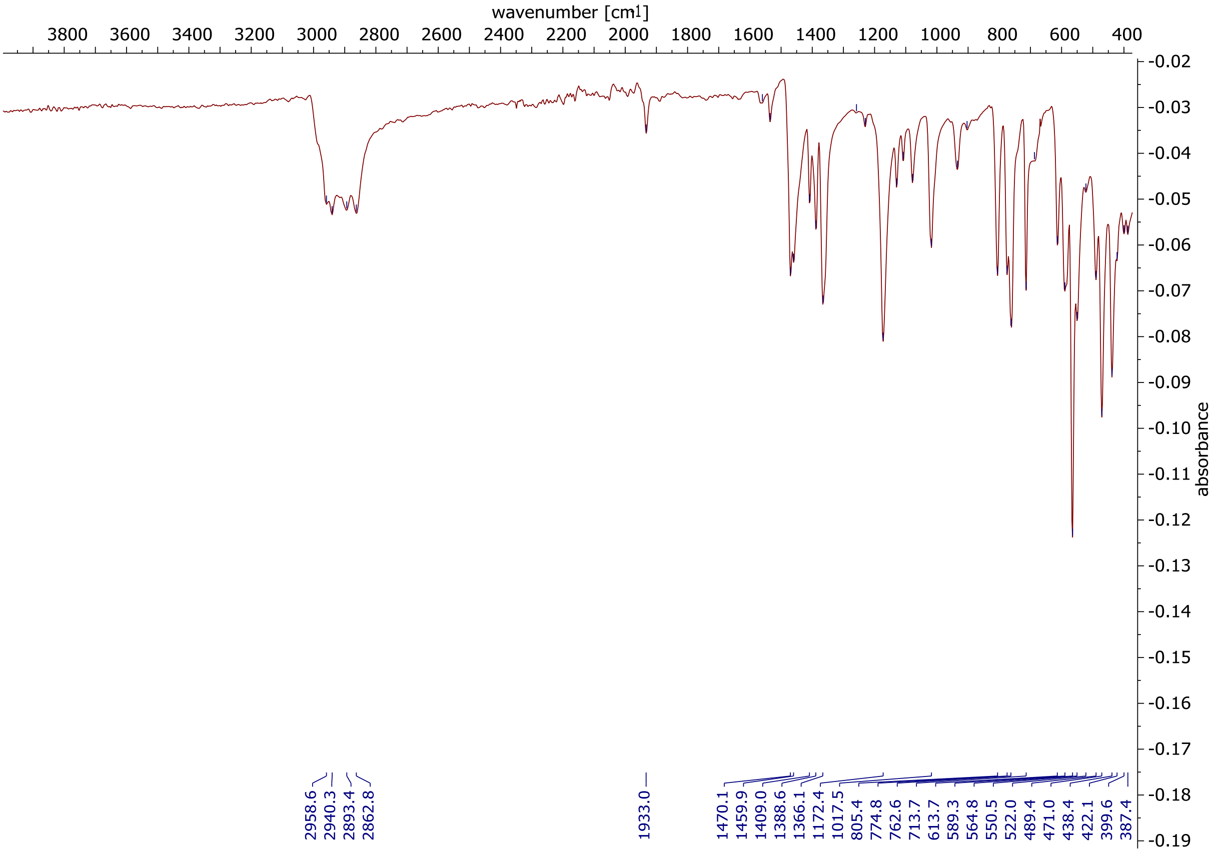

Figure S54. IR spectrum of complex **2-*t*Bu**.

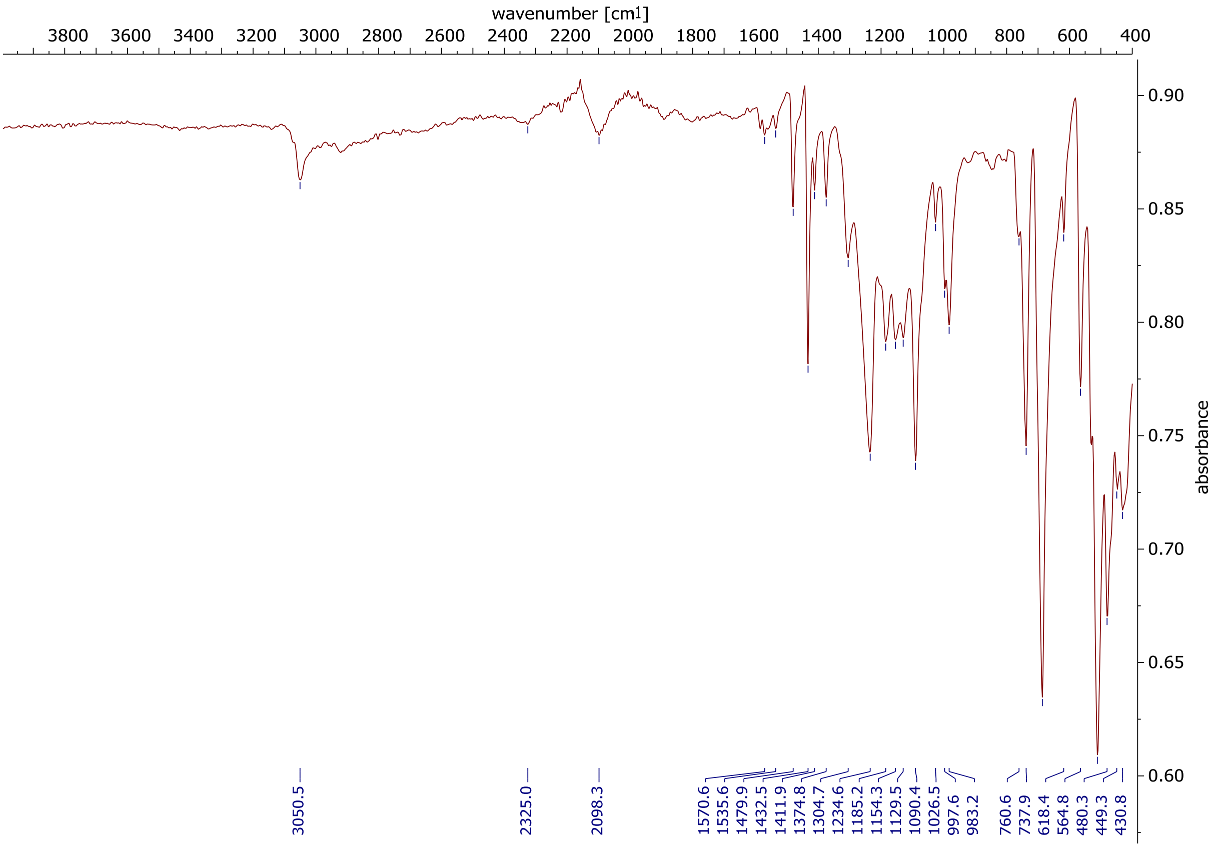

Figure S55. IR spectrum of complex **4**.

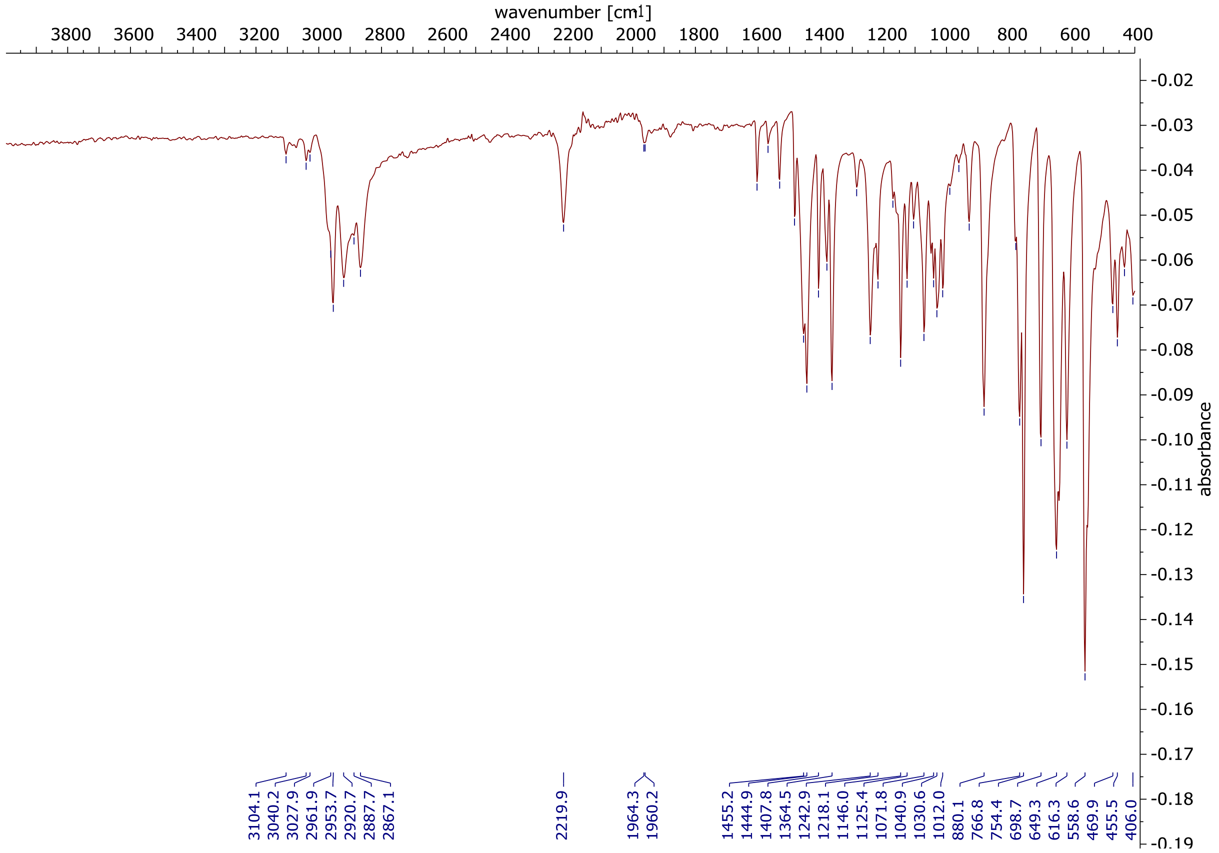

Figure S56. IR spectrum of complex **3-*i*Pr**.

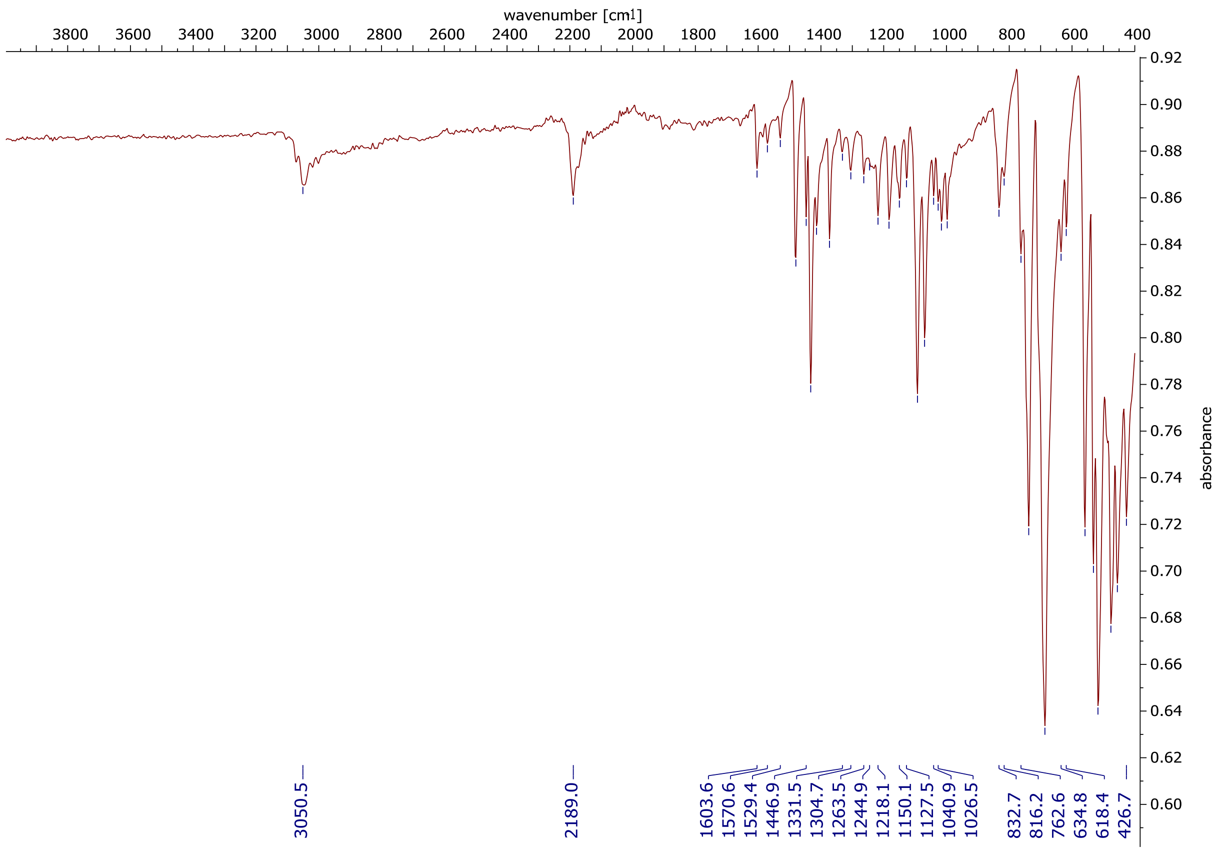

Figure S57. IR spectrum of complex **3-Ph**.

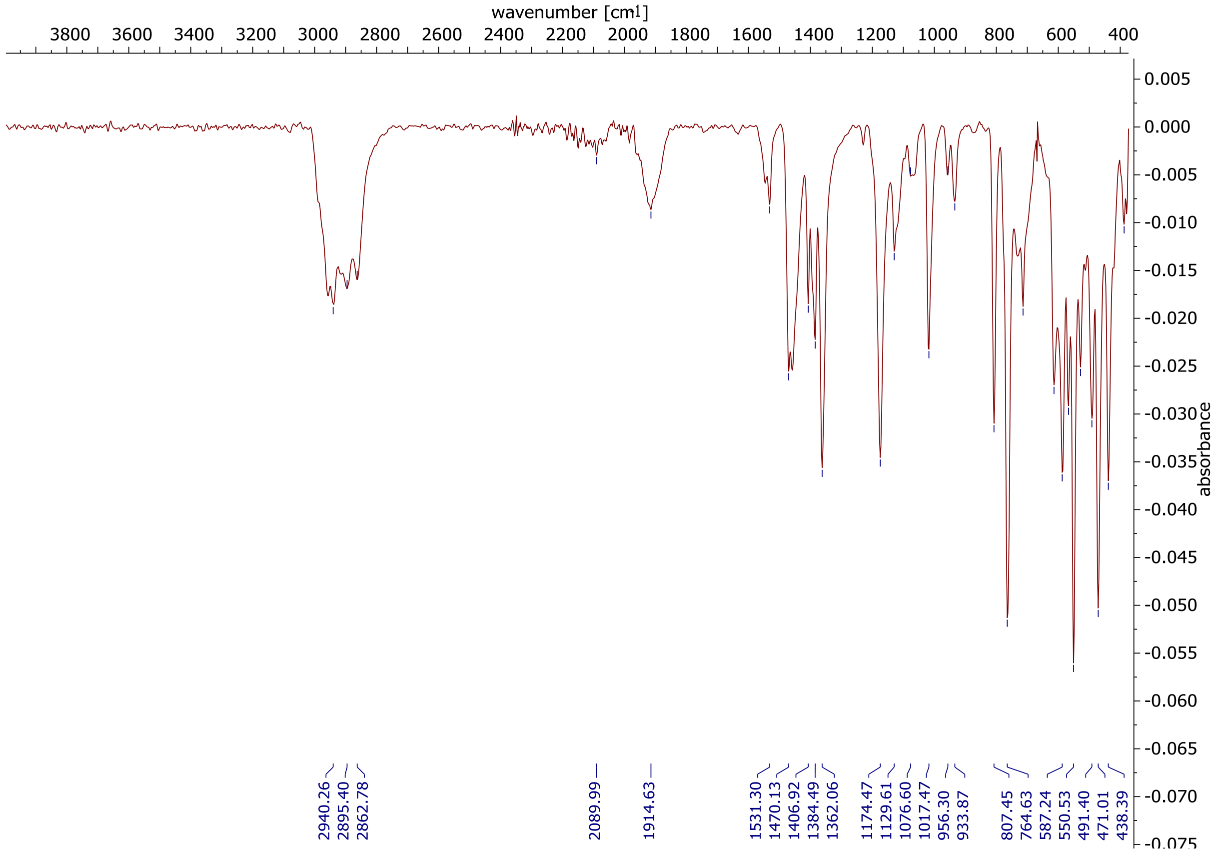

Figure S58. IR spectum of dihydride complex **6**.

8 Variable temperature NMR experiment

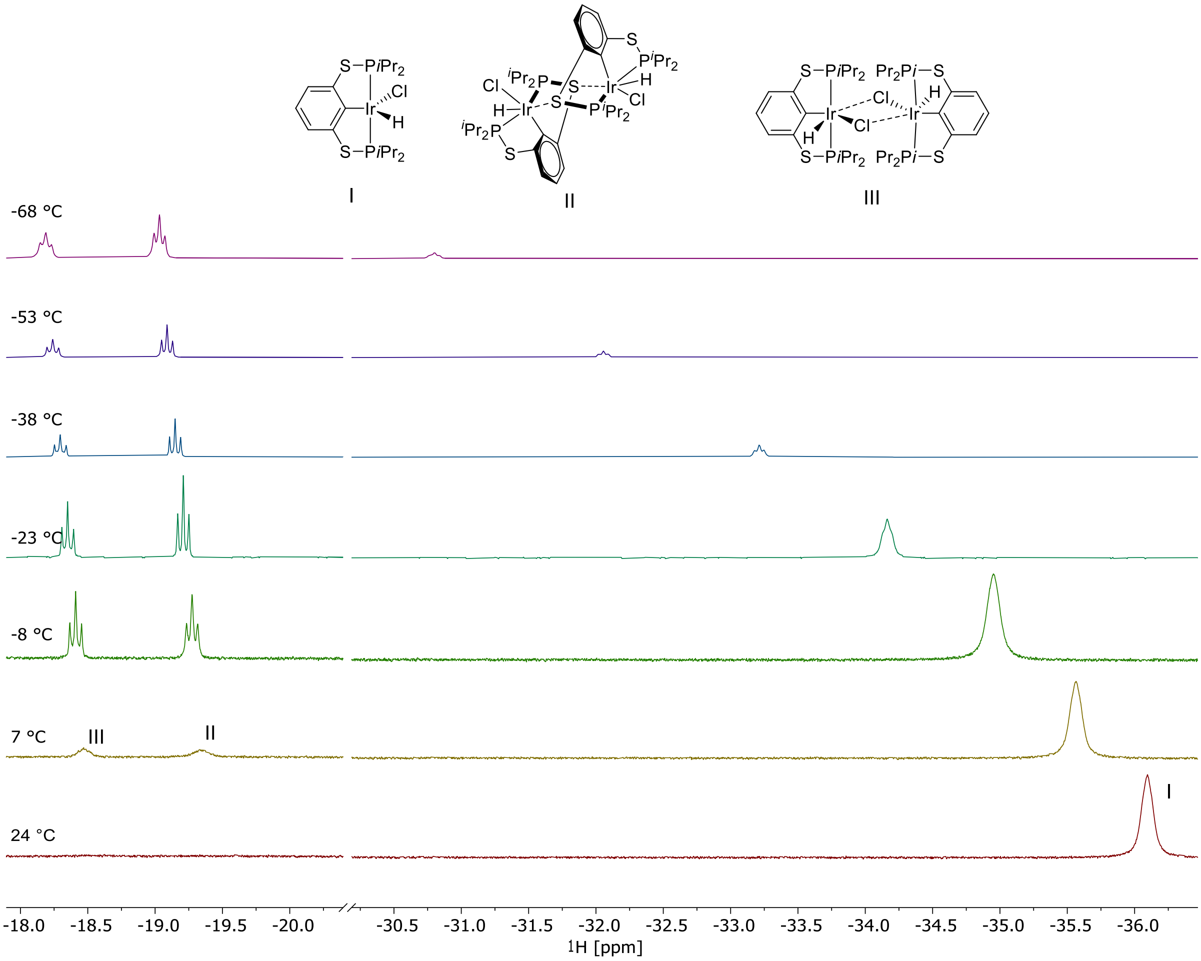

Figure S59. Variable temperature ^{1}H NMR spectra (CD_2Cl_2, 400 MHz, 297 K – 205 K) of complex **2-*i*Pr** with proposed isomers (I – III).

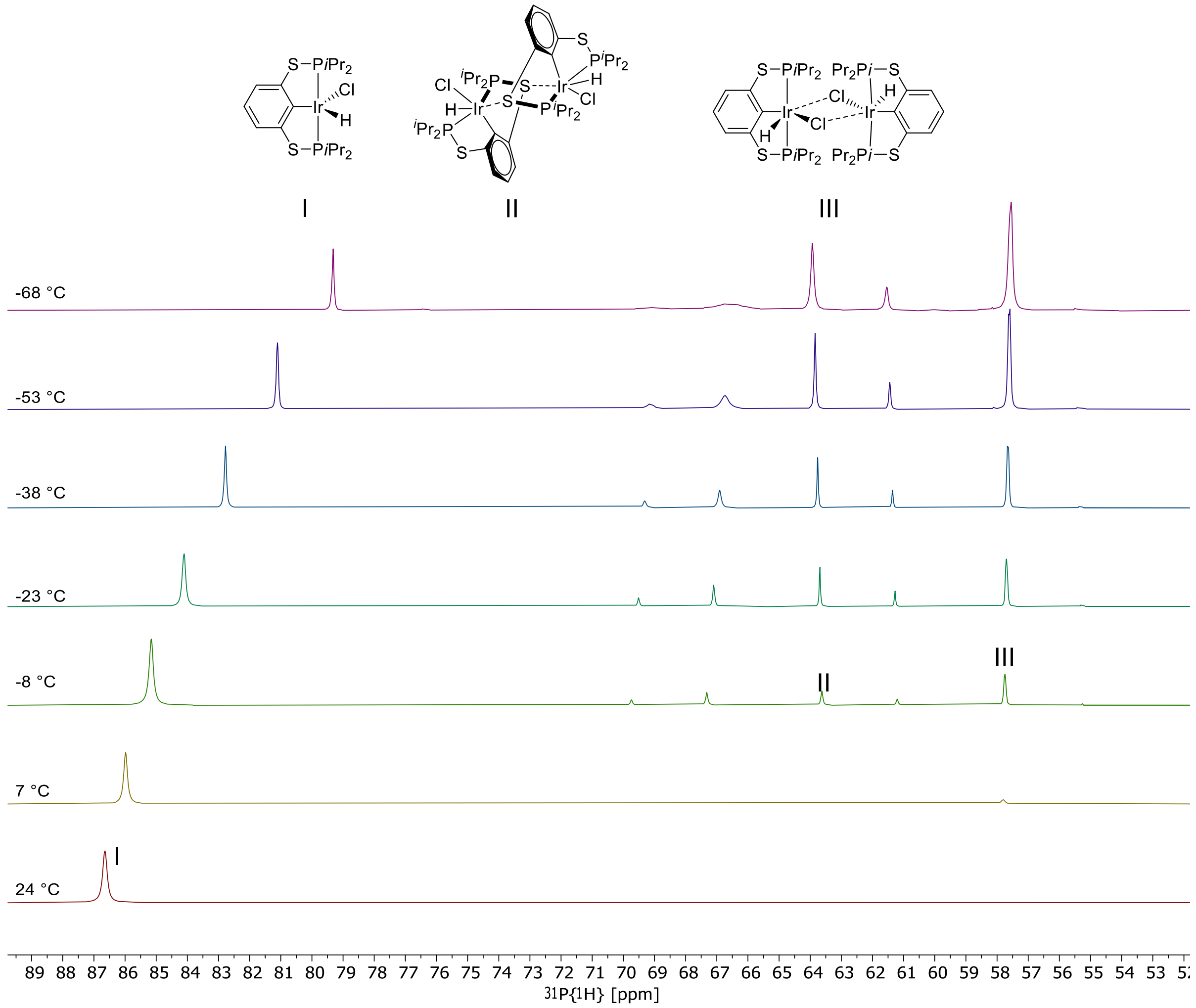

Figure S60. Variable temperature $^{31}P\{^{1}H\}$ NMR spectra (CD_2Cl_2, 162 MHz, 297 K – 205 K) of complex **2-*i*Pr** with proposed isomers (I – III).

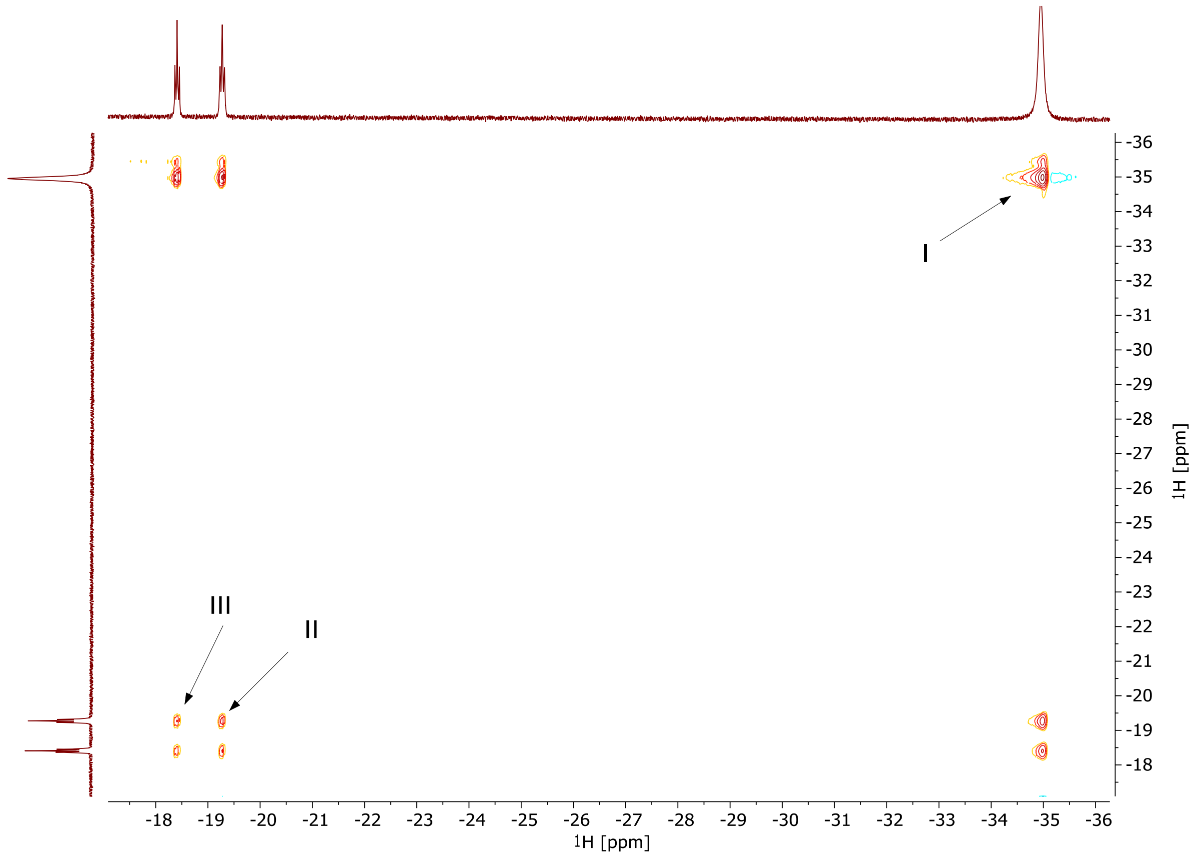

Figure S61. [1]H NOESY NMR spectrum (CD_2Cl_2, 400 MHz, 265 K) of complex **2-*i*Pr**.

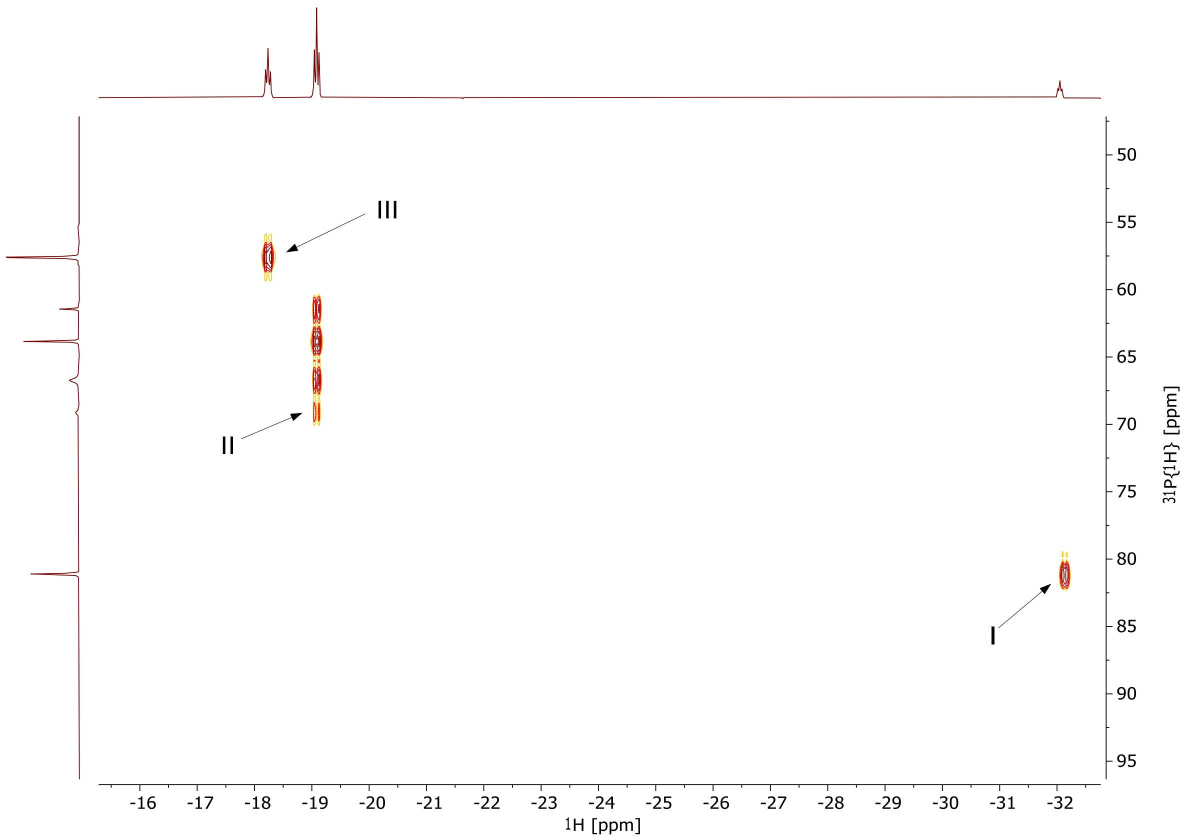

Figure S62. [1]H,[31]P{[1]H} HMBC NMR spectrum (CD_2Cl_2, 400 MHz, ,162 MHz, 220 K) of complex **2-*i*Pr**.

9 Computational details

9.1 General remarks

Computations were carried out using *Gaussian09*[10].

Structure optimisations employed the DFT functional PBE[11, 12] in conjunction with Grimme's dispersion correction D3(BJ)[13, 14] and the def2-TZVP basis set[15] in connection with Ahlrichs W06 density fitting approximation[15, 16] (notation PBE-D3/def2-TZVP/W06). Vibrational frequencies were also computed, to include zero-point vibrational energies in thermodynamic parameters and to characterise all structures as minima on the potential energy surface.

In addition to the electronic supporting information, we provide a multi-structure xyz-file including all calculated molecules.

Please note that all computations were carried out for single, isolated molecules in the gas phase (ideal gas approximation). There may well be significant differences between gas phase and condensed phase.

9.2 Thermochemistry

In this chapter we summarise the results of our thermodynamic calculations, which were performed on the PBE-D3/def2tzvp/W06 level of theory as described beforehand. To model the behaviour of the complexes in the liquid phase, also optimisations were performed at different level of theory. Hence, the self-consistent reaction field method was applied in two consecutive steps. First, the molecules were optimised with the polarisable continuum model (pcm)[17, 18] and confirmed as minima. Second, the resulting minimum structures were reoptimised with smd-approach[19], using the pcm-optimised structure as initial guess and reading out the force constants from the pcm optimisation and frequency analysis. Thermodynamic data were just reported for the gas phase and smd-approach because the former is recommended for computing ΔG of solvation.[20]

9.2.1 Thermodynamics of monomer-dimer-equilibrium of complexes 2-*i*Pr and 8

For optimisation of the proposed *μ*-chloro bridged dimer of complex **2-*i*Pr**, the molecular structure in the solid state of the lighter congener **8** was used as starting structure.[21] As a result, a dispersion stabilised dimer was found for **2-*i*Pr** instead of a *μ*-chloro bridged dimer (*c.f.* xyz-files). The opposite trend is found for the proposed linker atom bridged dimer of complex **8**: using the molecular structure in the solid state of complex **2-*i*Pr** as starting point for optimisation of the O-bridged dimer of **8**, delivered also a dispersion stabilised dimer (*c.f.* xyz-files).

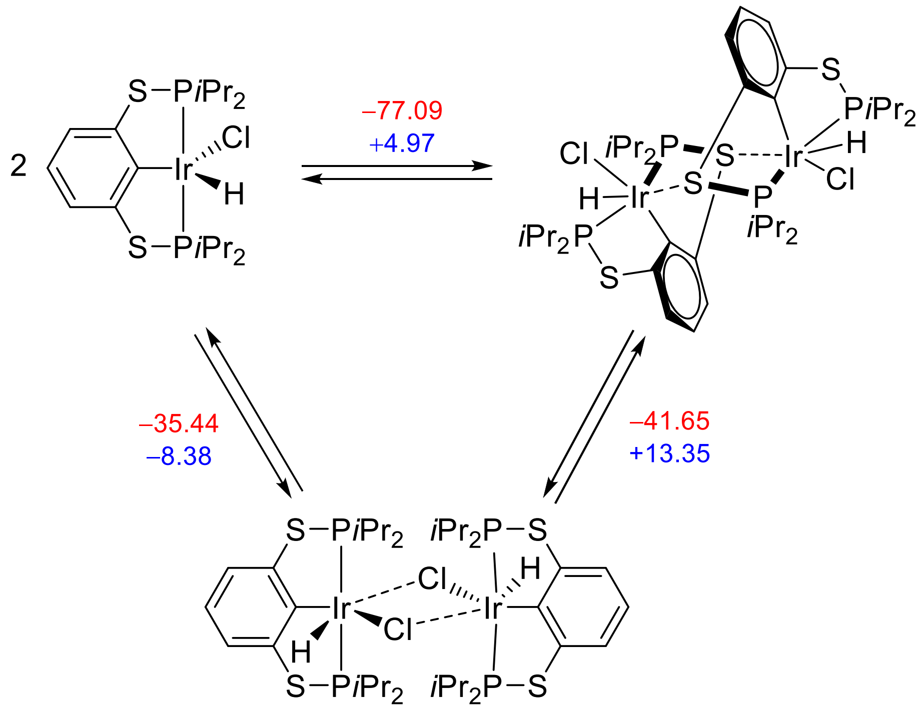

Figure S63. Proposed equilibrium between monomer and different dimers of complex **2-*i*Pr** with free reaction enthalpies $\Delta_R G^0$ in kJ·mol^{-1}: red values represent gas phase data, blue values were calculated with solvent correction (smd model) at PBE-D3/def2-TZVP/W06 level of theory.

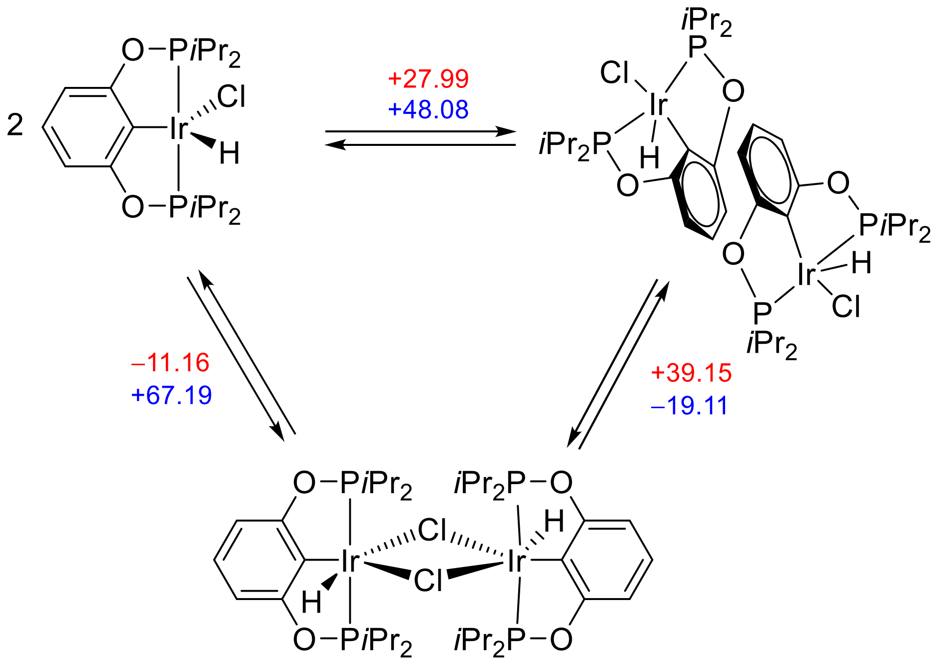

Figure S64. Proposed equilibrium between monomer and different dimers of complex [(^{iPr}POCOP)Ir(H)(Cl)] (**8**) with calculated free reaction enthalpies $\Delta_R G^0$ in kJ·mol^{-1}: red values represent gas phase data, blue values were calculated with solvent correction (smd model) at PBE-D3/def2-TZVP/W06 level of theory.

9.2.2 Thermodynamics of ligand dissociation of 4

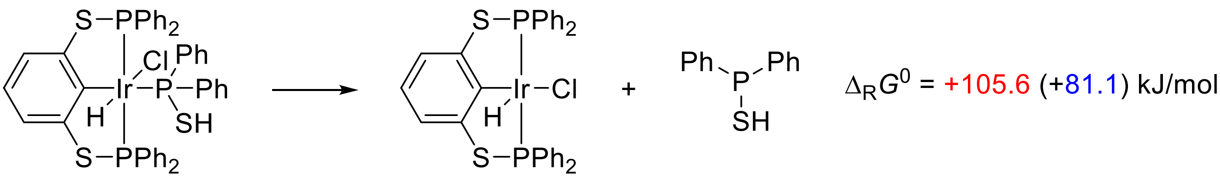

Figure S65. Thermodynamics of ligand dissociation from complex **4**. Free reaction enthalpy $\Delta_R G^0$ calculated for gas phase (red) and with smd solvent correction (blue) (PBE-D3/def2-TZVP/W06).

9.2.3 Report of total enthalpies and energies for all calculated molecules

Table S7. Summary of thermodynamic data of all calculated compounds. Different models of solvent correction were marked with different colours (pcm, smd).

Compound	PG	Nimag	HF [a. u]	ZPE [a.u]	H_{tot} [a.u.]	G_{tot} [a.u.]
[(^{iPr}PSCSP)Ir(H)(Cl)]-monomer	C_1	0	-2747.695381	-2747.244777	-2747.211217	-2747.308995
[(^{iPr}PSCSP)Ir(H)(Cl)] "Cl"-bridged	C_i	0	-5495.426240	-5494.524934	-5494.456410	-5494.631489
[(^{iPr}PSCSP)Ir(H)(Cl)] S-bridged	C_i	0	-5 495.4582763	-5 494.55148	-5494.485312	-5494.647353
[(iPrPSCSP)Ir(H)(Cl)] -monomer	C_1	0	-2747.708145	-2747.257557	-2747.224125	-2747.320449
[(iPrPSCSP)Ir(H)(Cl)] "Cl"-bridged	C_1	0	-5495.446745	-5494.542222	-5494.475066	-5494.643627
[(iPrPSCSP)Ir(H)(Cl)] S-bridged	C_i	0	-5495.471389	-5494.565497	-5494.49915	-5494.661707

Compound	**PG**	**Nimag**	**HF [a. u]**	**ZPE [a.u]**	**H_{tot} [a.u.]**	**G_{tot} [a.u.]**
[(iPrPSCSP)Ir(H)(Cl)] -monomer	C_1	0	-2747.733934	-2747.284031	-2747.250506	-2747.34712
[(iPrPSCSP)Ir(H)(Cl)] "Cl"-bridged	C_1	0	-5495.494592	-5494.59329	-5494.525408	-5494.697432
[(iPrPSCSP)Ir(H)(Cl)] S-bridged	C_i	0	-5495.501556	-5494.596579	-5494.530358	-5494.692347
[(^{iPr}POCOP)Ir(H)(Cl)] -monomer (Xray)	C_1	0	-2101.986211	-2101.530654	-2101.498221	-2101.592806
[(^{iPr}POCOP)Ir(H)(Cl)] "Cl"-bridged	C_i	0	-4204.012416	-4203.095563	-4203.031876	-4203.189861
[(^{iPr}POCOP)Ir(H)(Cl)] "O"-bridged	C_1	0	-4203.9904610	-4203.0762070	-4203.011139	-4203.174951
[(iPrPOCOP)Ir(H)(Cl)]-monomer (Xray)	C_1	0	-2101.9986917	-2101.5424610	-2101.510451	-2101.602861

Compound	PG	Nimag	HF [a. u]	ZPE [a.u]	H_{tot} [a.u.]	G_{tot} [a.u.]
[(iPrPOCOP)Ir(H)(Cl)] "Cl"-bridged	C_i	0	-4204.0233709	-4203.1075820	-4203.043750	-4203.201916
[(iPrPOCOP)Ir(H)(Cl)] "O"-bridged	C_1	0	-4203.9904609	-4203.0762080	-4203.011139	-4203.174956
[(iPrPOCOP)Ir(H)(Cl)]-monomer (Xray)	C_1	0	-2102.0231267	-2101.5681630	-2101.535991	-2101.629103
[(iPrPOCOP)Ir(H)(Cl)] "Cl"-bridged	C_i	0	-4204.0544759	-4203.1394460	-4203.075754	-4203.232615
[(iPrPOCOP)Ir(H)(Cl)] "O"-bridged	C_1	0	-4204.0560484	-4203.142945	-4203.078245	-4203.239892
PhPSCSPIrHClPPh2 SH in	C_1	0	-4402.618513	-4401.991950	-4401.942372	-4402.076694
PhPSCSPIrHCl (s ausgelenkt)	C_1	0	-3 199.7915925	-3 199.35535	-3199.319319	-3199.429425

Compound	PG	Nimag	HF [a. u]	ZPE [a.u]	H_{tot} [a.u.]	G_{tot} [a.u.]
Ph2PSH	C_1	0	-1202.751174	-1202.564543	-1202.550232	-1202.607064
PhPSCSPIrHClPPh2 SH in	C_1	0	-4402.624737	-4401.998143	-4401.948537	-4402.083035
PhPSCSPIrHCl (s ausgelenkt)	C_1	0	-3199.800117	-3199.363583	-3199.327641	-3199.437049
Ph2PSH	C_1	0	-1202.753566	-1202.566953	-1202.552623	-1202.609415
PhPSCSPIrHClPPh2 SH in	C_1	0	-4402.660137	-4402.033495	-4401.983815	-4402.118752
PhPSCSPIrHCl (s ausgelenkt)	C_1	0	-3199.8314927	-3199.3947140	-3199.358921	-3199.466317
Ph2PSH	C_1	0	-1202.7659382	-1202.5792540	-1202.564937	-1202.621564

10 References

1. G. Sheldrick, *Acta Crystallogr., Sect. A: Found. Adv.*, 2015, **71**, 3-8.
2. G. M. Sheldrick, *SHELXS 97, Program for the Solution of Crystal Structure*, 1990.
3. G. Sheldrick, *Acta Crystallogr., Sect. C: Struct. Chem.*, 2015, **71**, 3-8.
4. G. M. Sheldrik, *SADABS Version 2, University of Göttingen*, 2004.
5. A. Spek, *Acta Crystallogr., Sect. D: Struct. Biol.*, 2009, **65**, 148-155.
6. G. Vlahopoulou, S. Möller, J. Haak, P. Hasche, H. J. Drexler, D. Heller and T. Beweries, *Chem. Commun.*, 2018, **54**, 6292-6295.
7. L. P. Press, A. J. Kosanovich, B. J. McCulloch and O. V. Ozerov, *J. Am. Chem. Soc.*, 2016, **138**, 9487-9497.
8. I. Göttker-Schnetmann, P. S. White and M. Brookhart, *J. Am. Chem. Soc.*, 2004, **126**, 1804-1811.
9. W. Yao, Y. Zhang, X. Jia and Z. Huang, *Angew. Chem., Int. Ed.*, 2014, **53**, 1390-1394.
10. *R. E. Gaussian 09,* M. J. Frisch, G. W. Trucks, H. B. Schlegel, G. E. Scuseria, M. A. Robb, J. R. Cheeseman, G. Scalmani, V. Barone, G. A. Petersson, H. Nakatsuji, X. Li, M. Caricato, A. Marenich, J. Bloino, B. G. Janesko, R. Gomperts, B. Mennucci, H. P. Hratchian, J. V. Ortiz, A. F. Izmaylov, J. L. Sonnenberg, D. Williams-Young, F. Ding, F. Lipparini, F. Egidi, J. Goings, B. Peng, A. Petrone, T. Henderson, D. Ranasinghe, V. G. Zakrzewski, J. Gao, N. Rega, G. Zheng, W. Liang, M. Hada, M. Ehara, K. Toyota, R. Fukuda, J. Hasegawa, M. Ishida, T. Nakajima, Y. Honda, O. Kitao, H. Nakai, T. Vreven, K. Throssell, J. A. Montgomery, Jr., J. E. Peralta, F. Ogliaro, M. Bearpark, J. J. Heyd, E. Brothers, K. N. Kudin, V. N. Staroverov, T. Keith, R. Kobayashi, J. Normand, K. Raghavachari, A. Rendell, J. C. Burant, S. S. Iyengar, J. Tomasi, M. Cossi, J. M. Millam, M. Klene, C. Adamo, R. Cammi, J. W. Ochterski, R. L. Martin, K. Morokuma, O. Farkas, J. B. Foresman, and D. J. Fox, Gaussian, Inc., Wallingford CT, 2016.
11. J. P. Perdew, K. Burke and M. Ernzerhof, *Phys. Rev. Lett.*, 1996, **77**, 3865-3868.
12. J. P. Perdew, K. Burke and M. Ernzerhof, *Phys. Rev. Lett.*, 1997, **78**, 1396-1396.
13. S. Grimme, J. Antony, S. Ehrlich and H. Krieg, *J. Chem. Phys.*, 2010, **132**, 154104.
14. S. Grimme, S. Ehrlich and L. Goerigk, *J. Comput. Chem.*, 2011, **32**, 1456-1465.
15. F. Weigend and R. Ahlrichs, *Phys. Chem. Chem. Phys.*, 2005, **7**, 3297-3305.
16. F. Weigend, *Phys. Chem. Chem. Phys.*, 2006, **8**, 1057-1065.
17. J. Tomasi, B. Mennucci and R. Cammi, *Chem. Rev.*, 2005, **105**, 2999-3094.
18. G. Scalmani and M. J. Frisch, *J. Chem. Phys.*, 2010, **132**, 114110.
19. A. V. Marenich, C. J. Cramer and D. G. Truhlar, *J. Phys. Chem. B*, 2009, **113**, 6378-6396.
20. J. B. Foresman and Æ. Frisch, *Exploring Chemistry with Electronic Structure Methods*, Gaussian, Inc.: Wallingford, CT, 2015.
21. N. T. Mucha and R. Waterman, *Organometallics*, 2015, **34**, 3865-3872.